UNIVERSITY OF BELGRADE
FACULTY OF PHYSICS

Nataša B. Lazić

QUASI-CLASSICAL GROUND STATES AND MAGNONS IN MONOPERIODIC SPIN SYSTEMS

Doctoral Dissertation

Belgrade, 2016.

UNIVERZITET U BEOGRADU
FIZIČKI FAKULTET

Nataša B. Lazić

KVAZI-KLASIČNA OSNOVNA STANJA I MAGNONI U MONOPERIODIČNIM SPINSKIM SISTEMIMA

Doktorska Disertacija

Beograd, 2016.

Mentor: dr Milan Damnjanović, redovni profesor
Fizičkog fakulteta Univerziteta u Beogradu

Članovi komisije: dr Milan Damnjanović, redovni profesor
Fizičkog fakulteta Univerziteta u Beogradu

dr Zoran S. Popović, naučni savetnik
Instituta za nuklearne nauke "Vinča" u Beogradu

dr Tatjana Vuković, vanredni profesor
Fizičkog fakulteta Univerziteta u Beogradu

dr Đorđe Spasojević, vanredni profesor
Fizičkog fakulteta Univerziteta u Beogradu

dr Vladimir Damljanović, naučni saradnik
Instituta za Fiziku u Beogradu

Datum odbrane: _____

Ovaj rad je urađen u Nanolab grupi na Fizičkom fakultetu u Beogradu, pod rukovodstvom prof. dr Milana Damnjanovića. Njemu ujedno dugujem najveću zahvalnost na srdačnoj pomoći i podršci koju mi je pružio. Posebno bih istakla njegov entuzijazam i spremnost da sasluša i strpljivo odgovara na brojna pitanja. Iako mi je ponekad delovalo da diskusije poprimju žustriji ton, smatram ih najkorisnijim delom zajedničkog rada. Želela bih, takođe, da se zahvalim kolegama iz grupe na prijateljskoj atmosferi, a naročito prof. dr Tatjani Vuković i Marku Milivojeviću na njihovom doprinosu radu o magnetnim uređenjima. Korisne su bile sugestije prof. dr Zorana Radovića i doc. dr Mihajla Vanevića, koji je kritički pročitao rukopis o uređenjima kod ^{13}C nanotuba. Konačno, razumevanju komplikovanijih matematičkih problema doprineo je prof. dr Rade Živaljević.

Nataša Lazić

KVAZI-KLASIČNA OSNOVNA STANJA I MAGNONI U MONOPERIODIČNIM SPINSKIM SISTEMIMA

REZIME

Tema ovog rada je simetrijski zasnovana analiza sistema čiji atomi (čvorovi) imaju nenulte magnetne momente (spinove), a čija je dinamika diktirana Hamiltonijanima kvadratne forme po spinovima, tj. spin-spin interakcija je zadata tenzorom drugog reda. U ovoj oblasti se obično koristi isključivo translaciona periodičnost kristala, dok se ostale simetrije naknadno razmatraju. Stoga je osnovni cilj ove studije uključivanje kompletne simetrije sistema, pre svega u modeliranje magnetnih Hamiltonijana, a potom i u nalaženje njihovih mogućih rešenja u smislu kvazi-klasičnih osnovnih stanja i odgovarajućih nisko-energijskih (heli)magnonskih spektara. Da bi se to efikasno postiglo, rad je metodološki zasnovan na strogom formalizmu koji tretira sisteme čije su geometrijske konfiguiracije invarijantne na podgrupe Euklidske grupe, a interakcije obuhvataju proizvoljan nivo susedstva. Polazeći od osobina Lijeve algebre ugaonih momenata, u kvantno-mehaničkom prostoru stanja definiše se dejstvo grupe, koje, usled principa invarijantnosti hamiltonijana, izdvaja aksijalno-vektorsku reprezentaciju uz odgovarajuća ograničenja na tenzorsko polje interakcije. Zajedno sa tim, hermitičnost hamiltonijana omogućava generalizaciju Morijinih pravila na sve dozvoljene komponente interakcije. Zbog velike dimenzije kvantnog prostora stanja, koja se skalira eksponencijalno sa brojem čvorova, rešenja ovakvih modela su, osim u najjednostavnijim slučajevima, aproksimativna. Tako, ograničavanjem probnog skupa varijacionog problema na separabilna stanja energija postaje funkcional po klasičnim vektorima (na čvorovima), koji, u opštem slučaju, nemaju međusobno jednake dužine. Kako je potonji uslov podrazumevan u aproksimaciji srednjeg polja, u radu se razmatraju mogućnosti da ovako nađeno osnovno stanje bude regularno, tj. invarijantno na neku spinsku grupu. U tu svrhu se pokazuje da se klasifikacija spinskih grupa može izvršiti korišćenjem realnih trodimenzionalnih reprezentacija (spinske reprezentacije) kojima se direktno određuju i sva regularna uređenja (međusobno jednakih dužina). Polazeći dalje od pretpostavke da je model takav da je optimizovan regularno uređenim klasičnim

spinovima na čvorovima, a čuvajući njihovu prirodu ugaonog momenta, izvedeno je preslikavanje u bozonsku sliku otklona od osnovnog stanja. Time se dinamika niskoenergijskih pobuda svodi na svojstveni problem odgovarajuće beskonačnodimenzione dinamičke matrice koji se, opet zahvaljujući simetriji, lako rešava metodom modifikovanih grupnih projektora. Kako, međutim, u opštem slučaju grupa simetrije može biti smanjena, predlaže se algoritam za rešavanje svojstvenog problema dinamičke matrice koji efektivno koristi celu grupu. Za monoperiodične sisteme koji su opisani jednom od 13 familija linijskih grupa detaljno se analiziraju transformaciona svojstva tenzora interakcije i Morijina pravila, dok se pojmovi izotropnosti i homogenosti prilagođavaju kvazi-jednodimenzionalnoj geometriji. Izdvaja se prototipni Hamiltonijan koji pored XXZ Hajzenbergovog člana ima i Džalošinski-Morijin vektor usmeren duž ose sistema. Pored tenzora, podrobno se klasifikuju spinske reprezentacije i uređenja prve (najvažnije) familije linijskih grupa; uređenja ostalih familija se dobijaju iz prve, u radu predloženim algoritmom. Konačno, navedeni teorijski koncepti se primenjuju na nedavno sintetisanim ^{13}C nanotubama čiji su nuklearni spinovi putem lutajućih elektrona spregnuti dugo-dometnom Ruderman-Kitel-Kasuja-Josida interakcijom. Dobijena raznolikost helimagnetnih faza koje se kontrolišu naponom, osim toga što ukazuje na univerzalno ponašanje svih nanotuba, kandiduje ih, takođe, za spintroničke uređaje.

KLJUČNE REČI: Simetrija, kvazi-klasični magnetizam, spinski talasi, spinske grupe, helimagnetizam, ugljenične nanotube
NAUČNA OBLAST: Fizika
UŽA NAUČNA OBLAST: Kvantna i matematička fizika (Fizika kondenzovanog stanja materije)
UDK BROJ: 538.9

QUASI-CLASSICAL GROUND STATES AND MAGNONS IN MONOPERIODIC SPIN SYSTEMS

SUMMARY

Subject of this work is symmetry based analysis of systems whose atoms (sites) have non-vanishing magnetic moments (spins), and whose dynamics is governed by Hamiltonians of quadratic forms in spins, i.e. spin-spin interaction is given by the second rank tensor. Commonly, in this field, the translational periodicity of a crystal is used only, while the other symmetries are considered afterwards. Therefore, the main aim of this study is inclusion of the full symmetry of systems in the modeling of the magnetic Hamiltonians first, and then in finding their possible solutions, in particular the quasi-classical ground states and the corresponding low-energy (heli)magnons spectra. To achieve this efficiently, the work is methodologically based on rigorous formalism treating the systems whose geometrical configurations are invariant under the subgroups of the Euclidean group, and whose interactions involve arbitrary levels of neighbours. Starting from the properties of the angular momentum Lie algebra, in quantum-mechanical state space group action is defined, which, due to the invariance principle for Hamiltonian, singles out the axial-vector representation and its constrains on the interaction tensor field. Together with that, the hermiticity of Hamiltonian enables us to generalize the Moria's rules on all of the allowed components of the interaction. Because of the large dimension of the quantum state space, which is exponentially scaled by the numbers of sites, the solutions of such models are approximate, except in the simplest cases. Thus, restricting the trial set of the variational problem to the separable states, the energy becomes a functional over the site classical vectors, which, in general case, do not have mutually equal lengths. Since, in the mean-field approximation the latter condition is defaulted, in this work, the possibilities that the ground state found in this way is regular, i.e. invariant under a spin group, are considered. For this purpose, it is shown that the classification of the spin groups can be performed using orthogonal three-dimensional real representations (spin representations), by which all the regu-

lar arrangements (of mutually equal lengths) are directly determined also. Further on, starting from the assumption that a model is optimized by the regularly arranged classical site spins, and preserving their angular momentum nature, the mapping in the bosonic picture of deviations from the ground state is derived. Thereby, the dynamics of the low-energy excitations is reduced to the eigenproblem of the corresponding infinite-dimensional dynamical matrix, which, owing to symmetry again, is easy to solve by the modified group projectors technique. However, since in general case the symmetry group can be lowered, the algorithm for solving the dynamical matrix eigenproblem, which effectively uses the whole group is proposed. For monoperiodic systems, described by one of the 13 families of the line groups, the transformational properties of interaction tensors are analysed in detail, while the notions of isotropy and homogenity are accommodated to the quasi-one-dimensional geometry. The Hamiltonian prototype, which besides the XXZ Heisenberg term has also the Dzyaloshinskii-Moria vector directed along the system axis, is singled out. In addition to the tensors, spin representations and arrangements of the first (the most important) family line groups are classified thoroughly; the arrangements of the rest of the families are to be obtained from these by the algorithm proposed in the work. Finally, the specified theoretical concepts are applied to the recently synthesized ^{13}C nanotubes, whose nuclear spins are coupled by the long-ranged Ruderman-Kittel-Kasuya-Yosida interaction via itinerant electrons. Besides the obtained diversity of the gate-voltage controlabille helimagnetic phases reveals a universal behaviour of all the nanotubes, it makes them to be the candidates for spintronic devices, too.

KEYWORDS: Symmetry, quasi-classical magnetism, spin waves, spin groups, helimagnetism, carbon nanotubes
SCIENTIFIC FIELD: Physics
SCIENTIFIC DISCIPLINE: Quantum and mathematical physics (Condensed matter physics)
UDC NUMBER: 538.9

Contents

Introduction

Magnetism, being an ancient as well as a contemporary field of human interest, may be described, in short, as a diversity of phenomena caused by interactions of magnetic moments carriers. This, profoundly many-body problem, is in the core of many of fascinating properties of condensed matter [1]: the variety of possible new phases, critical phenomena, symmetries of the order parameter, the phenomenon of the magnetization plateaux [2], etc. On the other hand, besides the magnetic materials were crucial for technological breakthroughs [3], they are still in focus of the research community due to the potential applications in nanostorage devices, spintronics or quantum computing [1].

Inclusion of the spin degrees of freedom in the Schrödinger equation dates back to the works of Heisenberg and Dirac (1926): through the perturbation technique they arrived to today's well known pairwise spin Hamiltonian $J\hat{\boldsymbol{S}}_1\hat{\boldsymbol{S}}_2$. The coupling J originates from the electrostatic interaction of two electrons, and the (positive) negative J refers to (anti)ferromagnetic type of interaction. This means that spins, considered as classical vectors, tend to align (anti)parallel. Extension to an arbitrary lattice leads to the state space scaled exponentially by the number of sites (spins), and dynamics governed by the isotropic Dirac-Heisenberg Hamiltonian quickly abandons capability even of the conceivable computers. The chains of regularly arranged spins are textbook examples. Except utilizing the symmetry of a chain through the Bloch's theorem [4,5], there is no unified approach to the nature of ground states and elementary excitations. Thus, the classical picture of aligned spins is correct when the interaction is restricted to the adjacent spins of ferromagnetic type; however, it fails down for antiferromagnetic one due to large quantum fluctuations, which is justified by the Bethe ansatz [6–8]. If the antiferromagnetic interaction is not confined to the first neighbors only, it is not possible to arrange spins classically, i.e. magnetic moments are exposed to a kind of frustration. Magnetic frustration, arising from an interplay of a lattice geometry and competing interactions among spins is an attractive problem both within quantum and classical approach: it may result in exotic quantum phases and transitions, and/or in complex arrangements of magnetic moments such as spiral magnetic structures and skyrmions. Nevertheless, there are particular examples with found solutions, illustrating variety of ground states and excitations. E.g., for the Majumdar-Ghosh chain [9, 10], where the cou-

pling among the first neighbours is twice as large as the coupling among the second ones, the ground state is known, but the exact excitations are not; the Haldane-Shastry [11, 12] model is also exactly solvable and the ground state is spin-disorder with the non-interacted spinon as excitations [13]. There are indications that frustration or reduced dimensionality leads to spin liquid [14, 15], a highly correlated state that has no static order. One of the most intriguing example is the kagomé lattice [15, 16]. On the contrary, another typical illustration of frustration is the layer with spins arranged in the triangular lattice where antiferromagnetic interactions between the closest neighbours force them to be mutually anti-parallel. Classically, the resulting magnetic structure is infinitely degenerate, where the corner vectors of each triangle make the angles of 120 degrees. Numerical studies [17] confirm that in this case the system keeps the classical helical long-range order despite quantum fluctuations. However, the most of the lattices analyzed in literature are artificial, and it is expectable that for real systems, with more complex geometrical structures, the problem is even more complicated.

The influence of the geometry of a system on its magnetic properties is also visible through the perturbative inclusion of the spin-orbit interaction. This results in anisotropy (symmetric or antisymmetric) of the bilinear spin-spin form, i.e. the effective spin dynamics is not governed by a scalar as in the DH case, but rather by a tensor [18–20]. Dzyaloshinskii and Moria singled out the term $\boldsymbol{D} \cdot \hat{\boldsymbol{S}}_1 \times \hat{\boldsymbol{S}}_2$, allowed by the lattice symmetry, which favors canted spin arrangement. It turns out [19] that under some special symmetries of a crystal, particular components of the Dzyaloshinskii-Moria vector $\boldsymbol{D}$ vanish. Many of the recent studies point out that antisymmetric anisotropy is responsible for the multiferroicity [21–23].

Electrons are not only ingredients with magnetic moments in a crystal. The Ruderman-Kittel-Kasuya-Yosida interaction [24] is the key factor for magnetism in systems with localized magnetic moments embedded in metallic host materials, like magnetic impurities (nuclear spins) in Kondo systems [25–27]. It is governed by itinerant electrons whose wave functions, built in spin susceptibility tensor, comprise all mediated information (highly non-local) on the system. On the other hand, the long-range nature of the interaction implies that correlations of hundreds of thousands spin-spin interactions are to be handled to get the ground state of the effective Hamiltonian quadratic in spins. The problem is unsolvable within full quantum framework, and usually applied quasi-classical approach reduces it to the

variational optimization of energy functional over classical spin vectors.

The observation that magnetic structure is tightly bound to the symmetry of a lattice resulted in the Shubnikov's theory of black-and-white magnetic groups [28–30]. It assumes that spins are the axial (pseudo) vectors subdued to geometrical transformations and time reversal. Later on it is realized that this was incomplete description of the symmetry of magnetic materials. The lack is filled in by the concept of spin groups [31–33]. Spin space groups, and related methods [34] are widely used in decoding magnetic structures from neutron diffraction patterns [35]. They were also applied to magnetically ordered quasi-crystals [36, 37], while a similar approach was used in the analysis of quasi-two-dimensional systems [38]. Importantly, the spin groups generate spin arrangements which are apparently preferred candidates [38, 39] for the quasi-classical ground state. Moreover, the conspicuous symmetry of such states tremendously reduces the number of variational parameters, enabling optimizations even for the systems with long ranged interactions [39]. Regularity of a magnetic superstructure, constrained by the primary (geometrical) structure, is thus a starting point in the analysis of the symmetry allowed magnetic states, which would otherwise be overlooked.

Emerging intriguing physics [40] of quasi-one-dimensional helimagnetism, which appears in subsystems of some crystals (e.g. spin chains and several-leg spin ladders [41–43]), or in single crystal molecular chains [44] and nanowires [45], with the pronounced symmetry of the ordering, motivate exploring the allowed magnetic interactions and structures for all possible Q1D geometries. This refers to the systems periodic (translationally or helically) along one direction, whose symmetries are well studied, and classified within the 13 infinite families of the line groups [46] (briefly reviewed in Section 2.1.1). Indeed, the subject of this thesis is an implementation of the full symmetry of systems (generalizing the usually used Bloch's approach for the translational periodicity only) whose magnetic properties are modeled by the most general quadratic forms in spins. Despite a large amount of literature [13, 47–55] related to magnetism, the theses starts (Chapter 1) with an attempt to summarize systematically the origins of such Hamiltonians. Further on, establishing the rigorous theoretical framework (Chapter 2) for the lattices with arbitrary spins, the transition from the quantum to the quasi-classical model (Chapter 4) is elaborated, including several details of the mean-field approximation in the background. Such a methodologically new approach enables us an insight into the diverse possibilities of

the symmetry based analyses. Here comes the clarification how the magnetic interaction is, as far as the form of the corresponding tensor is considered, determined by the geometrical symmetry, which is thoroughly performed for Q1D systems (Chapter 3). In addition, the regular Q1D arrangements are studied (Chapter 5) utilizing the spin line groups which are classified through an original, spin representations based approach. This is incorporated in optimization procedure (Chapter 6) in order to obtain conditions for the symmetrical ground states. For such phases elementary excitations, also restricted by the symmetry, are accounted trough the linear theory of spin waves (Chapter 7). Finally, the power of these methodological innovations is justified (Chapter 8): all the previous results are successfully and efficiently (partly numerically) applied to the recently synthesized ^{13}C nanotubes.

To preserve the consistency and physical clarity of the main text, necessary group theoretical remainders, together with the mathematically nontrivial derivations (shaped in theorems with proofs) are postponed for the appendices. Here are also the lists of abbreviations, notations and conventions used, including a basic non-common terminology.

Chapter 1

Quadratic spin Hamiltonian

Bilinear spin-spin Hamiltonian is broad enough to describe the most of magnetic properties in crystals. It is an effective Hamiltonian obtained through perturbation techniques. The subject of this Chapter is an attempt to briefly review and describe in a systematic way various levels of approximations starting from basic ingredients. Thus, in the first Section, the many-electron Hamiltonian which takes into account the couplings of the electronic spins with the orbital degrees of freedom on a lattice is introduced and analysed; the most relevant terms are singled out and listed as commonly considered characteristic terms: hopping, exchange, SO etc. Those, significant in typical concrete physical situations are singled out, and within a perturbation technique (outlined in the second Section) are transformed to the well known models: DH, DM, Kondo, RKKY, etc, all being quadratic in spin operators.

1.1 Electronic Hamiltonian

Total quantum mechanical state space of a system of N electrons (with position operators $\hat{\boldsymbol{r}} = \{\hat{\boldsymbol{r}}_p \mid p = 1, \ldots, N\}$) and L sites (i.e. ions with position operators $\hat{\boldsymbol{R}} = \{\hat{\boldsymbol{R}}_P \mid P = 1, \ldots, L\}$) is $\mathcal{H}' \otimes \mathcal{H}$, where $\mathcal{H}'$ and $\mathcal{H}$ correspond to the ionic and the electronic part of the system, respectively. Hamiltonian is the sum of the kinetic energy operators ($\hat{T}$) of electrons and ions, the Coulomb interactions ($\hat{V}$) of electrons, of ions and between electrons and ions, and the electronic spin-orbit (SO) coupling ($\hat{H}^{\mathrm{SO}}$):

$$\hat{H}_{\mathrm{eI}} = \hat{T}_{\mathrm{e}} + \hat{T}_{\mathrm{I}} + \hat{V}_{\mathrm{ee}} + \hat{V}_{\mathrm{II}} + \hat{V}_{\mathrm{eI}} + \hat{H}^{\mathrm{SO}}. \tag{1.1}$$

The spin degrees of freedom of ions are neglected here.

The part of the total Hamiltonian relevant for the electronic system $\hat{H}_{\rm e} = \hat{H}_{\rm eI} - \hat{T}_{\rm I} - \hat{V}_{\rm II}$ commutes with ionic position operator, i.e. $[\hat{H}_{\rm e}, \hat{\boldsymbol{R}}] = 0$, and the total eigenstate $\mid \psi\rangle$ of the system may be chosen as $\mid \psi\rangle = \mid \boldsymbol{R}\rangle \otimes \mid \psi_{\rm e}; \boldsymbol{R}\rangle$. The partial scalar product of the both sides of $\hat{H}_{\rm e} \mid \psi\rangle = E \mid \psi\rangle$ with the state $\mid \boldsymbol{R}\rangle$ leads to $\hat{H}(\boldsymbol{R}) \mid \psi_{\rm e}; \boldsymbol{R}\rangle = E \mid \psi_{\rm e}; \boldsymbol{R}\rangle$, where $\hat{H}(\boldsymbol{R}) = \langle \boldsymbol{R}\mid \hat{H}_{\rm e} \mid \boldsymbol{R}\rangle$ is the electronic Hamiltonian in $\mathcal{H}(\boldsymbol{R}) = \mathcal{H}_{\rm o}(\boldsymbol{R}) \otimes \mathcal{H}_s$; actually, this is a family of the spaces parameterized by the positions of the ions. The single electron orbital part of the state space is $\mathcal{H}_{\rm o} = \mathcal{H}_{\rm o}(\boldsymbol{R}) = \oplus_{P=1}^{L} \mathcal{H}_{\rm o}(\boldsymbol{R}_P)$, of the dimension $|\mathcal{H}_{\rm o}| = \sum_{P=1}^{L} |\mathcal{H}_{\rm o}(\boldsymbol{R}_P)|$; here $\mathcal{H}_{\rm o}(\boldsymbol{R}_P)$ is a single site orbital state space, while the spin space is $\mathcal{H}_s$. A basis in $\mathcal{H}(\boldsymbol{R})$ is $\{|Pis\rangle \mid \; i = 1, \ldots, |\mathcal{H}_{\rm o}(\boldsymbol{R}_P)|; \; P = 1, \ldots, L; \; s = \{\uparrow, \downarrow\}\}$; namely, the index P counts the sites (ions), i counts the orbitals on the corresponding site and s is the projection of the electron spin on some quantization axis.

The terms $\langle \boldsymbol{R}\mid \hat{T}_{\rm e} \mid \boldsymbol{R}\rangle = \sum_{p=1}^{N} \hat{T}(\hat{\boldsymbol{r}}_p; \boldsymbol{R})$ and $\langle \boldsymbol{R}\mid \hat{V}_{\rm eI} \mid \boldsymbol{R}\rangle = \sum_{p=1}^{N} \sum_{P=1}^{L} \hat{V}(\hat{\boldsymbol{r}}_p, \boldsymbol{R}_P)$ are additive single electron operators where $\hat{t} = \hat{t}_p = \hat{T}(\hat{\boldsymbol{r}}_p; \boldsymbol{R}) + \sum_{P=1}^{L} \hat{V}(\hat{\boldsymbol{r}}_p, \boldsymbol{R}_P)$, while $\langle \boldsymbol{R} \mid \hat{V}_{\rm ee} \mid \boldsymbol{R}\rangle = \sum_{p_1,p_2=1}^{N} \hat{V}(\hat{\boldsymbol{r}}_{p_1}, \hat{\boldsymbol{r}}_{p_2}; \boldsymbol{R})$ with $\hat{v} = \hat{v}_{p_1p_2} = \hat{V}(\hat{\boldsymbol{r}}_{p_1}, \hat{\boldsymbol{r}}_{p_2}; \boldsymbol{R})$ is a two particle operator (both $\hat{t}$ and $\hat{v}$ act trivially in the spin factor space). Similarly, $\langle \boldsymbol{R}\mid \hat{H}^{\rm SO} \mid \boldsymbol{R}\rangle = \sum_{p=1}^{N} \hat{H}^{\rm SO}(\hat{\boldsymbol{r}}_p; \boldsymbol{R})$, where $\hat{h}^{\rm SO} = \hat{h}^{\rm SO}_p = \hat{H}^{\rm SO}(\hat{\boldsymbol{r}}_p; \boldsymbol{R}) \sim (\nabla \hat{V}_p(\boldsymbol{R}) \times \hat{\boldsymbol{p}}_p) \cdot \hat{\boldsymbol{S}}_p$ is a single-particle operator ($\hat{\boldsymbol{p}} = \hat{\boldsymbol{p}}_p$ and $\hat{\boldsymbol{S}} = \hat{\boldsymbol{S}}_p$ are momentum and spin angular momentum operators, respectively, while $\hat{V}(\boldsymbol{R}) = \hat{V}_p(\boldsymbol{R}) = \sum_P \hat{V}_p(\boldsymbol{R}_P)$ is an effective potential). With this notation the electronic Hamiltonian (for the fixed $\boldsymbol{R}$) is:

$$\hat{H} = \hat{H}(\boldsymbol{R}) = \sum_{p=1}^{N} (\hat{t}_p + \hat{h}^{\rm SO}_p) + \sum_{p_1,p_2=1}^{N} \hat{v}_{p_1p_2}. \tag{1.2}$$

Allowing the change of the number of electrons, the total state space is Fock space $\mathcal{F}_- = \oplus_N (\mathcal{H}_{\rm o} \otimes \mathcal{H}_s)^N_-$ (the subscript " $-$ " indicates an antisymmetric space) of the dimension $|\mathcal{F}_-| = \sum_{N=0}^{2|\mathcal{H}_{\rm o}|} \binom{2|\mathcal{H}_{\rm o}|}{N} = 4^{\sum_{P=1}^{L} |\mathcal{H}_{\rm o}(\boldsymbol{R}_P)|}$. For simplicity it will be assumed that each site has the same number of orbitals, $|\mathcal{H}_{\rm o}(\boldsymbol{R}_P)| = M$; accordingly, $|\mathcal{F}_-| = 4^{LM}$. Introducing creation $\hat{\hat{a}}_{Pis}$ and annihilation $\hat{a}_{Pis}$ operators, which obey the fermionic anti-commutation relations ($\hat{n}_{Pis} = \hat{a}^{\dagger}_{Pis} \hat{a}_{Pis}$ is the occupation number operator), in $\mathcal{F}_-$ can be defined the basis of the Slater determinants

$$\{|\boldsymbol{Pis}; N\rangle = |P_1 i_1 s_1 < \ldots < P_N i_N s_N\rangle = a^{\dagger}_{P_N i_N s_N} \cdots \hat{a}^{\dagger}_{P_1 i_1 s_1} \mid 0\rangle\},$$

with $N = 0, \ldots, 2LM$ ($P_k \in \{1, \ldots, L\}$, $i_k \in \{1, \ldots, M\}$ and $s_k \in \{\uparrow, \downarrow\}$ for all

k), where the vector order is implied [1]. Finally, in the representation of the second quantization the electronic Hamiltonian is:

$$\begin{aligned}\hat{H} &= \sum_{PP'ii's} \langle Pi|\,\hat{t}\,|P'i'\rangle \hat{a}^\dagger_{Pis}\hat{a}_{P'i's} + \sum_{PP'ii'ss'} \langle Pis|\,\hat{h}^{\mathrm{SO}}\,|P'i's'\rangle \hat{a}^\dagger_{Pis}\hat{a}_{Pi's'} + \\ &+ \frac{1}{2}\sum_{\substack{P_1P_1'i_1i_1's_1\\P_2P_2'i_2i_2's_2}} \langle P_1i_1P_2i_2|\,\hat{v}\,|P_1'i_1'P_2'i_2'\rangle \hat{a}^\dagger_{P_2i_2s_2}\hat{a}^\dagger_{P_1i_1s_1}\hat{a}_{P_1'i_1's_1}\hat{a}_{P_2'i_2's_2}. \end{aligned} \tag{1.3}$$

1.1.1 Components of the electronic Hamiltonian

The representation of the second quantization, with the operators singling out the basis states of the single-particle space, allows us to refine the ingredients in the Hamiltonian to the level of contributions of particular matrix elements. Grouping these components not only by the physical origin, but also according to their energy scale, a subtle classification emerges. It is the source of building of the models suited to concrete physical systems. The most common terms are here discussed in more details.

As for the orbital single-particle term $\hat{t}$, its matrix element $t^{ii'}_{PP'} = \langle Pi|\,\hat{t}\,|P'i'\rangle$ is the energy cost for the electron being in the orbital i' of the site P' to hope to the orbital i of the site P without the change of the spin. It must be expected that the following classification based on the involved pairs of orbitals reflects the hierarchy in magnitude:

1. single orbital Hamiltonian (where $t^{ii}_{PP} = \epsilon^i_P$)

$$\hat{H}_0 = \sum_{P,i,s} \epsilon^i_P \hat{n}_{Pis}, \tag{1.4a}$$

2. on-site (or inter-orbital) hopping

$$\hat{H}^{\text{on-site}}_t = \sum_P \sum_{i,i'(\neq i)} \sum_s t^{ii'}_{PP}\hat{a}^\dagger_{Pis}\hat{a}_{Pi's}, \tag{1.4b}$$

3. inter-site hopping

$$\hat{H}^{\text{inter-site}}_t = \sum_{P,P'(\neq P)} \sum_{i,i'} \sum_s t^{ii'}_{PP'}\hat{a}^\dagger_{Pis}\hat{a}_{P'i's}. \tag{1.4c}$$

[1] The ordered set of the vectors is $\{|\,P_1i_1s_1 < \ldots < P_Ni_Ns_N\rangle \mid P_k \leq P_{k+1}$; if $P_k = P_{k+1}$ then $i_k \leq i_{k+1}$, if also $i_k = i_{k+1}$ then $s_k < s_{k+1}\}$ (it is taken that $\uparrow<\downarrow$).

Analogously, the matrix element $v^{i_1 i_2 i'_1 i'_2}_{P_1 P_2 P'_1 P'_2} = \langle P_1 i_1 P_2 i_2 \mid \hat{v} \mid P'_1 i'_1 P'_2 i'_2 \rangle$ is the strength of the Coulomb interaction between electrons, satisfying $v^{i_1 i_2 i'_1 i'_2}_{P_1 P_2 P'_1 P'_2} = v^{i_2 i_1 i'_2 i'_1}_{P_2 P_1 P'_2 P'_1}$. The corresponding Hamiltonians are classified as on-site and inter-site. Among the first ones there are those which include[2]:

1. only one type of orbitals:

   (a) on-site (intra-orbital) repulsion

$$\hat{V}_U^{\text{on-site}} = \tfrac{1}{2} \sum_{P,i} \sum_{s,s'(\neq s)} v^{iiii}_{PPPP} \hat{n}_{Pis} \hat{n}_{Pis'}, \tag{1.4d}$$

2. two orbitals $i_1 \neq i_2$:

   (a) Hartree on-site term

$$\hat{V}_H^{\text{on-site}} = \tfrac{1}{2} \sum_{P} \sum_{i_1, i_2(\neq i_1)} \sum_{s_1, s_2} v^{i_1 i_2 i_1 i_2}_{PPPP} \hat{n}_{Pi_1 s_1} \hat{n}_{Pi_2 s_2}, \tag{1.4e}$$

   (b) Fock (direct exchange) on-site term

$$\hat{V}_F^{\text{on-site}} = \tfrac{1}{2} \sum_{P} \sum_{i_1, i_2(\neq i_1)} \sum_{s_1, s_2} v^{i_1 i_2 i_2 i_1}_{PPPP} \hat{a}^\dagger_{Pi_2 s_2} \hat{a}^\dagger_{Pi_1 s_1} \hat{a}_{Pi_2 s_1} \hat{a}_{Pi_1 s_2}, \tag{1.4f}$$

The inter-site terms may include two, three or four sites, and here the two site ones ($P_1 \neq P_2$) are listed:

1. Hartree

$$\hat{V}_H^{\text{inter-site}} = \tfrac{1}{2} \sum_{P_1, P_2(\neq P_1)} \sum_{i_1, i_2} \sum_{s_1, s_2} v^{i_1 i_2 i_1 i_2}_{P_1 P_2 P_1 P_2} \hat{n}_{P_2 i_2 s_2} \hat{n}_{P_1 i_1 s_1}, \tag{1.4g}$$

2. Fock (direct exchange)

$$\hat{V}_F^{\text{inter-site}} = \tfrac{1}{2} \sum_{P_1, P_2(\neq P_1)} \sum_{i_1, i_2} \sum_{s_1, s_2} v^{i_1 i_2 i_2 i_1}_{P_1 P_2 P_2 P_1} \hat{a}^\dagger_{P_2 i_2 s_2} \hat{a}^\dagger_{P_1 i_1 s_1} \hat{a}_{P_2 i_2 s_1} \hat{a}_{P_2 i_2 s_2}, \tag{1.4h}$$

The SO interaction in (1.3) is rewritten using the matrix elements $(\lambda \boldsymbol{L})^{ii'}_{PP'} \sim \langle Pi \,|\, (\nabla \hat{V} \times \hat{\boldsymbol{p}}) \,|\, P'i' \rangle$ and $\boldsymbol{S}_{ss'} = \langle s \,|\, \hat{\boldsymbol{S}} \,|\, s' \rangle$ (the both operators $\nabla \hat{V}(\boldsymbol{R}) \times \hat{\boldsymbol{p}}$ and $\hat{\boldsymbol{S}}$ have the angular momenta transformation properties) as an on-site term:

$$\hat{H}^{\text{SO}} = \sum_{P} \sum_{i, i'(\neq i)} \sum_{s, s'} (\lambda \boldsymbol{L})^{ii'}_{PP} \boldsymbol{S}_{ss'} \hat{a}^\dagger_{Pis} \hat{a}_{Pi's'}. \tag{1.4i}$$

[2]The matrix elements $v^{i_1 i_1 i_1 i_2}_{PPPP}$ and $v^{i_1 i_1 i_1 i_2}_{PPPP}$ are omitted in the given classification: there may be the matrix elements with three orbitals $i_1 \neq i_2 \neq i_3$, i.e. $v^{i_1 i_1 i_2 i_3}_{PPPP}$, $v^{i_1 i_2 i_1 i_3}_{PPPP}$ and $v^{i_1 i_2 i_3 i_1}_{PPPP}$, as well as four orbitals $v^{i_1 i_2 i'_1 i'_2}_{PPPP}$ with $i_1 \neq i_2 \neq i'_1 \neq i'_2$.

1.2 Modeling: effective Hamiltonians

A physical model is built up by properly chosen terms among (1.4) which are dominant in the considered physical situation. Then, the technique invoking certain perturbation theory, e.g. the standard or the Schrieffer-Wolff transformation [56], is applied. In this way many of the well known spin hamintonians are obtained. Actually, they are effective Hamiltonians, i.e. correction operators in some perturbation order, commonly expressed in the representation of the second quantization.

Namely, if $\hat{H} = \hat{H}^0 + \hat{H}'$, where the unperturbed Hamiltonian is given in its spectral form $\hat{H}^0 = \sum_n E_n \hat{P}_n$, and $\hat{H}'$ is a perturbation, then the effective Hamiltonian in the range of $\hat{P}_n$ is

$$\hat{H}_{\text{eff}} = \hat{P}_n \hat{H}' \sum_{k=0}^{\infty} (\sum_{m(\neq n)} \frac{\hat{P}_m \hat{H}'}{E_n - E_m})^k \hat{P}_n. \tag{1.5}$$

The first task is to find the operators of the type $\hat{P}_m \hat{H}' \hat{P}_{m'}$ where $m, m', \ldots$ labels excited states. Precisely, in different orders of the perturbation technique in (1.5) appear the operators $\hat{P}_n \hat{H}' \hat{P}_m \hat{H}' \hat{P}_{m'} \cdots \hat{P}_n$. On the other hand, the perturbation may be a sum $\hat{H}' = \hat{H}'_1 + \hat{H}'_2 + \cdots$, where $\hat{H}'_i$ is one of the terms from (1.4). Thus, the most general form of operators which are to be found is

$$\hat{P}_n \hat{H}'_j \hat{P}_m \hat{H}'_{j'} \hat{P}_{m'} \cdots \hat{P}_n = (\hat{P}_n \hat{H}'_j \hat{P}_m)(\hat{P}_m \hat{H}'_{j'} \hat{P}_{m'}) \cdots \hat{P}_n,$$

since projectors fulfil $\hat{P}_m = \hat{P}_m^2$.

In order to illustrate the algorithm for the determination of the operator $\hat{P}_m \hat{H}_j{}' \hat{P}_{m'}$, the case when the number of electrons is equal to the number of sites, $N = L$, is considered. Further, the half-filling is supposed in the sense that in the ground state the lowest energy orbital $i = 1$ on each site is occupied by a single electron. The projector onto the space of such states is $\hat{P}_0 = \sum_{s_1,\ldots,s_n} |11s_1, \ldots, N1s_N\rangle\langle 11s_1, \ldots, N1s_N| = \sum_{s_1,\ldots,s_n} \prod_{P=1}^{N} \hat{n}_{P1s_P}$. Consequently, the projector onto all excited states ($\hat{P}_m$, where $m > 0$ corresponds to a particular excited state) is $\hat{\mathbb{1}} - \hat{P}_0$.

Let us further take the perturbation $\hat{H}' = \hat{H}'_1 \sim \hat{a}^\dagger_{Pis} \hat{a}_{P'i's'}$ wich may capture the hoping or the SO term. In the ground state $|11s_1, \ldots, N1s_N\rangle$ only the electron with the spin s' which occupies $i' = 1$ orbital of the site P' may be annihilated; therefore $\hat{H}'_1 \hat{P}_0 = \hat{a}^\dagger_{Pis} \hat{a}_{P'1s'}$. There are several possibilities for the excited states.

- The electron is created on the same site $P = P'$ in the orbital $i > 1$ with the spin projection s. The projector onto all such states is denoted by $\hat{P}_1$.

- The electron with the spin s is created on the another site $P(\neq P')$, in the orbital $i = 1$. Since on the site P there is already an electron with the spin s_P, due to the Pauli exclusion principle s must be different from s_P. The range of $\hat{P}_2$ make the states with one empty site, one site with the double occupied ground state orbital and $N-2$ sites with the lowest orbitals being single occupied.

- The electron with the spin s is created on the site $P(\neq P')$, in the orbital $i > 1$. The projector $\hat{P}_3$ corresponds to the states with one empty site, one site with two electrons (the first electron is in the lowest orbital and the second is in an excited one) and $N-2$ sites with a single electron in the lowest orbital.

The effective Hamiltonian in the first perturbation order is $\hat{P}_0\hat{H}'_1\hat{P}_0 \sim \hat{a}^\dagger_{P1s}\hat{a}_{P1s'}$; similarly $\hat{P}_1\hat{H}'_1\hat{P}_0 = \hat{a}^\dagger_{P'is}\hat{a}_{P'1s'}$ where $i > 1$, $\hat{P}_2\hat{H}'_1\hat{P}_0 = \hat{a}^\dagger_{P1s}\hat{a}_{P'1s'}$, and with $i > 1$ also $\hat{P}_3\hat{H}'_1\hat{P}_0 = \hat{a}^\dagger_{Pis}\hat{a}_{P'1s'}$. Further, $\hat{H}'_2 \sim \hat{a}^\dagger_{P_2i_2s_2}\hat{a}^\dagger_{P_1i_1s_1}\hat{a}_{P'_1i'_1s'_1}\hat{a}_{P'_2i'_2s'_2}$ may be taken to capture the Coulomb interaction. In the similar manner it is easy to show that $\hat{P}_0\hat{H}'_2\hat{P}_1\hat{H}'_1\hat{P}_0 \sim 2\hat{a}^\dagger_{P'1s_2}\hat{a}^\dagger_{P1s_1}(\hat{a}_{P'_1is}\hat{a}_{P'1s'} - \hat{a}_{P'1s'}\hat{a}_{P'_1is})\hat{a}^\dagger_{P'is}\hat{a}_{P'1s'}$ where $i > 1$, etc.

Besides, in the case when two subsystems a and b with the non-interacting dynamics, described by $\hat{H}^0 = \hat{H}^a + \hat{H}^b$, has well separated low and high energy states, one may seek the influence of the small interaction part $\hat{H}' = c\hat{H}^{ab}$ on the low-energy regime. Then the effective Hamiltonian is to be obtained by the canonical Schrieffer-Wolff transformation [56]. The transformed Hamiltonian has the form $\tilde{\hat{H}} = \mathrm{e}^{\hat{A}}\hat{H}\mathrm{e}^{-\hat{A}} = [\hat{A}, [\hat{A}, [\ldots[\hat{A}, \hat{H}]]]\ldots]$, where $\hat{A}$ is the skew-hermitian operator $\hat{A}$ satisfying $[\hat{A}, \hat{H}^0] = -\hat{H}'$ (linear in c) which is to be found. In this way, the transformed Hamiltonian is $\tilde{\hat{H}} = \hat{H}^0 + \frac{1}{2}[\hat{A}, \hat{H}'] + \frac{1}{3}[\hat{A}, [\hat{A}, \hat{H}']] + \ldots$. Keeping the terms (usually, those up to some order in the small parameter c) that preserve the low-energy subspace with the projector $\hat{P}_n$, the effective Hamiltonian $\hat{H}_{\text{eff}} = \hat{P}_n\tilde{\hat{H}}\hat{P}_n$ is obtained.

Once the effective Hamiltonian for a particular problem is obtained it is convenient to express it in the terms of the second quantization form of spin operators $\hat{S}^\alpha_{Pi} = \sum_{s,s'}\frac{1}{2}\langle s|\,\sigma^\alpha\,|s'\rangle\hat{a}^\dagger_{Pis}\hat{a}_{Pis'}$ $(\alpha = 1, 2, 3)$. In this context the relation

$$\hat{a}^\dagger_{P1s}\hat{a}_{P1s'} = (1/2 + \hat{\boldsymbol{S}}_P\boldsymbol{\sigma})_{s's} \tag{1.6}$$

turns out to be very useful.

In the following, the hints for derivation of the frequently used effective Hamiltonians, quadratic in spin operators, are given.

1.2.1 Isotropic Dirac-Heisenberg Hamiltonian

The well known isotropic Heisenberg Hamiltonian is

$$\hat{H}^{\mathrm{XXX}} = \sum_{P,P'(\neq P)} J_{PP'} \hat{\boldsymbol{S}}_{P'} \hat{\boldsymbol{S}}_{P}, \tag{1.7}$$

and one way to derive it is based on the perturbative method starting from the Hubbard model. Actually, the state space is a single orbital per site; it is the same for all sites, which enables us to use the abbreviation $\{Ps\}$ for $\{P1s\}$. In the strong coupling limit, when the on-site Coulomb interaction dominates over the inter-site ones, the Hubbard model is obtained:

$$\hat{H} = \sum_{P,P'(\neq P)} \sum_{s} t_{P,P'} \hat{a}^{\dagger}_{Ps} \hat{a}_{P's} + U \sum_{P} \hat{n}_{P\uparrow} \hat{n}_{P\downarrow}; \tag{1.8}$$

here $U = v_{PPPP}$, $\epsilon_P = 0$, and the SO interaction is neglected.

Further, when $U \gg |t_{PP'}|$ (for all P and P'), the unperturbed Hamiltonian is $\hat{H}^0 = U\hat{M}$, where $\hat{M} \stackrel{\mathrm{def}}{=} \sum_P \hat{n}_{P\uparrow}\hat{n}_{P\downarrow}$, while $\hat{H}' = \sum_{P,P'} \sum_s t_{PP'} \hat{a}^{\dagger}_{Ps} \hat{a}_{P's}$ is the perturbation. The action of the operator $\hat{M}$ on the basis vector is

$$\hat{M} \,|\, \boldsymbol{Ps}; N\rangle = \sum_{j,k} \delta_{P_k,P_j} \delta_{s_k,\downarrow} \delta_{s_j,\uparrow} \,|\, \boldsymbol{Ps}; N\rangle. \tag{1.9}$$

This can be rewritten in the form $\hat{M} \mid \boldsymbol{Ps}; N; m\,\rangle = m \mid \boldsymbol{Ps}; N; m\,\rangle$, where $m = 0, 1, \ldots, L$ counts the number of the double occupied site obitals. This introduces another decomposition of the total state space $\mathcal{F}_- = \oplus_{m=0}^{L} \mathcal{F}_-^m$, where $\mathcal{F}_-^m = \mathrm{span}\{|\, \boldsymbol{Ps}; N; m\rangle\}$. For $N = L$, the subspace of the single occupied states (ground state space) is $\mathcal{F}_-^0$, while the first excited states (the states with a single double-occupied site orbital) form the eigensubspace $\mathcal{F}_-^1$ of $\hat{H}$ with the eigenvalue U.

The first order of the perturbation ((1.5), with $k = 0$) leads to the effective Hamiltonian $\hat{P}_0\hat{T}\hat{P}_0 = 0$. The second perturbation order ($k = 1$) gives:

$$\begin{aligned}
\sum_{m(\neq 0)} \tfrac{\hat{P}_0\hat{T}\hat{P}_m\hat{T}\hat{P}_0}{E_0 - E_m} = \quad & -\hat{P}_0\hat{T}\hat{P}_1\hat{T}\hat{P}_0/U = \\
& -\tfrac{1}{U} \sum_{P,P'(\neq P)} \sum_{s,s'} t_{PP'} t_{P'P} \hat{a}^{\dagger}_{P's'} \hat{a}_{Ps'} \hat{a}^{\dagger}_{Ps} \hat{a}_{P's} = \\
& -\tfrac{1}{U} \sum_{P,P'(\neq P)} \sum_{s,s'} t_{PP'} t_{P'P} \hat{a}^{\dagger}_{P's'} \hat{a}_{P's} (\delta_{ss'} - \hat{a}^{\dagger}_{Ps'} a_{Ps}).
\end{aligned}$$

Expressing this in terms of the spin operators using (1.6) one obtains

$$\hat{H}_{\text{eff}} = \sum_{P,P'(\neq P)} \frac{2t_{PP'}t_{P'P}}{U}(\hat{\boldsymbol{S}}_{P'}\hat{\boldsymbol{S}}_{P} - \tfrac{1}{4}).$$

Obviously, the isotropic Heisenberg Hamiltonian (1.7) with $J_{PP'} = \frac{2t_{PP'}t_{P'P}}{U}$ is obtained when the energy shift is neglected.

1.2.2 Dzyaloshinskii-Moria antisymmetric anisotropy

The Dzyaloshinskii-Moria [18, 19] Hamiltonian

$$\hat{H}^{\text{DM}} = \sum_{P,P'} \boldsymbol{D}_{PP'}(\hat{\boldsymbol{S}}_{P} \times \hat{\boldsymbol{S}}_{P'}) \tag{1.10}$$

is related to the SO interaction. Starting from the unperturbed Hamiltonian $\hat{H}^0 = \hat{H}_0 + \hat{V}_H^{\text{inter-site}}$, (1.10) may be obtained like:

1. superexchange, when the perturbation $\hat{H}' = \hat{H}_t^{\text{inter-site}} + \hat{H}^{\text{SO}}$ is taken in the third order (the second order in $\hat{H}_t^{\text{inter-site}}$ and the first in $\hat{H}^{\text{SO}}$), or

2. direct exchange, when the perturbation $\hat{H}' = \hat{V}_F^{\text{inter-site}} + \hat{H}^{\text{SO}}$ is taken in the second order (the first in both $\hat{V}_F^{\text{inter-site}}$ and $\hat{H}^{\text{SO}}$).

1.2.3 Symmetric anisotropy

The most general bilinear spin-spin interaction [19, 20],

$$\hat{H} = \sum_{P,P'} h_{PP'}\hat{\boldsymbol{S}}_{P}\hat{\boldsymbol{S}}_{P'}, \tag{1.11}$$

is determined by a rank two tensor $h_{PP'}$ consisted of the scalar $J_{PP'}$ from (1.7), the vector $\boldsymbol{D}_{PP'}$ from (1.10), and the additional symmetric tensor of anisotropy. Yildirim et al. [20] derived (1.11) using the eigenbasis of the Hamiltonian $\hat{H}_0 + \hat{H}^{\text{SO}}$. The relevant terms represented in that basis are $\tilde{\hat{H}}_0, \tilde{\hat{H}}^{\text{SO}}, \tilde{\hat{H}}_t^{\text{inter-site}}, \tilde{\hat{V}}_H^{\text{inter-site}}$, and $\tilde{\hat{V}}_F^{\text{inter-site}}$. The part $\tilde{\hat{U}}_H^{\text{inter-site}}$ of $\tilde{\hat{V}}_H^{\text{inter-site}}$ is also diagonal in that basis, and together with the single-particle terms $\tilde{\hat{H}}_0$ and $\tilde{\hat{H}}^{\text{SO}}$ it is used as the unperturbed Hamiltonian. The third order of the perturbation, i.e. the second in $\tilde{\hat{H}}_t^{\text{inter-site}}$ and the first in $\tilde{\hat{V}}_H^{\text{inter-site}} - \tilde{\hat{U}}_H^{\text{inter-site}} + \tilde{\hat{V}}_F^{\text{inter-site}}$, leads to the effective Hamiltonian (1.11).

1.2.4 Kondo model

One of the important aspects of magnetism in solids are the interactions of conduction electrons with a localized magnetic moment. To derive the simplest quadratic spin Hamiltonian (1.7), we consider the lattice with a single atomic orbital (say s-type) on $N-1$ sites and an additional site, impurity, with another kind of an orbital (e.g. d-type). It is supposed that there is the strong Coulomb repulsion $U = v_{QQQQ}$ only on the impurity site, and N electrons can freely hop from site to site on the rest of the lattice. Neglecting the SO interaction, the model reads

$$\hat{H} = \sum_{PP'(\neq Q),s} t_{PP'} \hat{a}^\dagger_{Ps} \hat{a}_{P's} + \sum_s \varepsilon_Q \hat{n}_{Qs} + U \hat{n}_{Q\uparrow} \hat{n}_{Q\downarrow} + \sum_{P(\neq Q),s} (t_{PQ} \hat{a}^\dagger_{Ps} \hat{a}_{Qs} + t_{QP} \hat{a}^\dagger_{Qs} \hat{a}_{Ps}). \tag{1.12}$$

Taking the new single-particle basis $\hat{a}^\dagger_{Ps} = \sum_k \langle ks \mid Ps \rangle \hat{a}^\dagger_{ks}$ in the subspace of the conduction electrons which diagonalizes the above Q-independent term, one obtains the Anderson Hamiltonian [56, 57]:

$$\hat{H}_{\text{Anderson}} = \sum_{k,s} \varepsilon_k \hat{n}_{ks} + \sum_s \varepsilon_Q \hat{n}_{Qs} + U \hat{n}_{Q\uparrow} \hat{n}_{Q\downarrow} + \sum_{k,s} (t_{kQ} \hat{a}^\dagger_{ks} \hat{a}_{Qs} + t_{Qk} \hat{a}^\dagger_{Qs} \hat{a}_{ks}), \tag{1.13}$$

where $\varepsilon_k = 2t_{kk}$. Obviously, the dynamics of the two subsystems is governed by the non-interacting part $\hat{H}^0 = \sum_{k,s} \varepsilon_k \hat{n}_{ks} + \sum_s \varepsilon_Q \hat{n}_{Qs} + U \hat{n}_{Q\uparrow} \hat{n}_{Q\downarrow}$ and the hybridization term $\hat{H}' = \sum_{k,s} (t_{kQ} \hat{a}^\dagger_{ks} \hat{a}_{Qs} + t_{Qk} \hat{a}^\dagger_{Qs} \hat{a}_{ks})$.

The basis that diagonalizes $\hat{H}^0$ includes the states where the impurity orbital is either unoccupied $|k_1 s_1 < \ldots < k_N s_N\rangle$, or occupied by a single electron of the spin s $|k_1 s_1 < \ldots < k_{N-1} s_{N-1}, Qs\rangle$, or double occupied $|k_1 s_1 < \ldots < k_{N-2} s_{N-2}, Qs, Q\overline{s}\rangle$ ($\overline{s} = -s$). The conduction electrons occupy the states near the Fermi energy $E_F = \sum_i^N \varepsilon_{k_i}$, thus $\varepsilon_k \approx E_F$ for every quantum number k. However, using the abbreviation $|n\rangle$ for any state, where $n = \{0, 1, 2\}$ is the occupation of the impurity orbital, the eigenproblem reads $\hat{H}^0 \mid 0\rangle = E_F \mid 0\rangle$, $\hat{H}^0 \mid 1\rangle = (E_F - \varepsilon_k + \varepsilon_Q) \mid 1\rangle$, and $\hat{H}^0 \mid 2\rangle = (E_F - \varepsilon_k - \varepsilon_{k'} + 2\varepsilon_Q + U) \mid 2\rangle$. Obviously, to have the localized magnetic moment, it is necessary that the energy of the single occupied impurity state is favorable in comparison with both unoccupied ($\varepsilon_Q < \varepsilon_k$) and double occupied states ($\varepsilon_{k'} < \varepsilon_Q + U$), i.e. $\varepsilon_Q < E_F < \varepsilon_Q + U$. Such low-energy dynamics of the conduction electrons with a localized magnetic moment is provided by $\hat{H}'$ subdued to the assumption $U \gg t_k$. Then, the Schrieffer-Wolff transformation, with

$$\hat{A} = \sum_{k,s} \frac{t_{kQ}}{\varepsilon_k - \varepsilon_Q - U} \hat{n}_{Q\overline{s}} \hat{a}^\dagger_{ks} \hat{a}_{Qs} + \frac{t_{kQ}}{\varepsilon_k - \varepsilon_Q} (1 - \hat{n}_{Q\overline{s}}) \hat{a}^\dagger_{ks} \hat{a}_{Qs} - \text{h.c.} \tag{1.14}$$

is utilized. After a tedious derivation, the commutator $\frac{1}{2}[\hat{A}, \hat{H}']$ becomes the sum of the following terms:

$$\tilde{\hat{H}}_1 = -\sum_{ks} t_{kQ} t_{Qk} [\frac{1}{\varepsilon_k - \varepsilon_Q} - (\frac{1}{\varepsilon_k - \varepsilon_Q} - \frac{1}{\varepsilon_k - \varepsilon_Q - U}) \hat{n}_{Q\bar{s}}] \hat{n}_{Qs}$$

,

$$\tilde{\hat{H}}_2 = \frac{1}{2} \sum_{kk's} t_{kQ} t_{Qk'} [\frac{1}{\varepsilon_k - \varepsilon_Q}] \hat{a}^\dagger_{ks} \hat{a}_{k's} + \text{h.c.}$$

$$\tilde{\hat{H}}_3 = \frac{1}{2} \sum_{kk'ss'} t_{kQ} t_{Qk'} [\frac{1}{\varepsilon_k - \varepsilon_Q} - \frac{1}{\varepsilon_k - \varepsilon_Q - U}] \hat{a}^\dagger_{Qs'} \hat{a}_{Qs} \hat{a}^\dagger_{ks} \hat{a}_{k's'} + \text{h.c.}$$

$$\tilde{\hat{H}}_4 = \frac{1}{2} \sum_{kk's} t_{kQ} t_{Qk'} [\frac{1}{\varepsilon_k - \varepsilon_Q} - \frac{1}{\varepsilon_k - \varepsilon_Q - U}] \hat{a}_{Qs} \hat{a}_{Q\bar{s}} \hat{a}^\dagger_{k\bar{s}} \hat{a}^\dagger_{k's} + \text{h.c.}$$

Denoting by $\hat{P}_1$ the projector onto the low-energy subspace (single occupied impurity states), the effective Hamiltonian is $\hat{H}_{\text{eff}} = \hat{P}_1(\hat{H}^0 + \sum_{i=1}^4 \tilde{\hat{H}}_i)\hat{P}_1$. However, one notes that the last term is not preserved in the low-energy subspace since it creates or annihilates two particles (with opposite spins) on the impurity, thus, $\hat{P}_1 \tilde{\hat{H}}_4 \hat{P}_1 = 0$. Similarly, due to $\hat{n}_{Q\bar{s}} \mid 1\rangle = 0$, one gets $\hat{P}_1 \hat{H}^0 \hat{P}_1 = E^0 \hat{\mathbb{1}}$, $\hat{P}_1 \tilde{\hat{H}}_1 \hat{P}_1 = -\sum_{ks} W^Q_{kk} \hat{n}_{Qs} = \Delta_Q \hat{\mathbb{1}}$, $\hat{P}_1 \tilde{\hat{H}}_2 \hat{P}_1 = \sum_{kk's} W^Q_{kk'} \hat{a}^\dagger_{ks} \hat{a}_{k's}$, where $W^Q_{kk'} = \frac{t_{kQ} t_{Qk'}}{2} [\frac{1}{\varepsilon_k - \varepsilon_Q} + \frac{1}{\varepsilon'_k - \varepsilon_Q}]$. Since the impurity orbital is half-filled, the relation (1.6) is used to rewrite the third term as $\tilde{\hat{H}}_3 = \hat{P}_1 \tilde{\hat{H}}_3 \hat{P}_1 = \frac{1}{2} \sum_{kk's} (\frac{1}{2} J^Q_{kk'} \hat{a}^\dagger_{ks} \hat{a}_{k's} + J^Q_{kk'} \hat{\boldsymbol{S}}_Q \sum_{ss'} \hat{a}^\dagger_{ks} \boldsymbol{\sigma}_{ss'} \hat{a}_{k's'}$, where $J^Q_{kk'} = t_{kQ} t_{Qk'} [\frac{1}{\varepsilon_k - \varepsilon_Q} - \frac{1}{\varepsilon_k - \varepsilon_Q - U} + \frac{1}{\varepsilon'_k - \varepsilon_Q} - \frac{1}{\varepsilon'_k - \varepsilon_Q - U}]$. Collecting all the obtained terms leads to

$$\hat{H}_{\text{eff}} = (E^0 + \Delta_Q)\hat{\mathbb{1}} + \sum_{kk's} (W^Q_{kk'} + \frac{1}{4} J^Q_{kk'}) \hat{a}^\dagger_{ks} \hat{a}_{k's} + \sum_{kk'} J^Q_{kk'} \hat{\boldsymbol{S}}_Q \sum_{ss'} \hat{a}^\dagger_{ks} \frac{\boldsymbol{\sigma}_{ss'}}{2} \hat{a}_{k's'}. \quad (1.15)$$

Again, one may transform $\{\hat{a}^\dagger_{ks}\}$ into the new single electron conduction basis $\{\hat{a}^\dagger_{qs}\}$ in order to diagonalize the Q-independent part; the effective Hamiltonian, known as Kondo (or s-d) model [56], now reads:

$$\hat{H}_{\text{Kondo}} = \sum_{qs} \varepsilon^Q_q \hat{n}_{qs} + \sum_{qq'} J^Q_{qq'} \hat{\boldsymbol{S}}_Q \sum_{ss'} \hat{a}^\dagger_{qs} \frac{\boldsymbol{\sigma}_{ss'}}{2} \hat{a}_{q's'}. \quad (1.16)$$

The term $\sum_{ss'} \hat{a}^\dagger_{qs} \frac{\boldsymbol{\sigma}_{ss'}}{2} \hat{a}_{q's'}$ is the spin density operator, and for $q \approx q' \approx q_F$ the interaction between the spin of the conduction electron and the impurity is of the Heisenberg form $\sum_q J^Q_q \hat{\boldsymbol{S}}_Q \hat{\boldsymbol{S}}_q$. Note that the same form has the dominant part of hyperfine interaction among the spin of a conduction electron and the nuclear spin [24].

1.2.5 Ruderman-Kittel-Kasuya-Yosida intearaction

For the case of multiple impurities, the Hamiltonian (1.16) is to be extended by the sum over the impurities Q

$$\hat{H} = \sum_{qs} \varepsilon_q \hat{n}_{qs} + \sum_{Qqq'} J^Q_{qq'} \hat{\boldsymbol{S}}_Q (\frac{1}{2} \sum_{ss'} \hat{a}^\dagger_{qs} \boldsymbol{\sigma}_{ss'} \hat{a}_{q's'}), \tag{1.17}$$

where $\varepsilon_q = \sum_Q \varepsilon^Q_q$. The Schrieffer-Wolff transformation with $\hat{H}^0$ and $\hat{H}'$ being the first and the second term of $\hat{H}$, gives the operator $\hat{A} = \sum_{Qqq'} \frac{J^Q_{qq'}}{\varepsilon_q - \varepsilon_{q'}} \hat{\boldsymbol{S}}_Q \sum_{ss'} \hat{a}^\dagger_{qs} \frac{\boldsymbol{\sigma}_{ss'}}{2} \hat{a}_{q's'}$. Evaluating the expression $\hat{P}_1(\frac{1}{2}[\hat{A}, \hat{H}'])\hat{P}_1$ (where $\hat{P}_1$ projects onto the single occupied impurities with no conduction electrons above the Fermi energy) results in the Ruderman-Kittel-Kasuya-Yosida interaction

$$\hat{H}^{\mathrm{RKKY}} = \frac{1}{2} \sum_{QQ'} \chi_{QQ'} \hat{\boldsymbol{S}}_Q \hat{\boldsymbol{S}}_{Q'}. \tag{1.18}$$

Here, the exchange interaction strength among the impurities is the susceptibility function $\chi_{QQ'} = \frac{1}{4} \sum_{qq'} J^Q_{qq'} J^{Q'}_{q'q} \frac{f_q - f_{q'}}{\varepsilon_q - \varepsilon_{q'}}$, where $f_q = f(\varepsilon_q)$ is the Fermi-Dirac distribution.

Chapter 2

Spin lattices

Crystal structures have regularly arranged atoms making various types of lattices. The regularity assumes that the arrangement of atoms remains unchanged under a set of Euclidean transformations (translations, rotations, and/or roto-reflections), which necessarily has the structure of group. If some property (spin, energy etc.) is a function (field) over the lattice then any of the transformations also affects this property in accordance with its physical characteristics sublimated as group-theoretical tensorial rules.

Thus, the first Section of this Chapter establishes the group-theoretical notions related to the geometrical structure of crystals. This is followed by a brief overview of the line groups comprising the symmetries of Q1D systems; the first family is singled out as the most important one. In the next Section, the relevant mathematical framework for study the spin lattices is given: the quantum mechanical state space, the quadratic spin Hamiltonian and the corresponding representation of the symmetry group. The spin-spin coupling is described by the interaction tensor field defined on a lattice. The pseudo-vector nature of the spin operator together with the invariance of the Hamiltonian determine its transformational properties.

2.1 G-lattice

$\boldsymbol{G}$-lattice (or lattice) is a set of atoms with positions $\boldsymbol{R} = \{\dots, \boldsymbol{r}_p^P, \dots\}$ invariant under a group[1] $\boldsymbol{G}$. The upper index P differs between atomic species, while p counts

[1]Here, geometric groups are considered only, including point, line, diperiodic or space groups. Their elements are the Euclidian transformations $g = (O|\boldsymbol{t})$ in the Koster-Seitz notation.

the atoms of the species P. An element g of $\boldsymbol{G}$ acts on the position vectors by

$$g\boldsymbol{R} = \{\dots, g\boldsymbol{r}_p^P, \dots\}, \tag{2.1}$$

permuting the atoms only within the same species. *Site symmetry group* (*stabilizer*) $\boldsymbol{F}^P$ gathers the group elements f^P which fix a *representative atom* $p = 0$ of the species P:

$$f^P \boldsymbol{r}_0^P = \boldsymbol{r}_0^P, \quad \forall f^P \in \boldsymbol{F}^P \tag{2.2}$$

In this way the group is partitioned into the cosets, $\boldsymbol{G} = \bigcup_p z_p^P \boldsymbol{F}^P$, where *transversal* $\boldsymbol{Z}^P = \{z_0^P, z_1^P, \dots\}$ is a set of the coset representatives. The group multiplication provides

$$g z_p^P = z_{gp}^P f^P(g, p), \quad \forall g \in \boldsymbol{G}. \tag{2.3}$$

The transversal generates the whole set of atoms of the species P as $\boldsymbol{r}_p^P = z_p^P \boldsymbol{r}_0^P$ (also, $\boldsymbol{r}_p^P = z_p^P f^P \boldsymbol{r}_0^P$ for any f^P); thus, the total number of the sites in a system is $N = \sum_P |\boldsymbol{Z}^P|$.

When the stabilizer consists of the identity element only, the orbit is called *generic*, and the transversal is the whole group. Clearly, the term species refers to the group *orbits*, i.e. the orbits are counted by the superscript P; within an orbit all the atoms are chemically the same, while the atoms from the distinct orbits are not necessarily chemically different. In other words, any $\boldsymbol{G}$-lattice consists of several orbits, and it is completely determined by a *symcell* being a set of the orbit representatives at $\boldsymbol{r}_0^P$, and the symmetry group $\boldsymbol{G}$.

Note that various analyses, including some of the symmetry based physical properties, may be performed orbit by orbit independently with subsequently combined results (usually in a straightforward manner). Then one effectively deals with single orbit systems, and the counter P may be omitted as superfluous; this convention is adopted throughout the text.

2.1.1 Quasi-one-dimensional lattices

Symmetries of Q1D compounds are described by the line groups [46]. Each of them is the product $\boldsymbol{L} = \boldsymbol{T}\boldsymbol{P}$ of a point group $\boldsymbol{P}$ preserving the system axis (the z-axis by convention) and an infinite *generalized translational group* $\boldsymbol{T}$, reflecting the structure of a regular Q1D system: a series of identical *monomers* (units with the internal symmetry $\boldsymbol{P}$) are arranged along the z-axis by $\boldsymbol{T}$. In detail, $\boldsymbol{P}$ is one of the *axial*

point group $\boldsymbol{C}_n$, $\boldsymbol{S}_{2n}$, $\boldsymbol{C}_{n\mathrm{h}}$, $\boldsymbol{D}_n$, $\boldsymbol{C}_{n\mathrm{v}}$, $\boldsymbol{D}_{n\mathrm{v}}$, $\boldsymbol{D}_{n\mathrm{h}}$, and $\boldsymbol{T}$ is either a *screw-axis* $\boldsymbol{T}_Q(f)$ or a *glide-plane* group $\boldsymbol{T}'(f)$. The generator of the screw-axis group is $(C_Q|f)$, i.e. the rotation for $2\pi/Q$ ($Q \geq 1$, real) around the z-axis, accompanied by the translation for f along the z-axis; the glide plane group is generated by $(\sigma_\mathrm{v}|f)$, which is the reflection in a vertical plane with the translation for f along the z-axis. Each line group $\boldsymbol{L} = \boldsymbol{L}^{(F)}$ ($F = 1, \ldots, 13$) belongs to one of the 13 line group families obtained by varying the factors $\boldsymbol{T}$ and $\boldsymbol{P}$.

Of a particular importance are the first family line groups $\boldsymbol{L}^{(1)} = \boldsymbol{T}_Q(f)\boldsymbol{C}_n$, gathering only roto-translations along the z-axis. In fact, they are subgroups of index 2 or 4 in the groups of higher families, as these extend $\boldsymbol{L}^{(1)}$ by one ($F = 2, \ldots, 8$) or two ($F = 9, \ldots, 13$) *parities* π_i. The parities are vertical and horizontal (σ_h) mirror planes, rotation for π around a horizontal x-axis (U) or roto-reflections ($\sigma_\mathrm{h}C_{2n}$). Accordingly, the general element of $\boldsymbol{L}^{(1)}$ is

$$\ell = \ell_{ts} = (C_Q|f)^t C_n^s, \quad t = 0, \pm 1, \ldots, \quad s = 0, \ldots, n-1; \tag{2.4}$$

the elements of the families $2-8$ are $\ell = \ell_{ts\alpha_1} = \ell_{ts}\pi_1^{\alpha_1}$ ($\alpha_1 = 0, 1$), being index two subgroups of the families $9-13$ with $\ell = \ell_{ts\alpha_1\alpha_2} = \ell_{ts}\pi_1^{\alpha_1}\pi_2^{\alpha_2}$ ($\alpha_1, \alpha_2 = 0, 1$). The line groups with their generators are given in the Table 2.1.

While for the groups with the glide-plane $\boldsymbol{T} = \boldsymbol{T}'(f)$ the translational period is $a = 2f$, helical systems, with $\boldsymbol{T} = \boldsymbol{T}_Q(f)$, have the translational period $a = fq/n$ only for a rational $Q = q/r$ (r and q are coprime integers and q is a multiple of n; in particular, for pure translational and glide-plane group $r = 1$, $q = n$); otherwise they are *incommensurate*, i.e. without the translational periodicity. Obviously, the *commensurate* groups have the pure translational group $\boldsymbol{T}(a)$ as a subgroup.

For all the line groups there are 75 different types of orbits [46], which are classified within 15 different conformation classes of Q1D geometries. They are sketched in Figure 2.1. In addition to the orbits of the first family described below, carbon nanotubes structure will be neatly analysed in Chapter 8.

Table 2.1: **Line groups [46].** For each family F different factorizations, roto-helical subgroup $\boldsymbol{L}^{(1)}$, generators and the isogonal point group $\boldsymbol{P}_{\rm I}$ are given in the first line. Bellow follow $N_F = |\boldsymbol{L}^{(F)}|/|\boldsymbol{L}^{(1)}|$, international symbol (of commensurate groups only), and the coset representatives $\ell_i^{(F)}$ for $i > 1$. $\boldsymbol{T}'_{\rm d}$ and $U_{\rm d}$ are glide plane and horizontal axis bisecting vertical mirror planes, while $S_{2n} = C_{2n}\sigma_h$. For families 1 and 5, the order q of the isogonal principle axis is given by $Q = q/r$ for commensurate groups, while $q = \infty$ otherwise.

F		Factorizations		$\boldsymbol{L}^{(1)}$	Generators	$\boldsymbol{P}_{\rm I}$
N_F	n even	International	n odd		$\ell_i^{(F)}$	
1		$\boldsymbol{T}_Q \otimes \boldsymbol{C}_n$		$\boldsymbol{T}_Q \otimes \boldsymbol{C}_n$	$(C_Q\|f), C_n$	$\boldsymbol{C}_q$
1		$\boldsymbol{L}q_p$				
2		$\boldsymbol{T} \wedge \boldsymbol{S}_{2n}$		$\boldsymbol{T} \otimes \boldsymbol{C}_n$	$(\mathbb{1}\|a), S_{2n}$	$\boldsymbol{S}_{2n}$
2	$\boldsymbol{L}\overline{2n}$		$\boldsymbol{L}\overline{n}$		S_{2n}	
3		$\boldsymbol{T} \wedge \boldsymbol{C}_{n\rm h}$		$\boldsymbol{T} \otimes \boldsymbol{C}_n$	$(\mathbb{1}\|a), C_n, \sigma_h$	$\boldsymbol{C}_{n\rm h}$
2	$\boldsymbol{L}n/m$		$\boldsymbol{L}\overline{2n}$		σ_h	
4		$\boldsymbol{T}^1_{2n}\boldsymbol{C}_{n\rm h} = \boldsymbol{T}^1_{2n}\boldsymbol{S}_{2n}$		$\boldsymbol{T}^1_{2n} \otimes \boldsymbol{C}_n$	$(C_{2n}\|a/2), C_n, \sigma_h$	$\boldsymbol{C}_{2n\rm h}$
2		$\boldsymbol{L}2n_n/m$			σ_h	
5		$\boldsymbol{T}_Q \wedge \boldsymbol{D}_n$		$\boldsymbol{T}_Q \otimes \boldsymbol{C}_n$	$(C_Q\|f), C_n, U$	$\boldsymbol{D}_q$
2	$\boldsymbol{L}q_p22$		$\boldsymbol{L}q_p2$		U	
6		$\boldsymbol{T} \otimes \boldsymbol{C}_{n\rm v} = \boldsymbol{C}_{n\rm v} \wedge \boldsymbol{T}'$		$\boldsymbol{T} \otimes \boldsymbol{C}_n$	$(\mathbb{1}\|a), C_n, \sigma_v$	$\boldsymbol{C}_{n\rm v}$
2	$\boldsymbol{L}nmm$		$\boldsymbol{L}nm$		σ_v	
7		$\boldsymbol{C}_n \wedge \boldsymbol{T}'$		$\boldsymbol{T} \otimes \boldsymbol{C}_n$	$(\sigma_v\|a/2), C_n$	$\boldsymbol{C}_{n\rm v}$
2	$\boldsymbol{L}ncc$		$\boldsymbol{L}nc$		$(\sigma_v\|a/2)$	
8		$\boldsymbol{C}_{n\rm v} \wedge \boldsymbol{T}^1_{2n} = \boldsymbol{C}_{n\rm v} \wedge \boldsymbol{T}'_{\rm d}$		$\boldsymbol{T}^1_{2n} \otimes \boldsymbol{C}_n$	$(C_{2n}\|a/2), C_n, \sigma_v$	$\boldsymbol{C}_{2n\rm v}$
2		$\boldsymbol{L}2n_nmc$			σ_v	
9		$\boldsymbol{T} \wedge \boldsymbol{D}_{n\rm d} = \boldsymbol{T}' \wedge \boldsymbol{D}_{n\rm d}$		$\boldsymbol{T} \otimes \boldsymbol{C}_n$	$(\mathbb{1}\|a), C_n, U_{\rm d}, \sigma_v$	$\boldsymbol{D}_{n\rm d}$
4	$\boldsymbol{L}\overline{2n}2m$		$\boldsymbol{L}\overline{n}m$		$\sigma_v, U_{\rm d}, S_{2n}$	
10		$\boldsymbol{T}'\boldsymbol{S}_{2n} = \boldsymbol{T}'_{\rm d}\boldsymbol{D}_n$		$\boldsymbol{T} \otimes \boldsymbol{C}_n$	$(\sigma_v\|a/2), S_{2n}$	$\boldsymbol{D}_{n\rm d}$
4	$\boldsymbol{L}\overline{2n}2c$		$\boldsymbol{L}\overline{n}c$		$(\sigma_v\|a/2), S_{2n}, (U_{\rm d}\|a/2)$	
11		$\boldsymbol{T} \wedge \boldsymbol{D}_{n\rm h} = \boldsymbol{T}'\boldsymbol{D}_{n\rm h}$		$\boldsymbol{T} \otimes \boldsymbol{C}_n$	$(\mathbb{1}\|a), C_n, U, \sigma_v$	$\boldsymbol{D}_{n\rm h}$
4	$\boldsymbol{L}n/mmm$		$\boldsymbol{L}\overline{2n}2m$		σ_v, U, σ_h	
12		$\boldsymbol{T}'\boldsymbol{C}_{n\rm h} = \boldsymbol{T}'\boldsymbol{D}_n$		$\boldsymbol{T} \otimes \boldsymbol{C}_n$	$(\sigma_v\|a/2), C_n, \sigma_h$	$\boldsymbol{D}_{n\rm h}$
4	$\boldsymbol{L}n/mcc$		$\boldsymbol{L}\overline{2n}2c$		$(\sigma_v\|a/2), U, (S_{2n}\|a/2)$	
13		$\boldsymbol{T}^1_{2n}\boldsymbol{D}_{n\rm h} = \boldsymbol{T}^1_{2n}\boldsymbol{D}_{n\rm d} = \boldsymbol{T}'_{\rm d}\boldsymbol{D}_{n\rm h} = \boldsymbol{T}'_{\rm d}\boldsymbol{D}_{n\rm d}$		$\boldsymbol{T}^1_{2n} \otimes \boldsymbol{C}_n$	$(C_{2n}\|a/2), C_n, U, \sigma_v$	$\boldsymbol{D}_{2n\rm h}$
4		$\boldsymbol{L}2n_n/mcm$			σ_v, U, σ_h	

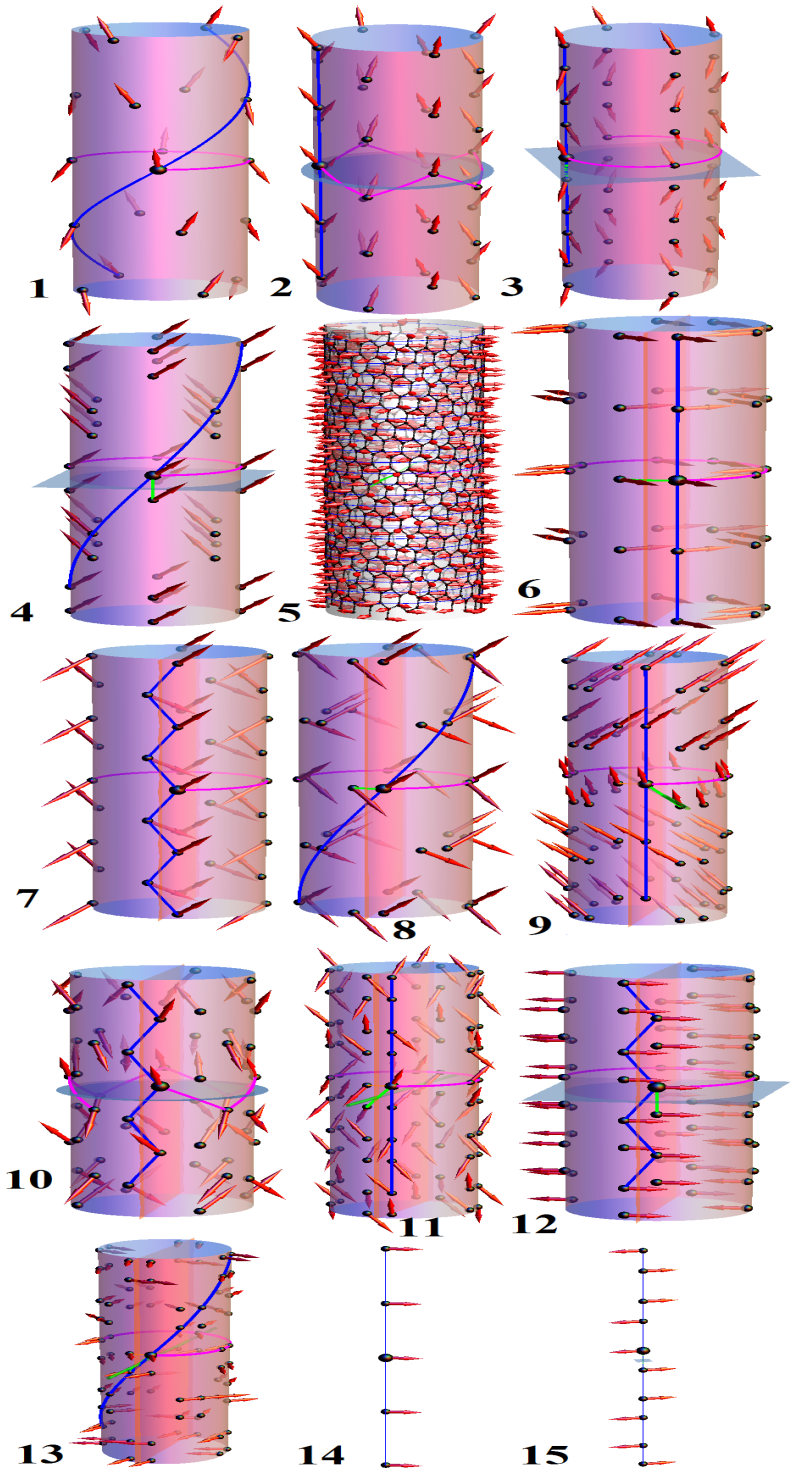

Figure 2.1: Conformation classes with examples of regular spin arrangements (see Chapter 5). Connected (in different colors) are the atoms generated from $\boldsymbol{r}_0$ (a bit larger) by the group generators; mirror planes and horizontal axis are additionally depicted.

Orbits of the first family

For these groups the generic orbit is obtained for the representative atom out of the z-axis, $\boldsymbol{r}_0 = (\rho > 0, \varphi_0, z_0)$ (cylindrical coordinates): then the other atoms are at

$$\boldsymbol{r}_{ts} = \ell_{ts}\boldsymbol{r}_0 = (\rho, \varphi_0 + 2\pi(\frac{t}{Q} + \frac{s}{n}), z_0 + ft), \tag{2.5}$$

with no ℓ_{ts} fixing $\boldsymbol{r}_0$. On the other hand, when $\boldsymbol{r}_0 = 0$, Equation (2.5) shows that $\boldsymbol{C}_n$ fixes it; thus another orbit of $\boldsymbol{L}^{(1)}$ is a linear chain along the z-axis with the period f and the transversal $\boldsymbol{T}(f)$.

2.2 Quantum spin lattice

Quantum $\boldsymbol{G}$-spin lattice of the spins $S^P = 0, \frac{1}{2}, 1, \ldots$ is obtained associating to the p-th site of the P-th orbit (for all p and P) the spin space $\mathcal{S}_p^P = \mathcal{S}^P$ of the dimension $2S^P + 1$. Quantum mechanical dynamical model on a $\boldsymbol{G}$-spin lattice is built by the standard construction of the total space $\mathcal{S}^{\mathrm{Tot}} = \otimes_{Pp}\mathcal{S}_p^P$ and Hamiltonian

$$\hat{H} = \frac{1}{2}\sum_{PQpq} \hat{\boldsymbol{S}}_p^P h_{Qq}^{Pp} \hat{\boldsymbol{S}}_q^Q, \quad \hat{\boldsymbol{S}}_p^P = \begin{pmatrix} \hat{S}_p^{P1} \\ \hat{S}_p^{P2} \\ \hat{S}_p^{P3} \end{pmatrix}. \tag{2.6}$$

Here, $h_{Qq}^{Pp} = h(\boldsymbol{r}_p^P, \boldsymbol{r}_q^Q)$ is an interaction tensor field, a three-dimensional matrix of coupling coefficients, while $\hat{\boldsymbol{S}}_p^P = \ldots \mathbb{1} \otimes \hat{\boldsymbol{S}} \otimes \mathbb{1} \ldots$ is a spin vector operator acting nontrivially in the corresponding factor space $\mathcal{S}_p^P$. Both the matrix and the tensor multiplications are assumed in the expression (2.6): the components $\hat{S}_p^{P\alpha} = \bar{\boldsymbol{x}}^\alpha \hat{\boldsymbol{S}}_p^P = \ldots \mathbb{1} \otimes \bar{\boldsymbol{x}}^\alpha \hat{\boldsymbol{S}} \otimes \mathbb{1} \ldots$ stem from the site spin operator projections $\hat{S}^\alpha = \bar{\boldsymbol{x}}^\alpha \hat{\boldsymbol{S}}$ on the axes of a global right-handed frame $\{\boldsymbol{x}^1, \boldsymbol{x}^2, \boldsymbol{x}^3\}$. They obey the well known commutation relations

$$[\hat{S}^\alpha, \hat{S}^\beta] = \mathrm{i}\varepsilon^{\alpha\beta\gamma}\hat{S}^\gamma, \ \alpha, \beta, \gamma = 1, 2, 3. \tag{2.7}$$

Their equations of motions in the Heisenberg picture are:

$$\mathrm{i}\frac{d\hat{S}^\alpha}{dt} = [\hat{S}^\alpha, \hat{H}], \quad \alpha = 1, 2, 3. \tag{2.8}$$

The commutator (2.7) defines the adjoint representation $\mathrm{ad}(\hat{S}^\alpha)\hat{S}^\beta = [\hat{S}^\alpha, \hat{S}^\beta]$ of su(2) algebra, and its matrices in the basis $\{\hat{S}^\alpha | \alpha = 1, 2, 3\}$ are well known.

The cross product is also the commutator (Lie multiplication) in $\mathbb{R}^3$, and using the definition of the right-handed frame:

$$\mathrm{ad}(\boldsymbol{x}^\alpha)\boldsymbol{x}^\beta = \boldsymbol{x}^\alpha \times \boldsymbol{x}^\beta = \varepsilon^{\alpha\beta\gamma}\boldsymbol{x}^\gamma,\ \alpha,\beta,\gamma = 1,2,3, \tag{2.9}$$

the adjoint representation in the basis $\{\boldsymbol{x}^\alpha \mid \alpha = 1,2,3\}$ is obtained:

$$\mathrm{ad}(\boldsymbol{x}^1) = \begin{pmatrix} 0 & 0 & 0 \\ 0 & 0 & -1 \\ 0 & 1 & 0 \end{pmatrix}, \quad \mathrm{ad}(\boldsymbol{x}^2) = \begin{pmatrix} 0 & 0 & 1 \\ 0 & 0 & 0 \\ -1 & 0 & 0 \end{pmatrix}, \quad \mathrm{ad}(\boldsymbol{x}^3) = \begin{pmatrix} 0 & -1 & 0 \\ 1 & 0 & 0 \\ 0 & 0 & 0 \end{pmatrix}. \tag{2.10}$$

Comparing (2.7) and (2.10) one gets the relations $\mathrm{ad}(\hat{S}^\alpha) = \mathrm{i}\,\mathrm{ad}(\boldsymbol{x}^\alpha)$, with the imaginary unit reflecting the principle of quantisation.

Accordingly, the Cartan-Weyl basis is $\{\hat{S}^\pm = \frac{1}{\sqrt{2}}(\hat{S}^1 \pm \mathrm{i}\hat{S}^2), \hat{S}^3\}$ (for each site space $\mathcal{S}_p^P$), with the standard commutation relations:

$$[\hat{S}^+, \hat{S}^-] = \hat{S}^3, \quad [\hat{S}^3, \hat{S}^\pm] = \pm\hat{S}^\pm. \tag{2.11}$$

Operators $\hat{\boldsymbol{S}}^2$ and $\hat{S}^3$ define the standard basis $\{|\, m_p^P\rangle \mid m_p^P = S^P, \ldots, -S^P\}$ in $\mathcal{S}_p^P$, such that:

$$\begin{aligned} \hat{\boldsymbol{S}}^2\,|\, m_p^P\rangle &= S^P(S^P+1)\,|\, m_p^P\rangle \\ \hat{S}^3\,|\, m_p^P\rangle &= m_p^P\,|\, m_p^P\rangle \\ \hat{S}^\pm\,|\, m_p^P\rangle &= S^\pm_{m_p^P\pm1}\,|\, m_p^P \pm 1\rangle, \quad S^\pm_{m_p^P\pm1} = \frac{1}{\sqrt{2}}\sqrt{(S^P \mp m_p^P)(S^P \pm m_p^P + 1)}. \end{aligned} \tag{2.12}$$

Since the Hamiltonian is a hermitian operator, the interaction tensors are interrelated:

$$\bar{h}^{Pp}_{Qq} = h^{Qq}_{Pp}. \tag{2.13}$$

Usually, the coupling coefficients in the global Cartesian frame are real valued fields. Taking the CWB instead of the Cartesian components of the site spin vector operators, the blocks h^{Pp}_{Qq} are changed into the $\chi^{Pp}_{Qq} = X h^{Pp}_{Qq} \bar{X}$, where $X = \left(\begin{smallmatrix} \mathrm{x} & 0 \\ 0 & 1 \end{smallmatrix}\right)$ with

$$\mathrm{x} = \frac{1}{\sqrt{2}} \begin{pmatrix} 1 & \mathrm{i} \\ 1 & -\mathrm{i} \end{pmatrix}. \tag{2.14}$$

2.2.1 Symmetry

Under the group action, the components $\hat{S}^\alpha$ of the spin vector operator $\hat{\boldsymbol{S}}$ are transformed as

$$\bar{u}^P(\tilde{\boldsymbol{G}})\hat{S}^\alpha u^P(\tilde{\boldsymbol{G}}) = \sum_\beta a^\alpha_\beta(\boldsymbol{G})\hat{S}^\beta, \quad \alpha,\beta = 1,2,3. \tag{2.15}$$

Here, $u^P(\tilde{\boldsymbol{G}}) = u^P(T_3{\wedge}\mathrm{SU}(2)) \downarrow \tilde{\boldsymbol{G}}$ is a representation of $\tilde{\boldsymbol{G}}$ in $\mathcal{S}^P$ where $\tilde{\boldsymbol{G}}$ is the double (covering) group [30, 47] of $\boldsymbol{G}$. It is a subgroup of the universal covering $T_3{\wedge}\mathrm{SU}(2)$ of the Euclidean group. While to each element $\tilde{g}$ in $\tilde{\boldsymbol{G}}$ corresponds a unique element in $\boldsymbol{G}$ denoted by g, to each element g correspond two elements of $\tilde{\boldsymbol{G}}$. Since in $\tilde{\boldsymbol{G}}$ the translations are represented trivially, $u^P(\tilde{\boldsymbol{G}})$ is effectively a subduced representation of SU(2). If $u^P = u^{(S^P)}$ is an irreducible representation of SU(2) (for the maximal weight S^P) subduced on $\tilde{\boldsymbol{G}}$, then $a(\boldsymbol{G})$ is the (three-dimensional) axial representation of $\boldsymbol{G}$, giving the standard characterization of the spin components. Note that for integer S^P the representation $u^P(\tilde{\boldsymbol{G}})$ is also a representation of $\boldsymbol{G}$, and double group may not be considered.

The group action $U(\tilde{\boldsymbol{G}})$ in the total spin space is automatically derived in non-correlated basis $|\ldots, m_p^P, \ldots\rangle = \ldots \otimes |m_p^P\rangle \otimes \ldots$ (here $|m_p^P\rangle$ denotes single-particle basis vector in $\mathcal{S}_p^P$):

$$U(\tilde{g})\ |\ldots, m_p^P, \ldots\rangle \stackrel{\mathrm{def}}{=} |\ldots, u^P(\tilde{g}) m^P_{\bar{g}p}, \ldots\rangle. \tag{2.16}$$

It is a representation of $\tilde{\boldsymbol{G}}$ (as shown by Theorem B.3.1), interchanging (permuting) site spins only within the orbits of the geometrical group action.

Spin lattice with a symmetry group $\boldsymbol{G}$ means that Hamiltonian (2.6) commutes with $U(\tilde{\boldsymbol{G}})$, i.e. $[\hat{H}, U(\tilde{\boldsymbol{G}})] = 0$, implying the transformation rule for the interaction tensor field (Theorem B.3.2):

$$h^{Pp}_{Qq} = a(g) h^{P,\bar{g}p}_{Q,\bar{g}q} a(\bar{g}). \tag{2.17a}$$

This becomes

$$h^{Pp}_{Qq} = a(z_q^Q) h^{P,\bar{z}_q^Q p}_{Q0} a(\bar{z}_q^Q), \tag{2.17b}$$

for $g = z_q^Q$, while for $g = f^Q$ and $q = e$

$$h^{Pp}_{Q0} = a(f^Q) h^{P,\bar{f}^Q p}_{Q0} a(\bar{f}^Q). \tag{2.17c}$$

The above symmetry constraints determine the forms of tensors, which is elaborated in Chapter 3.

2.2.2 Changing a frame

If the *global* frame $\{\boldsymbol{x}_p^{P\alpha} = \boldsymbol{x}^\alpha \mid \alpha = 1, 2, 3\}$ (the same for each site) is changed to a new (site dependent) one $\{\boldsymbol{t}_p^{P\alpha} \mid P, p, \alpha\}$, which is right-handed,

$$\boldsymbol{t}_p^{P\alpha} \times \boldsymbol{t}_p^{P\beta} = \varepsilon^{\alpha\beta\gamma} \boldsymbol{t}_p^{P\gamma},\ \alpha, \beta, \gamma = 1, 2, 3 \tag{2.18}$$

then the corresponding components of the spin vector operator $\hat{\boldsymbol{S}}$ are projections onto the new frame axes $\hat{S}^{t_p^P\alpha} = \bar{\boldsymbol{t}}_p^{P\alpha}\hat{\boldsymbol{S}}$. The columns of the site frame vectors are columns of the transition matrices, $t_p^P = [\boldsymbol{t}_p^{P1}, \boldsymbol{t}_p^{P2}, \boldsymbol{t}_p^{P3}]$ ($\boldsymbol{t}_p^{P\alpha} = \sum_\beta \bar{t}_{p\beta}^{P\alpha}\boldsymbol{x}^\beta$). Therefore, in order to preserve the spin commutations relations analogous to (2.7), t_p^P must be from $\mathrm{SO}(3,\mathbb{R})$, which is ensured by the right-handedness of the site frames.

With these triples of the site spin operators the Hamiltonian (2.6) reads (as before, the spin operators in the whole space are $\tilde{\hat{S}}_p^{P\alpha} = \ldots \mathbb{1} \otimes \hat{S}^{t_p^{P\alpha}} \otimes \mathbb{1} \ldots$):

$$\hat{H} = \frac{1}{2}\sum_{PQpq\alpha\beta} \tilde{\hat{S}}_p^{P\alpha}\tilde{h}_{Qq\beta}^{Pp\alpha}\tilde{\hat{S}}_q^{Qt\beta}, \quad \tilde{h}_{Qq\beta}^{Pp\alpha} = \bar{\boldsymbol{t}}_p^{P\alpha}h_{Qq}^{Pp}\boldsymbol{t}_q^{Q\beta}. \tag{2.19}$$

Taking CWB ($\alpha = \{+,-,3\}$) instead of the Cartesian one ($\alpha = \{1,2,3\}$), the operators $\hat{\boldsymbol{S}}^2$ and $\hat{S}^{t_p^{P3}}$ define the transformed basis $\{|m_p^P; t_p^P\rangle \mid m_p^P = -S^P, \ldots, S^P\}$ in the factor space $\mathcal{S}_p^P$, satisfying the relations (analogous to (2.12)):

$$\begin{aligned}
\hat{\boldsymbol{S}}^2\,|m_p^P; t_p^P\rangle &= S^P(S^P+1)\,|m_p^P; t_p^P\rangle \\
\hat{S}^{t_p^{P3}}\,|m_p^P; t_p^P\rangle &= m_p^P\,|m_p^P; t_p^P\rangle \\
\hat{S}^{t_p^{P\pm}}\,|m_p^P; t_p^P\rangle &= S^\pm_{m_p^P\pm1}\,|m_p^P \pm 1; t_p^P\rangle.
\end{aligned} \tag{2.20}$$

The adjoint representation for these components is $\mathrm{ad}(\hat{S}^{t_p^{P\alpha}}) = \mathrm{i}\,\mathrm{ad}(\boldsymbol{t}_p^{P\alpha})$. Note that the last matrices $t_p^P = [\boldsymbol{t}_p^{P+}, \boldsymbol{t}_p^{P-}, \boldsymbol{t}_p^{P3}]$, as compositions of $\mathcal{I}$ and rotations, are not from $\mathrm{SO}(3,\mathbb{R})$ any more. For the transformed frames the relation (2.15) becomes

$$\bar{u}^P(\tilde{g})\hat{S}^{t_p^{P\alpha}}u^P(\tilde{g}) = \sum_\beta [t_p^P a(g)\bar{t}_p^P]_\beta^\alpha \hat{S}^{t_p^{P\beta}}, \quad \alpha,\beta = 1,2,3. \tag{2.21}$$

Accordingly, the rule (2.17a) for the interaction tensors $\tilde{h}_{Qq}^{Pp} = t_p^P h_{Qq}^{Pp}\bar{t}_q^Q$ is

$$\tilde{h}_{Qq}^{Pp} = [t_p^P a(g)\bar{t}_{\bar{g}p}^P]\tilde{h}_{Q,\bar{g}q}^{P,\bar{g}p}[t_{\bar{g}q}^Q a(\bar{g})\bar{t}_q^Q]. \tag{2.22}$$

Chapter 3

Interaction tensor field

The specific symmetry of Q1D systems is directly manifested in the form of the magnetic interactions and presented general analysis singles out natural physically distinct components of the interaction tensor, establishing the starting point for the symmetry adapted modeling of dynamics and related analyses. For all these components specific symmetry dependent constraints are found, generalizing Moryia's rules for DM vector. The distinguished z-axis, along a quasi-one-dimensional system, reduces the isotropy to $\mathrm{SO}(2,\mathbb{R})$ group, splitting DH type interaction into independent parts, irreducible tensors. Moreover, the z-component of DM vector is a scalar, and must be taken into account in the most general form of the interaction, unless it is forbidden by other symmetries.

3.1 Standard tensor components

The relation (2.17a) in the form explicating the Cartesian components, allows us to analyse the action of the symmetry transformation g (from $\boldsymbol{G}$). The transformed tensor becomes $h^{Pgp\alpha}_{Qgq\beta} = \sum_{\alpha'\beta'} a^{\alpha}_{\alpha'}(g) a^{\beta'}_{\beta}(g) h^{Pp\alpha'}_{Qq\beta'}$, meaning that h (the indices are omitted) is transformed according to the tensor product $(a \otimes a)(\boldsymbol{G})$ of the axial-vector representation a of the group $\boldsymbol{G}$. The classification of the physical components of magnetic interactions is obtained considering their transformation properties with respect to the accompanying decomposition of $a \otimes a$. As the translational part of the geometrical transformations has no impact to the axial representation, the tensor form is effectively determined by the isogonal point group.

In fact, the well known physical components of the magnetic interactions

$$h = J \begin{pmatrix} 1 & 0 & 0 \\ 0 & 1 & 0 \\ 0 & 0 & 1 \end{pmatrix} + \begin{pmatrix} 0 & D^3 & -D^2 \\ -D^3 & 0 & D^1 \\ D^2 & -D^1 & 0 \end{pmatrix} + \begin{pmatrix} T^1+T^2 & A^3 & A^2 \\ A^3 & T^1-T^2 & A^1 \\ A^2 & A^1 & 2T^1 \end{pmatrix}, \tag{3.1}$$

for a three-dimensional spin lattice are obtained considering its transformation properties with respect to the rotations of the corresponding space group. The axial representation of the orthogonal part of a space group forms a subgroup of the full rotational group $\mathrm{SO}(3,\mathbb{R})$, and h is a rank two tensor of this group. The irreducible representations $d^{(l)}$ of $\mathrm{SO}(3,\mathbb{R})$ are determined by the value $l = 0, 1, 2, \ldots$, and their dimension is $2l+1$. It is obvious that the axial representation a corresponds to the representation with $l = 1$ (the polar and axial-vector representations are the same when only rotations are considered). Using the Clebsch-Gordan series, $d^{(l)} \otimes d^{(l')} = \sum_{l''=|l-l'|}^{l+l'} d^{(l'')}$, the reduction

$$\mathrm{SO}(3,\mathbb{R}): \quad d^{(1)} \otimes d^{(1)} = d^{(0)} \oplus d^{(1)} \oplus d^{(2)} \tag{3.2}$$

is obtained. This explicates that among h^α_β there is one component that is transformed as a scalar (according to $d^{(0)}$) giving rise to the isotropic Heisenberg (isotropic symmetric exchange) term, determined by an exchange coupling $J(\boldsymbol{r}_p^P, \boldsymbol{r}_q^Q)$); three of them are transformed according to $d^{(1)}$, that is the Dzyaloshinskii-Moriya term (antisymmetric anisotropy) characterized by an antisymmetric axial vector field $\boldsymbol{D}(\boldsymbol{r}_p^P, \boldsymbol{r}_q^Q)$); the remaining five components, with tensorial transformation properties (corresponding to $d^{(2)}$), make the symmetric anisotropic part of the Hamiltonian (gathering $T^\alpha(\boldsymbol{r}_p^P, \boldsymbol{r}_q^Q)$ with $\alpha = 1, 2$, and $A^\alpha(\boldsymbol{r}_p^P, \boldsymbol{r}_q^Q)$ with $\alpha = 1, 2, 3$). For a concrete spin lattice, its symmetry refines the properties of the obtained interaction components.

In the physics of low dimensional (Q1D and Q2D) crystals, the underlying type of symmetry modifies some of the above general conclusions, including the classification of the components. The role of the full rotational group for three-dimensional lattices takes the subgroup $\mathrm{SO}(2,\mathbb{R}) \cong \boldsymbol{C}_\infty$ of rotations $R_z(\varphi)$ for the angle φ around the z-axis. Its RIRs are classified by the z-component of the angular momentum, i.e. by the quantum number m: while for $m = 0$ all the rotations are represented by 1 (unit representation A_0), for $m = 1, 2, \ldots$ the corresponding representations are two-dimensional $E_m(\varphi) = \left(\begin{smallmatrix} \cos m\varphi & -\sin m\varphi \\ \sin m\varphi & \cos m\varphi \end{smallmatrix}\right)$. The decomposition of the axial representation $a(\mathrm{SO}(2,\mathbb{R})) = A_0(\mathrm{SO}(2,\mathbb{R})) \oplus E_1(\mathrm{SO}(2,\mathbb{R}))$ implies

$$\mathrm{SO}(2,\mathbb{R}): \quad (A_0 \oplus E_1) \otimes (A_0 \oplus E_1) = 3A_0 \oplus 2E_1 \oplus E_2. \tag{3.3}$$

Analogously to (3.2), this gives the following partition of the interaction tensor accommodated to the magnetism of low-dimensional systems:

$$\begin{aligned} h &= \begin{pmatrix} J^1 & 0 & 0 \\ 0 & J^1 & 0 \\ 0 & 0 & J^3 \end{pmatrix} + \begin{pmatrix} 0 & D^3 & 0 \\ -D^3 & 0 & 0 \\ 0 & 0 & 0 \end{pmatrix} + \\ &+ \begin{pmatrix} 0 & 0 & -D^2 \\ 0 & 0 & D^1 \\ D^2 & -D^1 & 0 \end{pmatrix} + \begin{pmatrix} 0 & 0 & A^2 \\ 0 & 0 & A^1 \\ A^2 & A^1 & 0 \end{pmatrix} + \begin{pmatrix} T^1 & T^2 & 0 \\ T^2 & -T^1 & 0 \\ 0 & 0 & 0 \end{pmatrix}. \end{aligned} \tag{3.4}$$

Its symmetric part is the Heisenberg XXZ term including two scalars, $J^1(\boldsymbol{r}_p^P, \boldsymbol{r}_q^Q)$ and $J^3(\boldsymbol{r}_p^P, \boldsymbol{r}_q^Q)$, while the antisymmetric one is consisted of the third scalar coupling, the z-component of DM vector $D^3(\boldsymbol{r}_p^P, \boldsymbol{r}_q^Q)$. Obviously, the isotropy is reduced to the xy-plane only.

The first two matrices of the second row in (3.4) describe the couplings which interrelates the xy-plane and the z-axis. Their components form two-dimensional vectors $\boldsymbol{d}(\boldsymbol{r}_p^P, \boldsymbol{r}_q^Q) = (D^1(\boldsymbol{r}_p^P, \boldsymbol{r}_q^Q), D^2(\boldsymbol{r}_p^P, \boldsymbol{r}_q^Q))$ (the rest of the antisymmetric DM term) and $\boldsymbol{a}(\boldsymbol{r}_p^P, \boldsymbol{r}_q^Q) = (A^1(\boldsymbol{r}_p^P, \boldsymbol{r}_q^Q), A^2(\boldsymbol{r}_p^P, \boldsymbol{r}_q^Q))$ (a part of the symmetric anisotropy); corresponding to the quantum number $m = 1$, their transformations are vectorial: $\boldsymbol{d}(R_z(\varphi)\boldsymbol{r}_p^P, R_z(\varphi)\boldsymbol{r}_q^Q) = E_1(\varphi)\boldsymbol{d}(\boldsymbol{r}_p^P, \boldsymbol{r}_q^Q)$, $\boldsymbol{a}(R_z(\varphi)\boldsymbol{r}_p^P, R_z(\varphi)\boldsymbol{r}_q^Q) = E_1(\varphi)\boldsymbol{a}(\boldsymbol{r}_p^P, \boldsymbol{r}_q^Q)$. They gather the xy-components of anisotropy, being in low-dimensional systems *a priori* decoupled from the other anisotropy components.

Finally, the last term is the remaining symmetric second rank tensor, described by the two-component pair $\boldsymbol{t}(\boldsymbol{r}_p^P, \boldsymbol{r}_q^Q) = (T^1(\boldsymbol{r}_p^P, \boldsymbol{r}_q^Q), T^2(\boldsymbol{r}_p^P, \boldsymbol{r}_q^Q))$. Its quantum number is $m = 2$, due to the transformation law $\boldsymbol{t}(R_z(\varphi)\boldsymbol{r}_p^P, R_z(\varphi)\boldsymbol{r}_q^Q) = E_2(\varphi)\boldsymbol{t}(\boldsymbol{r}_p^P, \boldsymbol{r}_q^Q)$ (not vector like) of this intrinsic, xy-plane, symmetric anisotropy.

For the system whose isogonal group has the principle axis of order q greater than 2 (for the line groups this means that at least one of n and Q is neither 1 nor 2), the presented tensor components are the same as for the group $\mathrm{SO}(2,\mathbb{R})$=$\boldsymbol{C}_\infty$. In the very simplified cases, even further reduction occurs: as for $q = 2$ (e.g. ribbons in the case of Q1D systems) there is no representation with $m = 2$, the last term splits into two scalars, while for $q = 1$ (various chains) all the components are scalars of the symmetry group.

For a concrete spin lattice, its symmetry refines the properties of the obtained interaction components. The additional symmetries for the line groups are parities (Section 2.1.1). There is a rotation U for π around a horizontal axis; here it is assumed that this is the x-axis (U). Mirror planes are either horizontal, σ_h, being in some groups combined with rotations into $\sigma_\mathrm{h}C_{2n}$, or vertical, σ_v (the xz-plane will

Table 3.1: Transformation rules of components $C(\boldsymbol{r}_{ij})$ (Equation (3.4)) of interaction tensors in Q1D systems. Polar- ($d^{\rm pv}$) and axial-vector (a) representations of orthogonal parts of the elements ℓ of the line groups are listed. The action of ℓ on its effective arguments $\boldsymbol{r}_{ij}$ is given first, omitting the non-changed one; then, for each allowed component of the interaction tensor its value $\ell C(\boldsymbol{r}_{ij})$ is expressed in the column corresponding to ℓ. Here, u is two-dimensional matrix diag$[1,-1]$.

ℓ	$C_q \quad (q>2)$	C_2	U	$\sigma_{\rm v}$	$\sigma_{\rm h}$
$d^{\rm pv}(\bar{\ell})$	$R_z(\frac{2\pi(q-1)}{q})$	$R_z(\pi)$	diag$[1,-1,-1]$	diag$[1,-1,1]$	diag$[1,1,-1]$
$a(\ell)$	$R_z(\frac{2\pi}{q})$	$R_z(\pi)$	diag$[1,-1,1]$	diag$[1,1,-1]$	diag$[-1,-1,1]$
$\boldsymbol{r}_{ij}$	$(\rho_i,\varphi_i,z_i,\rho_j,\varphi_j,z_j)$				
$\bar{\ell}\boldsymbol{r}_{ij}$	$\varphi_{i/j}+\frac{2\pi(q-1)}{q}$	$\varphi_{i/j}+\pi$	$-\varphi_{i/j},-z_{i/j}$	$-\varphi_{i/j}$	$-z_{i/j}$
$J^1(\boldsymbol{r}_{ij})$	$J^1(\bar{C}_q\boldsymbol{r}_{ij})$	$J^1(C_2\boldsymbol{r}_{ij})$	$J^1(U\boldsymbol{r}_{ij})$	$J^1(\sigma_{\rm v}\boldsymbol{r}_{ij})$	$J^1(\sigma_{\rm h}\boldsymbol{r}_{ij})$
$J^3(\boldsymbol{r}_{ij})$	$J^3(\bar{C}_q\boldsymbol{r}_{ij})$	$J^3(C_2\boldsymbol{r}_{ij})$	$J^3(U\boldsymbol{r}_{ij})$	$J^3(\sigma_{\rm v}\boldsymbol{r}_{ij})$	$J^3(\sigma_{\rm h}\boldsymbol{r}_{ij})$
$D^3(\boldsymbol{r}_{ij})$	$D^3(\bar{C}_q\boldsymbol{r}_{ij})$	$D^3(C_2\boldsymbol{r}_{ij})$	$-D^3(U\boldsymbol{r}_{ij})$	$-D^3(\sigma_{\rm v}\boldsymbol{r}_{ij})$	$D^3(\sigma_{\rm h}\boldsymbol{r}_{ij})$
$\boldsymbol{d}(\boldsymbol{r}_{ij})$	$E_1(\frac{2\pi}{q})\boldsymbol{d}(\bar{C}_q\boldsymbol{r}_{ij})$	$-\boldsymbol{d}(C_2\boldsymbol{r}_{ij})$	$u\boldsymbol{d}(U\boldsymbol{r}_{ij})$	$-u\boldsymbol{d}(\sigma_{\rm v}\boldsymbol{r}_{ij})$	$-\boldsymbol{d}(\sigma_{\rm h}\boldsymbol{r}_{ij})$
$\boldsymbol{a}(\boldsymbol{r}_{ij})$	$E_1(\frac{2\pi}{q})\boldsymbol{a}(\bar{C}_q\boldsymbol{r}_{ij})$	$-\boldsymbol{a}(C_2\boldsymbol{r}_{ij})$	$u\boldsymbol{a}(U\boldsymbol{r}_{ij})$	$-u\boldsymbol{a}(\sigma_{\rm v}\boldsymbol{r}_{ij})$	$-\boldsymbol{a}(\sigma_{\rm h}\boldsymbol{r}_{ij})$
$\boldsymbol{t}(\boldsymbol{r}_{ij})$	$E_2(\frac{2\pi}{q})\boldsymbol{t}(\bar{C}_q\boldsymbol{r}_{ij})$	$\boldsymbol{t}(C_2\boldsymbol{r}_{ij})$	$u\boldsymbol{t}(U\boldsymbol{r}_{ij})$	$u\boldsymbol{t}(\sigma_{\rm v}\boldsymbol{r}_{ij})$	$\boldsymbol{t}(\sigma_{\rm h}\boldsymbol{r}_{ij})$

be considered). Summarizing, it is sufficient to consider only U, $\sigma_{\rm h}$, $\sigma_{\rm v}$, besides the rotations around the z-axis.

To resume, the action of some group element $\ell=(O|\boldsymbol{f})$ of the line group $\boldsymbol{L}$ on the interaction tensor is $\ell h(\boldsymbol{r}_{pq}^{PQ}) \stackrel{\rm def}{=} a(\bar{\ell})h(\bar{\ell}\boldsymbol{r}_{pq}^{PQ})a(\ell)$, i.e. it is the similarity transformation by the axial representation of the orthogonal part O. Concerning the arguments $\boldsymbol{r}_{pq}^{PQ} \stackrel{\rm def}{=} \{\boldsymbol{r}_p^P,\boldsymbol{r}_q^Q\}$, the group element acts by its Koster-Seitz form, where the corresponding orthogonal part is the polar-vector transformation: $\bar{\ell}\boldsymbol{r}_{pq}^{PQ}=\{(d^{\rm pv}(\bar{O})|-\boldsymbol{f})\boldsymbol{r}_p^P,(d^{\rm pv}(\bar{O})|-\boldsymbol{f})\boldsymbol{r}_q^Q\}$. Obviously, the invariance (2.17a) reads $h(\boldsymbol{r}_{pq}^{PQ})=\ell h(\boldsymbol{r}_{pq}^{PQ})$. Q1D lattices are suitably described by the cylindrical coordinates $\boldsymbol{r}_p^P=(\rho_p^P,\varphi_p^P,z_p^P)$ of their atoms, and none of the line group elements changes the coordinate ρ. The transformation of the tensorial components (3.4) under the listed line group elements are in Table 3.1. The parities impose additional restrictions on the interaction tensor, which are manifested as special properties of these components. It is easy to derive that J^i $(i=1,3)$ and T^1 are even functions with respect to all the parities, while D^3 and T^2 are even with respect to $\sigma_{\rm h}$, and changes the sign under U and $\sigma_{\rm v}$. The vectors $\boldsymbol{d}$ and $\boldsymbol{a}$ are axial ones.

3.2 Generalized Moryia's rules

The dependence on coordinates is a characteristic of the interaction, but its invariance obtained in the form (2.17) by the action of a symmetry transformation on positions vectors, sublimates general rules of compatibility of the interaction tensor with the symmetry group. Still, there are two situations when some special position of the interacting pair of spins (i.e. of the bond between them) with regard to a particular symmetry, allows us to explicate these rules even for the most general interaction type.

First, when both sites are unchanged by some symmetry element, i.e. when ℓ is in the stabilizer of the both sites, Equation (2.17b) gives

$$\boldsymbol{r}^{P/Q}_{p/q} = \ell \boldsymbol{r}^{P/Q}_{p/q} : \; a(\bar{\ell}) h(\boldsymbol{r}^{P}_{p}, \boldsymbol{r}^{Q}_{q}) a(\ell) = h(\boldsymbol{r}^{P}_{p}, \boldsymbol{r}^{Q}_{q}). \tag{3.5}$$

The second case is related to the pair of sites of the same orbit, when they are connected by a symmetry element ℓ: $\boldsymbol{r}^{P}_{p'} = \ell \boldsymbol{r}^{P}_{p}$. Then (2.17b) combined with (2.13) yields

$$h(\boldsymbol{r}^{P}_{p}, \bar{\ell}\boldsymbol{r}^{P}_{p}) = a(\bar{\ell}) \bar{h}(\boldsymbol{r}^{P}_{p}, \ell \boldsymbol{r}^{P}_{p}) a(\ell). \tag{3.6}$$

This means that couplings between $\boldsymbol{r}^{P}_{p}$ and its oppositely arranged neighbours $\ell \boldsymbol{r}^{P}_{p}$ and $\bar{\ell}\boldsymbol{r}^{P}_{p}$ are mutually related. For the parities, when ℓ^2 is the identity element, sites $\boldsymbol{r}^{P}_{p'}$ and $\boldsymbol{r}^{P}_{p}$ are interchanged, and (3.6) is

$$\boldsymbol{r}^{P}_{p/p'} = \ell \boldsymbol{r}^{P}_{p'/p} : \; h(\boldsymbol{r}^{P}_{p}, \boldsymbol{r}^{P}_{p'}) = a(\bar{\ell}) \bar{h}(\boldsymbol{r}^{P}_{p}, \boldsymbol{r}^{P}_{p'}) a(\ell). \tag{3.7}$$

These equations are the rules constraining the components of interaction for such bonds, even annihilating some of them. For example, when $\ell = \sigma_{\mathrm{h}}$, the both situations may occur. If $\boldsymbol{r}^{P}_{p}$ and $\boldsymbol{r}^{P}_{p'}$ are in the xy-plane, they are fixed by σ_{h}, and (3.5) combined with the properties in Table 3.1 gives $\boldsymbol{a}(\boldsymbol{r}^{P}_{p}, \boldsymbol{r}^{P}_{p'}) = \boldsymbol{d}(\boldsymbol{r}^{P}_{p}, \boldsymbol{r}^{P}_{p'}) = 0$; also, if $\boldsymbol{r}^{P}_{p}$ and $\boldsymbol{r}^{P}_{p'}$ are symmetrically above and below the xy-plane, the bond is reversed, and (3.7) imposes $\boldsymbol{a}(\boldsymbol{r}^{P}_{p}, \boldsymbol{r}^{P}_{p'}) = D^{3}(\boldsymbol{r}^{P}_{p}, \boldsymbol{r}^{P}_{p'}) = 0$. The exhaustive set of these rules is presented in the Table 3.2. They generalize Moriya's rules [19] derived for the Dzyaloshinskii-Moriya interaction to all of the components of the interaction.

It is important to note that for the most general interaction the rules in Table 3.2 apparently refer only to the pairs of sites (i.e. the corresponding Hamiltonian submatrices) in special positions with respect to action of a symmetry ℓ. However, the tensorial properties of the components (listed in Table 3.1) extend this rules, giving

Table 3.2: Generalized Moryia's rules. For each symmetry ℓ in the first column, the second and the third column give vanishing components of the interaction between the sites in the special positions (defined in the first row) with respect to ℓ. It is assumed that $q > 2$ for C_q, and C_2 is singled out.

ℓ	$\boldsymbol{r}_{i/j} = \ell\boldsymbol{r}_{i/j}$	$\boldsymbol{r}_{i/j} = \ell\boldsymbol{r}_{j/i}$
C_q	$\boldsymbol{t}, \boldsymbol{a}, \boldsymbol{d}$	/
C_2	$\boldsymbol{a}, \boldsymbol{d}$	$\boldsymbol{a}, D^3$
U	T_1, A^2, D^2, D^3	T_1, A^2, D^1
σ_{h}	$\boldsymbol{a}, \boldsymbol{d}$	$\boldsymbol{a}, D^3$
σ_{v}	T_1, A^1, D^1, D^3	T_1, A^1, D^2
$\mathcal{I}$	/	$\boldsymbol{d}, D^3$

analogous restrictions for other pairs derived from the initial ones by any symmetry ℓ'; this manifests the fact that the new pair is in the analogous relation to the conjugated symmetry $\ell'\ell\bar{\ell}'$. Still, homogeneity or isotropy of a spin lattice, introduced in the next Section, may additionally extend the rules.

3.3 Homogeneity and isotropy of Q1D lattices

A general analysis of the isotropy and the homogeneity of Q1D systems is important since it leads to a reduced form of the matrices $h(\boldsymbol{r}_p^P, \boldsymbol{r}_q^Q)$ which are frequently the values (for the singled out arguments) of some tensor field, e.g. spin susceptibility (considered in Chapter 8 for nanotubes).

In Section 3.1 it is clarified that isotropy in the physics of Q1D systems is reduced to the invariance under the group $\mathrm{SO}(2,\mathbb{R})$. Also, it is discussed that the principle axis of a rotation of the order greater than 2 suffices to provide this property of tensor fields (counterexample are the ribbons with symmetric opposite edges, with $\boldsymbol{C}_2$ invariance). Taking suitable cylindrical coordinates to describe the positions of interacting spins, it is clear that *isotropic tensor field* depends on the difference $\varphi_{pq}^{PQ} = \varphi_p^P - \varphi_q^Q$ (and not both φ_p^P and φ_q^Q), and the remaining (non-angular) coordinates. Thus, its effective arguments are $\boldsymbol{r}_{pq}^{PQ} = \{\rho_p^P, z_p^P, \rho_q^Q, z_q^Q, \varphi_{pq}^{PQ}\}$. Since the rotations around the z-axis do not change ρ and z coordinates, for a system with $q > 2$ the isotropic interaction is consisted of the scalar components J^1, J^3 and D^3 of (3.4) only, while for $q = 2$ there are the additional scalars T_1 and T_2.

On the other hand, the homogeneity of a lattice is its invariance under trans-

lations $\ell = (\mathbb{1}|f)$. Since a Q1D system is localized to a finite distance from the z-axis, i.e. within the cylinder of a finite radius, the homogeneity refers only to the z-axis; the dependence on the pair of z-coordinates is reduced to the dependence on their difference $z_{pq}^{PQ} = z_p^P - z_q^Q$, leaving $\boldsymbol{r}_{pq}^{PQ} = \{\rho_p^P, \varphi_p^P, \rho_q^Q, \varphi_q^Q, z_{pq}^{PQ}\}$ as effective arguments. If such system is also isotropic, the interaction depends on the difference φ_{pq}^{PQ} rather than on the separate angular coordinates. Such tensors, where $\boldsymbol{r}_{pq}^{PQ} = \{\rho_p^P, \rho_q^Q, \varphi_{pq}^{PQ}, z_{pq}^{PQ}\}$, will be called *cylindrical*. While for three-dimensional systems, according to (3.1), the isotropic Heisenberg model is achieved, for Q1D ones the rotations around the z-axis are allowed, and line groups single out the three scalar components in (3.4) giving the XXZ model with the z-component of the Dzyaloshinskii-Moriya interaction

$$\begin{pmatrix} J^1 & D^3 & 0 \\ -D^3 & J^1 & 0 \\ 0 & 0 & J^3 \end{pmatrix} \tag{3.8}$$

if there are nontrivial rotations, and the additional two scalars

$$\begin{pmatrix} T^1 & T^2 & 0 \\ T^2 & -T^1 & 0 \\ 0 & 0 & 0 \end{pmatrix} \tag{3.9}$$

if the order of the isogonal axis is 2.

A consequence illustrating the importance of these results is that the quasi-classical ground state of the quadratic spin Hamiltonian involving the cylindrical tensor of interaction is a ether planar (in the xy-plane) helimagnet or a linear (along the z-axis) arrangement. This anticipates the detailed discussion in Chapter 8.

Chapter 4

Quasi-classical approximation

Being a prototypic many-body problem, the exact dynamics of a quantum spin lattice is not exactly solvable. In the simplest, commonly used mean-field type of the quasi-classical approximation, spin operators are substituted by their averages, which are the classical vectors of fixed length. Precisely, neglecting quantum correlations the expectation value of the quantum Hamiltonian becomes an energy functional over the sets of these classical vectors. In general, for an arbitrary spin (spin 1/2 is an exception), the lengths of the vectors on different sites are not necessarily equal. Nevertheless, the requirement of the equal lengths of classical spin vectors seems to be naturally imposed, with appropriate refinement by symmetry. In addition, the assumed equal contribution of the sites interrelated by symmetry to the total energy is emphasized as another manifestation of symmetry.

4.1 Model

The total energy of the spin lattice in the state $\hat{\rho}$ is the Hamiltonian (2.6) expectation value $\varepsilon^{\mathrm{Tot}} = \mathrm{Tr}\hat{H}\hat{\rho}$. The partial trace over all factor spaces except Pp-th and Qq-th gives the energy expressed by the reduced two-particle statistical operators $\hat{\rho}^{Pp}_{Qq}$:

$$\varepsilon^{\mathrm{Tot}} = \frac{1}{2}\sum_{PQpq} \mathrm{Tr}_{Pp,Qq}\hat{\boldsymbol{S}}^{P}_{p} h^{Pp}_{Qq}\hat{\boldsymbol{S}}^{Q}_{q}\hat{\rho}^{Pp}_{Qq}, \quad \hat{\rho}^{Pp}_{Qq} = \mathrm{Tr}_{\widehat{Pp,Qq}}\hat{\rho}. \tag{4.1}$$

Two-particle correlation operator can be defined as $\hat{\rho}^{\mathrm{C}} = \hat{\rho}^{Pp}_{Qq} - \hat{\rho}^{P}_{p} \otimes \hat{\rho}^{Q}_{q}$, where $\hat{\rho}^{P}_{p} = \mathrm{Tr}_{Qq}\hat{\rho}^{Pp}_{Qq}$ is a single-particle reduced state. Using the total separable state $\hat{\rho}_0 = \ldots \otimes \hat{\rho}^{P}_{p} \otimes \ldots$, correlation free, so called *quasi-classical* part of the energy is

expressed as

$$\varepsilon^{\mathrm{Cl}}[\dots \boldsymbol{s}_p^P \dots] = \mathrm{Tr}\hat{H}\hat{\rho}_0 = \frac{1}{2}\sum_{PQpq} \bar{\boldsymbol{s}}_p^P h_{Qq}^{Pp} \boldsymbol{s}_q^Q, \quad \boldsymbol{s}_p^P = \begin{pmatrix} s_p^{P1} \\ s_p^{P2} \\ s_p^{P3} \end{pmatrix} = \mathrm{Tr}_{Pp}\hat{\boldsymbol{S}}\hat{\rho}_p^P = \mathrm{Tr}\hat{\boldsymbol{S}}_p^P\hat{\rho}_0. \tag{4.2}$$

It is a functional over the *sets of the classical spin vectors* $\{\dots \boldsymbol{s}_p^P \dots\}$. The equation of motion of classical spin vectors,

$$\frac{d\boldsymbol{s}_p^P}{dt} = -\boldsymbol{s}_p^P \times \frac{d\varepsilon^{\mathrm{Cl}}}{d\boldsymbol{s}_p^P}, \quad \frac{d\varepsilon^{\mathrm{Cl}}}{d\boldsymbol{s}_p^P} = \sum_{Qq} h_{Qq}^{Pp}\boldsymbol{s}_q^Q. \tag{4.3}$$

is derived by the inserting the commutation relation of spin operator components (2.7) in the quantum-mechanical equation of motion (2.8) for the Hamiltonian (2.6), taking into account that $\frac{d\hat{\rho}_p^P}{dt} = 0$ within the Heisenberg picture. For stationary states, $\frac{d\boldsymbol{s}_p^P}{dt} = 0$, the solutions of (4.3) depend on the direction of $\boldsymbol{s}_p^P$, i.e. $\frac{d\varepsilon^{\mathrm{Cl}}}{d\boldsymbol{s}_p^P} \propto \boldsymbol{s}_p^P$. The group $\boldsymbol{G}$ acts on classical spin vectors as (Theorem B.3.3)

$$g\boldsymbol{s}_p^P = a(\bar{g})\boldsymbol{s}_{\bar{g}p}^P. \tag{4.4}$$

The neglected part of the total energy is a quantum correlation energy:

$$\varepsilon^{\mathrm{Cor}} = \frac{1}{2}\sum_{PQpq} \mathrm{Tr}_{Pp,Qq}\hat{\tilde{\boldsymbol{S}}}_p^P h_{Qq}^{Pp}\hat{\boldsymbol{S}}_q^Q\hat{\rho}^{\mathrm{C}}. \tag{4.5}$$

To summarize, the eigenproblem is unsolvable within the full quantum framework, except in few cases when there are some results on ground states, the parts of the spectra or iterative numerical attempts. Thus, the usually applied quasi-classical approach reduces it to the variational optimization of the energy functional over classical spin vectors. In other words, the minima of a classical energy is obtained by the variation over the trial set of all separable states yielding the spin vectors of the lengths $0 \leq ||\boldsymbol{s}_p^P|| \leq S^P$. Only *a posteriori* correlations may be studied to some extent.

4.2 Spin arrangement

To preserve the picture invoked mainly by symmetry, in the rest of the text it is assumed that classical spins are of the same length for all the sites of the same orbit of a $\boldsymbol{G}$-lattice. Such a spin set $\{\dots, \boldsymbol{s}_p^P, \dots\}$ is called *spin arrangement*. The

fixed spin length along the orbit will be also denoted by S^P, even if it is less then the maximal one[1]. Besides this constant classical spins can be described by unit norm vectors $\boldsymbol{t}_p^{P3}$ such that $\boldsymbol{s}_p^P = S^P \boldsymbol{t}_p^{P3}$. Each of these vectors is determined by two parameters (the angles of spherical coordinates), i.e. the *classical state space* is the $2N$-dimensional manifold $\mathcal{S}^{\mathrm{Cl}} = \cup_{Pp} S^2(\boldsymbol{r}_p^P, S^P)$ (where $S^2(\boldsymbol{r}_p^P, S^P)$ is the 2-sphere of the radius S^P centered at $\boldsymbol{r}_p^P$).

Two spin arrangements over the same orbit are *equivalent* if there is a non-singular three-dimensional matrix X mapping each spin of the first arrangement into the corresponding spin of the second one: $X\boldsymbol{s}_p^P = \boldsymbol{s}'^P_p$. *Dimensionality* (1, 2 or 3) of an arrangement is determined by a corresponding *spin set*, which is the set of all site spin vectors (placed at the same origin).

4.2.1 Framework for classical formalism

To enable the application of algebraic techniques, the ambient space $\mathbb{R}^{3N}$ is used, i.e. each site sphere is embedded as a manifold in the vector space $\mathbb{R}^3$. Any point of the classical states manifold $\mathcal{S}^{\mathrm{Cl}}$ is a spin arrangement, and as a vector from $\mathbb{R}^{3N}$ it may be rewritten in a convenient form:

$$\boldsymbol{S} = \sum_{Pp} E^{Pp} \otimes \boldsymbol{s}_p^P = \sum_P S^P \sum_p E^{Pp} \otimes \boldsymbol{t}_p^{P3}, \qquad \|\boldsymbol{s}_p^P\| = S^P; \tag{4.6}$$

here, the columns E^{Pp} form the absolute basis in $\mathbb{R}^N$ (see Appendix A.2).

The $3N$-dimensional matrix of the *classical Hamiltonian* H is composed of the 3-dimensional blocks of the interaction tensor of the quantum Hamiltonian $\hat{H}$:

$$H = \sum_{PQpq} E_{Qq}^{Pp} \otimes h_{Qq}^{Pp}. \tag{4.7}$$

Again, the $E_{Qq}^{Pp} = E^{Pp} \otimes E_{Qq} = E^{Pp} E_{Qq}$ are the absolute basis in the space of $3N$-dimensional matrices (see Appendix A.2).

Accordingly, the classical energy functional (4.2) may be rewritten as

$$\varepsilon^{\mathrm{Cl}}[\boldsymbol{S}] = \frac{1}{2} \bar{\boldsymbol{S}} H \boldsymbol{S}, \qquad \|\boldsymbol{s}_p^P\| = S^P. \tag{4.8}$$

[1] As far as spin $\frac{1}{2}$ is considered this corresponds to the trial set of pure states.

In addition, since for infinite systems the energy value diverges, a finite valued, *averaged energy*

$$\varepsilon_0[\boldsymbol{S}] = \frac{1}{2}\frac{\bar{\boldsymbol{S}}H\boldsymbol{S}}{\bar{\boldsymbol{S}}\boldsymbol{S}}, \quad \bar{\boldsymbol{S}}\boldsymbol{S} = \sum_P {S^P}^2|\boldsymbol{Z}^P|, \qquad \|\boldsymbol{s}_p^P\| = S^P, \tag{4.9}$$

is introduced as a quantity convenient in optimization.

The group action in $\mathbb{R}^{3N}$ is generated from (2.16). It is the induced axial representation of $\boldsymbol{G}$:

$$A(g) = \sum_{Pp} E_{Pp}^{P,gp} \otimes a(g), \tag{4.10}$$

where the matrices $E_{Pp}^{P,gp}$ implement the ground group action over the sites. The commutation of the quantum action $\hat{U}(\boldsymbol{G})$ with the quantum hamiltonian, through the relations (2.17a), ensures (Theorem B.3.3)

$$[A(\boldsymbol{G}), H] = 0, \tag{4.11}$$

i.e. $\boldsymbol{G}$ is the symmetry group of the classical Hamiltonian.

4.2.2 Arrangements with equally contributing sites

An intuitive idea of symmetry inspires an additional natural dynamical assumption for quasi-classical states. To this end note that the contribution of a particular site Qq to the classical energy (4.8) is

$$\varepsilon_q^Q \stackrel{\text{def}}{=} \frac{1}{2}\sum_{Pp} \bar{\boldsymbol{s}}_q^Q h_{Pp}^{Qq} \boldsymbol{s}_p^P. \tag{4.12}$$

An arrangement $\boldsymbol{S}$ is *equally contributing sites* (ECS) vector if all the sites from the same orbit Q contribute equally, $\varepsilon_q^Q = \varepsilon_0^Q$, to the total energy.

Indeed, an extension of the group action to this quantity, i.e. to site energy contributions, assumes that the action is described for each orbit by a real (to preserve the reality of energy) one-dimensional (thus irreducible, either an alternating or the unit) representation of $\boldsymbol{G}$, say $B^Q(\boldsymbol{G})$, such that $B^Q(g)\varepsilon_q^Q = \varepsilon_{gq}^Q$. Then the sum of the site energies is

$$\sum_{Qq} \varepsilon_q^Q = \sum_{Qq} B^Q(z_q^Q)\varepsilon_0^Q = \sum_Q \frac{1}{|\boldsymbol{F}^Q|}\sum_{qf^Q} B^P(z_q^Q f^Q)\varepsilon_0^Q = \sum_Q |\boldsymbol{Z}^Q|\boldsymbol{G}(B^Q)\varepsilon_0^Q,$$

where the projector $\boldsymbol{G}(B^Q) = \frac{1}{|\boldsymbol{G}|}\sum_g B^Q(g)$ can be either 1 or 0. From the orthogonality theorem follows that $\boldsymbol{G}(B^Q) = 1$ for the unit representation $B^Q = \mathbb{1}$, and $\boldsymbol{G}(B^Q) = 0$ for any alternating one. If ε_0^Q vanishes, then the total contribution of the orbit to the energy vanishes.

Chapter 5

Regular spin arrangements

Within the quasi-classical approximation, when magnetic moments are the classical spin vectors arranged over a lattice, symmetry considerations are neither exhaustively nor systematically elaborated in the literature: basically, there exist only Bloch-type arguments in the discussions of ferromagnetic order and its slight generalizations. On the other hand, it is expectable that arrangements on the $\boldsymbol{G}$-lattices are deeply related to the lattice symmetry. This is justified by many examples of the systems with obviously regular spin arrangements, but with the spin vectors not distributed by the axial representation (as expected, Chapter 1 and Chapter 4) of the geometrical symmetry group. Magnetic groups are an attempt to overwhelm this problem, with a very restricted success. Their generalization, spin groups [32], completely describe the systems which can be called symmetric in any intuitive sense. They are based on spin representations, which are objective of this Chapter.

5.1 Spin groups

We begin with a brief reminder about the originally introduced notion of spin groups [33] in order to relate it to the equivalent spin representation approach developed here and recently applied [58–60].

As usual, let an atomic configuration (regardless of the spins) have a symmetry group $\boldsymbol{G}$, with elements g. Then the spin group is a subgroup in $E(3)\times \mathrm{O}(3,\mathbb{R})$. Precisely, the elements of the spin group are pairs (g,b), where g and b belong respectively to $\boldsymbol{G}$ and to the subgroup $\boldsymbol{B}$ of $\mathrm{O}(3,\mathbb{R})$. It was shown that derivation of the spin groups was reduced to the classification of the *nontrivial spin groups*, thus spin arrangement of a system is completely defined by one of the latter. Linear and

planar arrangements possess an additional *spin-only group* ($\boldsymbol{B}'$ equal to $\boldsymbol{C}_\infty$ and $\boldsymbol{C}_{1\mathrm{h}}$, respectively) completing their full symmetry (spin group); for a three-dimensional spin arrangement the spin-only group contains only the identity element. A nontrivial spin group $N(\boldsymbol{G})$ is determined by the isomorphism $N(\boldsymbol{G})/\boldsymbol{G}' \cong \boldsymbol{B}^*$, where $\boldsymbol{G}'$ is a normal subgroup of $\boldsymbol{G}$ ($\boldsymbol{G} = \boldsymbol{G}' + g_2\boldsymbol{G}' + \dots$), while $\boldsymbol{B}^*$ is the group of the coset representatives $\{e, b_2, \dots\}$ (coset decomposition $\boldsymbol{B} = \boldsymbol{B}' + b_2\boldsymbol{B}' + \dots$ with normal subgroup $\boldsymbol{B}'$). The isomorphism (denoted by β) between the quotient group $N(\boldsymbol{G})/\boldsymbol{G}'$ and $\boldsymbol{B}^*$ (which maps each coset $g_i\boldsymbol{G}'$ into the element $\beta(g_i\boldsymbol{G}') = b_i$ from $\boldsymbol{B}^*$) generates the homomorphism $d(g) = \beta(g\boldsymbol{G}')$ of $\boldsymbol{G}$ onto $\boldsymbol{B}^*$ (every element g is mapped to an orthogonal matrix). Bearing in mind that a representation is the homomorphism of $\boldsymbol{G}$ into the group of nonsingular matrices of some carrier space, one concludes that d is a representation of $\boldsymbol{G}$, called spin representation, in $\mathbb{R}^3$. Therefore, the nontrivial spin group is completely determined by the spin representation, with kernel being the normal subgroup $\boldsymbol{G}'$.

For some fixed group $\boldsymbol{G}$, different nontrivial spin groups are those with inequivalent spin representations. In other words, nontrivial spin groups with the spin representations $d_1(\boldsymbol{G})$ and $d_2(\boldsymbol{G})$ are equivalent if there is a matrix R from $\mathrm{SO}(3,\mathbb{R})$ such that $Rd_1(\boldsymbol{G})\bar{R} = d_2(\boldsymbol{G})$. In fact, the usual equivalence relation, i.e. conjugation by some nonsingular matrix O, leads to the condition that O can be taken from $\mathrm{O}(3,\mathbb{R})$ too, as $Od_1(\boldsymbol{G})\bar{O}$ has to be a spin representation. This means that O can be a rotation $O = R$ or roto-inversion $O = \mathcal{I}R$, but conjugation under these two gives the same spin representation. Therefore, all the representations

$$^{R}d = Rd\bar{R}, \quad R = R(\alpha, \beta, \gamma), \tag{5.1}$$

obtained by an arbitrary rotation R (specified by the Euler angles α, β and γ) are also spin representations equivalent to d.

The procedure for the classification of nontrivial spin groups proposed by Litvin and Opechowski [33] assumes that one finds all normal subgroups $\boldsymbol{G}'$ of the geometrical group $\boldsymbol{G}$ and orthogonal group $\boldsymbol{B}^*$ establishing the isomorphism β. The spin groups may be also found directly, by construction of non-equivalent spin representations d, utilizing real (or physically) irreducible representations (RIRs) of the group $\boldsymbol{G}$. The approaches are equivalent (as equivalent representations have the same kernels).

Magnetic Groups

It is important to realize that magnetic groups are special cases of the spin groups; it is thus not possible to describe all the spin systems which are within the scope of the spin groups by magnetic groups only. A magnetic group is isomorphic to the group of geometrical transformations of a particular system, but together with the Euclidean transformations it involves also the time reversal Θ. Precisely, for a given system with the geometrical group $\boldsymbol{G}$ there are two types of magnetic groups (we omit here grey groups as they refer to systems with vanishing spins): besides the *ordinary* group $\boldsymbol{G}$, a *black-and-white magnetic groups* is obtained from a halving subgroup $\boldsymbol{G}'$ of $\boldsymbol{G}$:

$$\boldsymbol{G}' + \Theta g' \boldsymbol{G}'; \tag{5.2}$$

here, g' is an arbitrary element of the coset $\boldsymbol{G} \setminus \boldsymbol{G}'$. Since the time reversal changes the orientation of a spin vector, whereas the geometrical transformations act on a spin field by the axial (pseudo) vector representation $a(\boldsymbol{G})$, it follows that the magnetic groups are nontrivial spin groups with the particular spin representation $d(g) = \delta_g a(g)$, where δ_g is equal to 1 when g belongs to $\boldsymbol{G}'$, and -1 otherwise.

5.2 Spin representations

A classical spin arrangement emerges when each site $\boldsymbol{r}_p^P$ of a $\boldsymbol{G}$-lattice carries the spin vector $\boldsymbol{s}_p^P$ of the length S^P, i.e. it is the set $\{\dots, (\boldsymbol{r}_p^P, \boldsymbol{s}_p^P), \dots\}$, where $\|\boldsymbol{s}_p^P\| = S^P$ for all p. An arrangement is *regular* if it is invariant under a *spin group* [32, 59], which extends the geometrical action of $\boldsymbol{G}$ to the spin space of the orbit P by a real three-dimensional *spin representation* d^P of $\boldsymbol{G}$ such that (2.1) is extended to:

$$g\{\dots, (\boldsymbol{r}_p^P, \boldsymbol{s}_p^P), \dots\} = \{\dots, (g\boldsymbol{r}_p^P, d^P(g)\boldsymbol{s}_p^P), \dots\}. \tag{5.3}$$

The uniqueness of the site spins requires that the *orbit representative spin* $\boldsymbol{s}_0^P$ is fixed by the stabilizer:

$$(f^P \boldsymbol{r}_0^P, d^P(f^P)\boldsymbol{s}_0^P) = (\boldsymbol{r}_0^P, \boldsymbol{s}_0^P), \quad \forall f^P \in \boldsymbol{F}^P. \tag{5.4}$$

As for the positions, the transversals $\boldsymbol{Z}^P$ generate the whole arrangement from the orbit representative spins, because $\boldsymbol{s}_p^P = d^P(z_p^P)\boldsymbol{s}_0^P$. In the form of the vector (4.6)

from $\mathbb{R}^{3N}$, a regular spin arrangement is invariant under the representation $D(\boldsymbol{G})$:

$$D(g) = \sum_{Pp} E^{P,gp}_{Pp} \otimes d^P(g), \quad D(\boldsymbol{G})\boldsymbol{S} = \boldsymbol{S} = \sum_{Pp} E^{Pp} \otimes d^P(z^P_p)\boldsymbol{s}^P_0, \tag{5.5}$$

Obviously, the lengths of the site spin vectors along the P-th orbit are preserved and equal to $\|\boldsymbol{s}^P_0\| = S^P$.

Since the group acts independently over the orbits, each carrying its own spin representation d^P, the classification of the regular arrangements along the group orbits suffices to describe the regular arrangements for an arbitrary $\boldsymbol{G}$-lattice. Concerning the arrangements over the orbits, only the inequivalent spin representations are relevant. In fact, for the arrangements generated by the equivalent spin representations d and ${}^R d$, Equation (5.1) implies $d(g)\bar{R}\boldsymbol{s}_0 = {}^R d(g)\bar{R}\boldsymbol{s}_0$ for their mutual equivalence.

5.2.1 Parity of spin representations

The matrices of the axial representation $a(\boldsymbol{G})$ are a subgroup in $\mathrm{SO}(3,\mathbb{R})$; on the contrary, the matrices of the spin representation $d^P(\boldsymbol{G})$ are subgroups in $\mathrm{O}(3,\mathbb{R})$. Following the framework of the magnetic groups, a change of the spin vectors from site to site by roto-reflections may be connected with time reversal symmetry of a spin arrangement.

Precisely, to each element g in $\boldsymbol{G}$ and each spin representation $d^P(\boldsymbol{G})$, the *spin-parity*

$$\pi^P(g) \stackrel{\text{def}}{=} \det d^P(g) = (-1)^{\Pi^P(g)}, \quad \Pi^P(g) \stackrel{\text{def}}{=} \frac{1-\pi^P(g)}{2}, \tag{5.6}$$

is assigned. In general, for each orbit P, $\pi^P(\boldsymbol{G})$ is a representation of $\boldsymbol{G}$. There are two types: the trivial spin-parity (unit representation, $\pi^P(g) = 1$), and the spin-parities with one half of the group elements positive, $\pi^P(g) = 1$, and the other half negative, $\pi^P(g) = -1$ (alternating representation).

Each nontrivial spin-parity defines the Lagrange partition $\boldsymbol{G} = \boldsymbol{G}^P_+ + g^P_-\boldsymbol{G}_+$, where $\boldsymbol{G}^P_+ = \{g \in \boldsymbol{G} | \pi^P(g) = 1\}$ (the invariant index-two subgroup of $\boldsymbol{G}$) and $\pi^P(g^P_-) = -1$. Let us denote by $\boldsymbol{Z}^P_+$ and $\boldsymbol{Z}^P_-$ the sets of the opposite spin-parities of the transversal elements, i.e. $\boldsymbol{Z}^P = \boldsymbol{Z}^P_+ \bigcup \boldsymbol{Z}^P_-$. When the stabilizer of the P-th orbit representative site $\boldsymbol{r}^P_0$ is also partitioned by the spin-parity, $\boldsymbol{F}^P = \boldsymbol{F}^P_+ + f^P_-\boldsymbol{F}^P_+$, a new, completely positive transversal, $\boldsymbol{Z}^P_+ \bigcup \boldsymbol{Z}^P_- f^P_-$ may be chosen, and $\boldsymbol{G}^P_+ = (\boldsymbol{Z}^P_+\boldsymbol{F}^P_+) \bigcup (\boldsymbol{Z}^P_- f^P_- \boldsymbol{F}^P_+)$; for those transversals where $\boldsymbol{Z}^P_- = \emptyset$, it follows that $\boldsymbol{G}^P_+ =$

$\boldsymbol{Z}^P\boldsymbol{F}_+^P$. In these cases the positive groups $\boldsymbol{G}_+^P$, containing transversals, generate all the $\boldsymbol{G}$-orbit sites by their action on $\boldsymbol{r}_0^P$ for all P. Otherwise, when there is no stabilizer's element of the negative spin-parity, $\boldsymbol{F}^P = \boldsymbol{F}_+^P$, the positive group is $\boldsymbol{G}_+^P = \boldsymbol{Z}_+^P\boldsymbol{F}^P$; only a half of any transversal is positive, and $\boldsymbol{G}_+^P$ builds up the whole P-th orbit from the two sites $\boldsymbol{r}_0$ and $g_-\boldsymbol{r}_0$, while the transversal $\boldsymbol{Z}_-^P$ may be chosen such that $\boldsymbol{Z}_-^P = g_-^P\boldsymbol{Z}_+^P$. In this way, the *positive subgroup* $\boldsymbol{G}_+ = \bigcap_P \boldsymbol{G}_+^P$ of $\boldsymbol{G}$ may be found.

From this viewpoint, for the magnetic group (5.2), the subgroup $\boldsymbol{G}'$ is the positive subgroup, while g' is the element of the negative spin-parity.

5.2.2 Classification of spin representations

According to the Wigner's classification [61], a representation $D(\boldsymbol{G})$ of the group $\boldsymbol{G}$ can be:

1. of *the first kind* if $D(\boldsymbol{G}) \sim D^*(\boldsymbol{G})$ and there is an equivalent real representation;

2. of *the second kind* if $D(\boldsymbol{G}) \sim D^*(\boldsymbol{G})$, but there is no an equivalent real representation;

3. of *the third kind* if $D(\boldsymbol{G}) \nsim D^*(\boldsymbol{G})$.

Using this criterion and starting from the irreducible representations $d^{(\mu)}(\boldsymbol{G})$ (Greek superscript counts irreducible representations) of the dimension $|\mu|$ (the relevant are one, two and three-dimensional), all inequivalent spin representations $d(\boldsymbol{G})$ can be constructed as follows.

1. If $d^{(\mu)}(\boldsymbol{G}), d^{(\nu)}(\boldsymbol{G}), d^{(\lambda)}(\boldsymbol{G})$ are inequivalent representations of the first kind and $|\mu| = |\nu| = |\lambda| = 1$ (automatically RIRs). They give rise to the inequivalent spin representations:

   (a) $3d^{(\mu)}(\boldsymbol{G})$ (the same form for ν and λ),

   (b) $2d^{(\mu)}(\boldsymbol{G}) \oplus d^{(\nu)}(\boldsymbol{G})$ (the same 2+1 form for the other combinations),

   (c) $d^{(\mu)}(\boldsymbol{G}) \oplus d^{(\nu)}(\boldsymbol{G}) \oplus d^{(\lambda)}(\boldsymbol{G})$.

2. If $d^{(\mu)}(\boldsymbol{G})$ is of the second or of the third kind and $d^{(\nu)}(\boldsymbol{G})$ is of the first kind, and $|\mu| = |\nu| = 1$, then one constructs the spin representation

(a) $\bar{\mathrm{x}}(d^{(\mu)}(\boldsymbol{G}) \oplus d^{(\mu*)}(\boldsymbol{G}))\mathrm{x} \oplus d^{(\nu)}(\boldsymbol{G})$ (x given by (2.14)).

3. If $d^{(\mu)}(\boldsymbol{G}), d^{(\nu)}(\boldsymbol{G})$ are of the first kind and $|\mu| = 2$, $|\nu| = 1$, then spin representation is

   (a) $d^{(\mu)}(\boldsymbol{G}) \oplus d^{(\nu)}(\boldsymbol{G})$.

4. If $d^{(\mu)}(\boldsymbol{G})$ is of the first kind and $|\mu| = 3$, it provides the spin representation

   (a) $d^{(\mu)}(\boldsymbol{G})$.

Recall that only inequivalent forms of the spin representations are given here. E.g. the spin representation $d^{(\mu)}(\boldsymbol{G}) \oplus d^{(\nu)}(\boldsymbol{G}) \oplus d^{(\lambda)}(\boldsymbol{G})$ from the first case is equivalent to any spin representation of the same form obtained by permuting μ, ν, λ; similarly, there is equivalence $2d^{(\mu)}(\boldsymbol{G}) \oplus d^{(\nu)}(\boldsymbol{G}) \sim d^{(\nu)}(\boldsymbol{G}) \oplus 2d^{(\mu)}(\boldsymbol{G})$. Obviously, a spin representation carry the set $\boldsymbol{\mu}$ of the quantum numbers of the included RIRs. Taking into account (5.1), the general specification of a spin representation is ${}^{R}d^{\boldsymbol{\mu}}$.

5.3 Quasi-one-dimensional regular spin arrangements

The introduced concepts are applied [39, 59, 60] to the line groups: after their spin representations are found, all the regular spin arrangements of the quasi-one-dimensional systems are classified. Some of them are illustrated in Figure 2.1. This classification was sufficient to predict the cross sections for neutron diffraction [60], in a way enabling an experimental characterization of magnetically ordered samples.

5.3.1 Spin representations of line groups

Based on the theory exposed in Section 5.2.2 spin representations, as three-dimensional, may be of the two general types:

$$d = E + C = \left(\begin{smallmatrix} E & 0 \\ 0 & C \end{smallmatrix}\right), \tag{5.7a}$$

$$d = C_1 + C_2 + C_3 = \left(\begin{smallmatrix} C_1 & 0 & 0 \\ 0 & C_2 & 0 \\ 0 & 0 & C_3 \end{smallmatrix}\right); \tag{5.7b}$$

here C and E stand for arbitrary one- and two-dimensional RIRs, respectively. Precisely, the RIRs of the line groups are of the dimensions 1,2 and 4, hence, inequivalent

combinations (5.7) of the RIRs C and E classify the spin representations of the line groups. Note that an one-dimensional RIR may be either the unit representation or an alternating one, and A or B respectively is used instead of C when this distinction is significant.

Further, RIRs of the line groups are characterized by quantum numbers of *helical* $\tilde{k}$ (real) and *angular momenta* $\tilde{m}$ (integer), and parities Π_i (± 1) for each geometrical parity π_i in the group. Thus, the most general labels are ${}_{\tilde{k}}E_{\tilde{m}}$, ${}_{\tilde{k}}E^{\Pi}_{\tilde{m}}$, ${}_{\tilde{k}}C_{\tilde{m}}$, ${}_{\tilde{k}}C^{\Pi}_{\tilde{m}}$ and ${}^{\Pi_1}_{\tilde{k}}C^{\Pi_2}_{\tilde{m}}$ (A, ${}_{\tilde{k}}B_{\tilde{m}}$, ${}_{\tilde{k}}B^{\Pi}_{\tilde{m}}$ and ${}^{\Pi_1}_{\tilde{k}}B^{\Pi_2}_{\tilde{m}}$). For the commensurate groups, instead of the helical also the *linear momenta* k and m may be used; helical and linear momenta coincide in the families where the generalized translation group is a pure translational or a glide plane group. The one- and two-dimensional RIRs of the line groups are tabulated [60].

Spin representation of the first family line groups

The irreducible representations of the first family line groups are one-dimensional [46] (as $\boldsymbol{L}^{(1)}$ is abelian). To an arbitrary element (2.4) such a representation assigns the number ${}_{\tilde{k}}C_{\tilde{m}}(\ell_{ts}) = \mathrm{e}^{\mathrm{i}\phi^{\tilde{k}\tilde{m}}_{ts}}$, where

$$\phi^{\tilde{k}\tilde{m}}_{ts} = \tilde{k}ft + \frac{2\pi}{n}\tilde{m}s, \tag{5.8}$$

and the helical quasi-momentum $\tilde{k}$ takes values from the helical Brillouin zone $(-\pi/f, \pi/f]$, while the angular momentum $\tilde{m}$ may be an integer from the interval $(-n/2, n/2]$. It is obvious that these representations are complex (the third kind according to the Wigner's classification, Section 5.2.2), except

$${}_0A_0(\ell_{ts}) = 1,\ {}_{\frac{\pi}{f}}B_0(\ell_{ts}) = (-1)^t,\ {}_0B_{\frac{n}{2}}(\ell_{ts}) = (-1)^s,\ {}_{\frac{\pi}{f}}B_{\frac{n}{2}}(\ell_{ts}) = (-1)^{t+s}, \tag{5.9}$$

which are real (the first kind). Alternatively, the latter are written in an unified way as $(-1)^c$ with $c = 0, t, s, t+s$, corresponding respectively to the quantum numbers $(\tilde{k}, \tilde{m}) = (0,0), (\pi/f, 0), (0, n/2), (\pi/f, n/2)$. The representations with $\tilde{m} = n/2$ exist only for the groups with even n.

To classify corresponding RIRs, we note that each pair of the mutually conjugated complex representations ${}_{\tilde{k}}C_{\tilde{m}}$ and ${}_{\tilde{k}}C^{*}_{\tilde{m}} = {}_{-\tilde{k}}C_{-\tilde{m}}$ gives (by the similarity transformation with the matrix (2.14)) the two-dimensional real representation equivalent to their direct sum ${}_{\tilde{k}}C_{\tilde{m}} \oplus {}_{-\tilde{k}}C_{-\tilde{m}}$:

$${}_{\tilde{k}}E_{\tilde{m}}(\ell_{ts}) = \begin{pmatrix} \cos\phi^{\tilde{k}\tilde{m}}_{ts} & -\sin\phi^{\tilde{k}\tilde{m}}_{ts} \\ \sin\phi^{\tilde{k}\tilde{m}}_{ts} & \cos\phi^{\tilde{k}\tilde{m}}_{ts} \end{pmatrix}, \tag{5.10}$$

with $\phi_{ts}^{\tilde{k}\tilde{m}}$ given by (5.8). To count all these inequivalent representations $\tilde{k}$ takes the values only from the right half $[0, \pi/f]$ of the helical Brillouin zone, while the range of $\tilde{m}$ is the same as in the complex case. Therefore, the real irreducible representations of $\boldsymbol{L}^{(1)}$ are one-dimensional (5.9) and two-dimensional (5.10).

There are only two ways to form three-dimensional real representations according to (5.7). First, any two-dimensional representation ${}_{\tilde{k}}E_{\tilde{m}}$ can be combined only with one of the representations (5.9); in this way, four different *classes* of spin representations are obtained:

$$ {}_{\tilde{k}}d^{c}_{\tilde{m}}(\ell_{ts}) = \begin{pmatrix} \cos(\phi_{ts}^{\tilde{k}\tilde{m}}) & -\sin(\phi_{ts}^{\tilde{k}\tilde{m}}) & 0 \\ \sin(\phi_{ts}^{\tilde{k}\tilde{m}}) & \cos(\phi_{ts}^{\tilde{k}\tilde{m}}) & 0 \\ 0 & 0 & (-1)^c \end{pmatrix}, \quad c = 0, t, s, t+s, \quad \begin{smallmatrix} \tilde{k}\in[0,\frac{\pi}{f}] \\ \tilde{m}\in(-\frac{n}{2},\frac{n}{2}] \end{smallmatrix}. \tag{5.11a} $$

In the given class c, the choice of the pairs $(\tilde{k}, \tilde{m})$ gives a particular spin representation, i.e. $\boldsymbol{\mu} = \{(\tilde{k}, \tilde{m}), (\tilde{k}_c, \tilde{m}_c)\}$. Note that in (5.11a) the upper left two-by-two block corresponds to the rotation in the xy-plane. It follows that for the class $c = 0$, the spin representation of the group element ℓ_{ts} is the rotation $R_z(\phi_{ts}^{\tilde{k}\tilde{m}})$ for $\phi_{ts}^{\tilde{k}\tilde{m}}$ around the z-axis. In the remaining three classes, $c = t, s, w$, the halving subgroup containing elements with c even is represented by the rotations $R_z(\phi_{ts}^{\tilde{k}\tilde{m}})$, while the other elements, with c odd (the remaining coset), are reflections $-R_z(\phi_{ts}^{\tilde{k}\tilde{m}} + \pi)$.

The second possibility to build a spin representation is to combine the three representations (5.9). However, note that when in the construction of ${}_{\tilde{k}}E_{\tilde{m}}$ any of these representations is used, the result is the diagonal representation $\mathrm{diag}[(-1)^c, (-1)^c]$. Therefore, the classes (5.11a) include also four the scalar spin representations composed of the three identical real representations, $\mathrm{diag}[(-1)^c, (-1)^c, (-1)^c]$, as well as those representations consisting of two mutually equal and one different real irreducible representation $\mathrm{diag}[(-1)^{c_1}, (-1)^{c_1}, (-1)^{c_2}]$. Hence, only the representations $\mathrm{diag}[(-1)^{c_1}, (-1)^{c_2}, (-1)^{c_3}]$ with three different components (5.9) are not included in the classes (5.11a). This makes four *exceptional* spin representations:

$$ \begin{aligned} \mathrm{diag}[(-1)^t, (-1)^s, (-1)^{t+s}], \quad & \mathrm{diag}[(-1)^s, (-1)^{t+s}, 1], \\ \mathrm{diag}[(-1)^t, (-1)^{t+s}, 1], \quad & \mathrm{diag}[(-1)^t, (-1)^s, 1], \end{aligned} \tag{5.11b} $$

with $\boldsymbol{\mu} = \{(\tilde{k}_{c_1}, \tilde{m}_{c_1}), (\tilde{k}_{c_2}, \tilde{m}_{c_2}), (\tilde{k}_{c_3}, \tilde{m}_{c_3})\}$. Thus, in all of the four exceptional cases the identity matrix is associated to the elements of $\boldsymbol{L}^{(1)}$ with even t and s simultaneously. This means that the kernel of these representations is an index four subgroup of $\boldsymbol{L}^{(1)}$, and its three cosets correspond to the remaining three different

matrices. These matrices are involutions (their square is the identity matrix), and describe rotations or reflections.

To summarize, there are the four classes (5.11a) and the four exceptional (5.11b) spin representations of the line groups of the first family with even n. When n is odd, there are only the two classes $c = 0, t$ of spin representations (no exceptional representations and classes $c = s, s + t$). Of course, these are standardized forms of spin representations, and the other equivalent representations ${}^{R}d^{\boldsymbol{\mu}}$ are obtained by the similarity transformation.

Regular spin arrangements of the first family line groups

When the spin representations are found, the inequivalent spin arrangements may be determined in the next step. The results are explicated for the standardized form (5.11), and for the equivalent representations ${}^{R}d^{\boldsymbol{\mu}}$, the presented spin vectors and domains in Table 5.1 should be mapped by R.

The regular spin arrangement over the orbit (2.5) is given by $\boldsymbol{s}_{ts} = d(\ell_{ts})\boldsymbol{s}_0$. Assuming that $(1, \theta, \phi_0)$ are cylindrical coordinates of $\boldsymbol{s}_0$, the spin vectors of the obtained regular arrangements are

$$\boldsymbol{s}_{ts} \;=\; \begin{pmatrix} \sin\theta\cos(\phi_{ts}^{\tilde{k}\tilde{m}}+\phi_0) \\ \sin\theta\sin(\phi_{ts}^{\tilde{k}\tilde{m}}+\phi_0) \\ C(\ell_{ts})\cos\theta \end{pmatrix}, \tag{5.12a}$$

for the spin representation of the type (5.11a), while the spin representation (5.11b) yields

$$\boldsymbol{s}_{ts} \;=\; \begin{pmatrix} C_1(\ell_{ts})\sin\theta\cos\phi_0 \\ C_2(\ell_{ts})\sin\theta\sin\phi_0 \\ C_3(\ell_{ts})\cos\theta \end{pmatrix}. \tag{5.12b}$$

Altogether 19 (6) types of the inequivalent spin arrangements are obtained for n even (odd), and they are depicted in Figure 5.1. For each of them the basic characteristics are in the Table 5.1: the superscript "o" emphasizes those arrangements allowed also for odd n, the dimension D and the spin representation d generating the arrangement from the spin vector $\boldsymbol{s}_0$ from the domain specified in the column Domain. Arrangements allowed for the linear orbit are singled out in column LO (by + or by additional conditions). Within 11-15, the types defined by various $\tilde{k}$ and $\tilde{m}$ are grouped. Representation C may be either A, ${}_{\pi}B_0$, ${}_0B_{n/2}$, ${}_{\pi}B_{n/2}$ (π stands for π/f).

Table 5.1: Spin arrangements of the first family line groups.

No.	D	d	Domain	LO
1^o	1	$3A$	xyz	+
		${}_0B_{n/2}({}_\pi B_0,{}_\pi B_{n/2}) + 2A$	yz	+
		${}_0B_{n/2} +_\pi B_0 + A$	z	+
		${}_0B_{n/2} +_\pi B_{n/2} + A$	z	+
		${}_\pi B_0 +_\pi B_{n/2} + A$	z	+
		${}_{\tilde{k}}E_{\tilde{m}} + A$	z	+
2^o	1	$3_\pi B_0$	xyz	+
		$A({}_0B_{n/2},{}_\pi B_{n/2}) + 2_\pi B_0$	yz	+
		$A +_0 B_{n/2} +_\pi B_0$	z	+
		$A +_\pi B_{n/2} +_\pi B_0$	z	+
		${}_0B_{n/2} +_\pi B_{n/2} +_\pi B_0$	z	+
		${}_{\tilde{k}}E_{\tilde{m}} +_\pi B_0$	z	+
3		$3_0B_{n/2}$	xyz	
		$A({}_\pi B_0,{}_\pi B_{n/2}) + 2_0B_{n/2}$	yz	
		$A +_\pi B_0 +_0 B_{n/2}$	z	
		$A +_\pi B_{n/2} +_0 B_{n/2}$	z	
		${}_\pi B_0 +_\pi B_{n/2} +_0 B_{n/2}$	z	
		${}_{\tilde{k}}E_{\tilde{m}} +_0 B_{n/2}$	z	
4		$3_\pi B_{n/2}$	xyz	
		$A({}_\pi B_{0,0} B_{n/2}) + 2_\pi B_{n/2}$	yz	
		$A +_\pi B_0 +_\pi B_{n/2}$	z	
		$A +_0 B_{n/2} +_\pi B_{n/2}$	z	
		${}_\pi B_0 +_0 B_{n/2} +_\pi B_{n/2}$	z	
		${}_{\tilde{k}}E_{\tilde{m}} +_\pi B_{n/2}$	z	
5^o	2	$2A +_\pi B_0$	$(xy \cup z)^C$	+
		$A + 2_\pi B_0$	$(x \cup yz)^C$	+
		$A +_\pi B_0 +_0 B_{n/2}$	$xy \backslash (x \cup y)$	+
		$A +_\pi B_0 +_\pi B_{n/2}$	$xy \backslash (x \cup y)$	+
6		$2A +_0 B_{n/2}$	$(xy \cup z)^C$	
		$A + 2_0B_{n/2}$	$(x \cup yz)^C$	
		$A +_0 B_{n/2} +_\pi B_0$	$xy \backslash (x \cup y)$	
		$A +_0 B_{n/2} +_\pi B_{n/2}$	$xy \backslash (x \cup y)$	
7		$2A +_\pi B_{n/2}$	$(xy \cup z)^C$	
		$A + 2_\pi B_{n/2}$	$(x \cup yz)^C$	
		$A +_\pi B_{n/2} +_\pi B_0$	$xy \backslash (x \cup y)$	
		$A +_\pi B_{n/2} +_0 B_{n/2}$	$xy \backslash (x \cup y)$	
8		${}_0B_{n/2} + 2_\pi B_0$	$(x \cup yz)^C$	
		${}_\pi B_0 + 2_0B_{n/2}$	$(x \cup yz)^C$	
		${}_\pi B_0 +_0 B_{n/2} + A$	$xy \backslash (x \cup y)$	
		${}_\pi B_0 +_0 B_{n/2} +_\pi B_{n/2}$	$xy \backslash (x \cup y)$	
9		${}_0B_{n/2} + 2_\pi B_{n/2}$	$(x \cup yz)^C$	
		${}_\pi B_{n/2} + 2_0B_{n/2}$	$(x \cup yz)^C$	
		${}_0B_{n/2} +_\pi B_{n/2} + A$	$xy \backslash (x \cup y)$	
		${}_0B_{n/2} +_\pi B_{n/2} +_\pi B_0$	$xy \backslash (x \cup y)$	
10		${}_\pi B_0 + 2_\pi B_{n/2}$	$(x \cup yz)^C$	
		${}_0B_{n/2} + 2_\pi B_{n/2}$	$(x \cup yz)^C$	
		${}_\pi B_0 +_\pi B_{n/2} + A$	$xy \backslash (x \cup y)$	
		${}_\pi B_0 +_\pi B_{n/2} +_0 B_{n/2}$	$xy \backslash (x \cup y)$	
11^o		${}_{\tilde{k}}E_{\tilde{m}} + C$	xy	$\tilde{m} = 0$
12^o	3	${}_{\tilde{k}}E_{\tilde{m}} + A$	$(xy \cup z)^C$	$\tilde{m} = 0$
13^o		${}_{\tilde{k}}E_{\tilde{m}} +_\pi B_0$	$(xy \cup z)^C$	$\tilde{m} = 0$
14		${}_{\tilde{k}}E_{\tilde{m}} +_0 B_{n/2}$	$(xy \cup z)^C$	
15		${}_{\tilde{k}}E_{\tilde{m}} +_\pi B_{n/2}$	$(xy \cup z)^C$	
16		$A +_0 B_{n/2} +_\pi B_{n/2}$	$(xy \cup yz \cup xz)^C$	
17		$A +_\pi B_0 +_\pi B_{n/2}$	$(xy \cup yz \cup xz)^C$	
18		$A +_\pi B_0 +_0 B_{n/2}$	$(xy \cup yz \cup xz)^C$	
19		${}_\pi B_0 +_0 B_{n/2} +_\pi B_{n/2}$	$(xy \cup yz \cup xz)^C$	

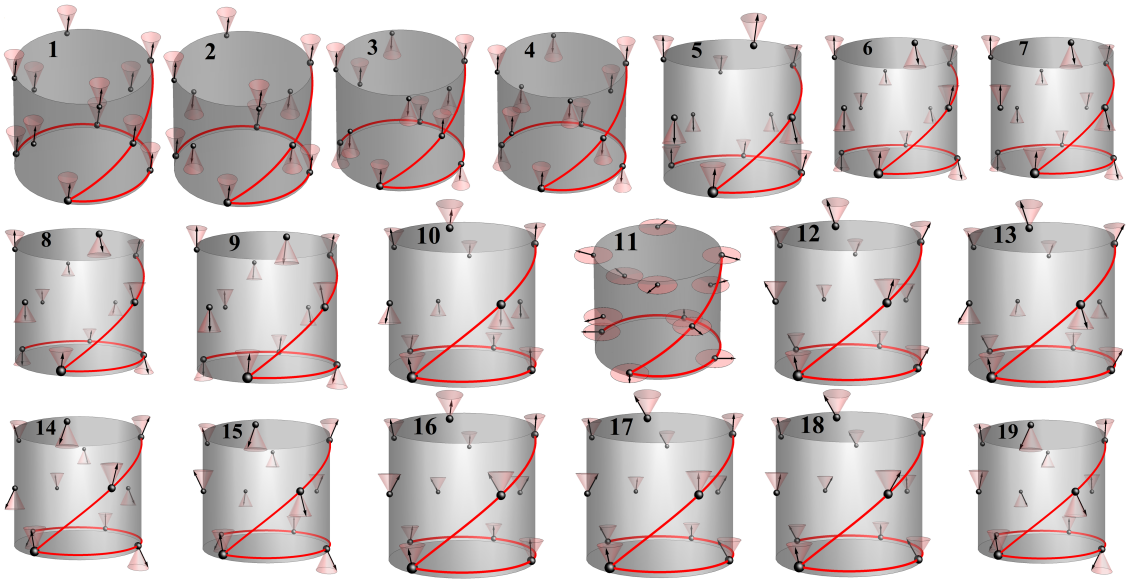

Figure 5.1: Spin arrangements of the generic orbit of the first family line group $\boldsymbol{T}_{56/9}(f)\boldsymbol{C}_4$, labeled by the ordinals in the Table 5.1.

A one-dimensional spin arrangement can be ferromagnetic $\boldsymbol{s}_{ts} = \boldsymbol{s}_0$ (No. 1 in Table 5.1) and antiferromagnetic (Nos. 2-4). The latter can appear due to spin flip by $(C_Q|f)$ only ($\boldsymbol{s}_{ts} = (-1)^t\boldsymbol{s}_0$, ferromagnetic monomers are mutually antiferromagnetically ordered; No. 2), by C_n only ($\boldsymbol{s}_{ts} = (-1)^s\boldsymbol{s}_0$, aligned antiferromagnetic monomers, No. 3), or by both ($\boldsymbol{s}_{ts} = (-1)^{t+s}\boldsymbol{s}_0$, antiferromagnetic order both within monomers and between them; No. 4).

Two-dimensional spin arrangements 5-10 are generated by the diagonal spin representations (5.7b) acting on the orbit representative spin with vanishing one of the Cartesian components; the other two, $\boldsymbol{s}_0 = (s_0^1, s_0^2)$, single out the effective components of the spin representation. Among such arrangements there are those consisting of two different spins only, alternated by the spin representation; alternation may be along the helix with ferromagnetic monomer ($\boldsymbol{s}_{ts} = (s_0^1, (-1)^t s_0^2)$; No. 5), or within mutually aligned monomers ($\boldsymbol{s}_{ts} = (s_0^1, (-1)^s s_0^2)$; No. 6), or when both the generators alternate spins in the same way ($\boldsymbol{s}_{ts} = (s_0^1, (-1)^{t+s} s_0^2)$; No. 7). Besides, there are arrangements with four spins in total; the arrangements are completely analogous to the previous case: antiferromagnetic monomer, with the alternation along the helix ($\boldsymbol{s}_{ts} = ((-1)^s s_0^1, (-1)^{t+s} s_0^2)$; No. 9), the alternation within the monomer with the flipped adjacent monomers ($\boldsymbol{s}_{ts} = ((-1)^t s_0^1, (-1)^{t+s} s_0^2)$; No.

10), or the opposite alternation ($\boldsymbol{s}_{ts} = ((-1)^s s_0^1, (-1)^t s_0^2)$; No. 8) in both directions. Finally, there is a class of planar helimagnets ($\boldsymbol{s}_{ts} = (s_0^1 \cos\phi_{ts}^{\tilde{k}\tilde{m}}, s_0^2 \sin\phi_{ts}^{\tilde{k}\tilde{m}})$; No. 11) obtained by the representations (5.11a) where $\phi_{ts}^{\tilde{k}\tilde{m}} = \tilde{k}ft + \tilde{m}(2\pi/n)s$.

In three-dimensional cases spins are in general positions provided out of the domain for one- and two-dimensional arrangements of the same spin representation. Representations of the type (5.7a) generate arrangements 12-15 acting on $\boldsymbol{s}_0 = (s_0^1, s_0^2, s_0^3)$. When matrices d are rotations, the conical helimagnets are with the spins on a single cone ($\boldsymbol{s}_{ts} = (s_0^1 \cos\phi_{ts}^{\tilde{k}\tilde{m}}, s_0^2 \sin\phi_{ts}^{\tilde{k}\tilde{m}}, s_0^3)$; No. 12), while the others (roto-reflections) are with the spins on both cones ($\boldsymbol{s}_{ts} = (s_0^1 \cos\phi_{ts}^{\tilde{k}\tilde{m}}, s_0^2 \sin\phi_{ts}^{\tilde{k}\tilde{m}}, (-1)^\alpha s_0^3)$; Nos. 13-15, for $\alpha = t, s, t+s$). The rest of the arrangements, related to (5.7b), are with four different spin vectors on a single cone ($\boldsymbol{s}_{ts} = (s_0^1, (-1)^s s_0^2, (-1)^{t+s} s_0^3)$, $\boldsymbol{s}_{ts} = (s_0^1, (-1)^t s_0^2, (-1)^{t+s} s_0^3)$, $\boldsymbol{s}_{ts} = (s_0^1, (-1)^t s_0^2, (-1)^s s_0^3)$; 16-18), and on both cones ($\boldsymbol{s}_{ts} = ((-1)^t s_0^1, (-1)^s s_0^2, (-1)^{t+s} s_0^3)$; No. 19).

For the groups with n odd the described types of arrangements are reduced to the 6 different types only, as the total number of spin groups is lowered. Further, for a linear orbit (chain) $\boldsymbol{s}_0$ must be chosen to fulfill the conditions (5.4): there are exactly 6 different (the last column) such spin orderings. In fact, as chains are the same for any n, the corresponding spin orbits coincide with the arrangements allowed for odd n. Also, these spin orbits correspond to those over generic orbits for the groups with $n = 1$ (when atoms form a single helix).

It is important to note that the arrangements 11-15 of Table 5.1 are commensurate (in the sense that the same spin vectors appear periodically) only if $f\tilde{k}/\pi$ is rational (then the spin set is finite); otherwise, all the spin vectors are mutually different (and the spin set is infinite). In particular, for a system with translational periodicity (Q rational), rational $\tilde{k}$ implies commensurability of the two lattices, i.e. translational periodicity of the spin arrangement (with period being multiple of the period of the system), while irrational $\tilde{k}$ means that periodicity of the total system is completely broken, due to the incompatibility of the atomic and the spin lattices.

5.3.2 Other line groups: a general induction algorithm

Here we show how the spin representations and the spin arrangements of the other families of the line groups can be found using the derived ones. Examples of the regular spin arrangements are illustrated in Figure 2.1.

Let $\boldsymbol{L}$ be an index-two subgroup in $\boldsymbol{L}'$, i.e. $\boldsymbol{L}' = \boldsymbol{L} + \ell'\boldsymbol{L}$. First, note that

any spin-representation $D(\boldsymbol{L}')$ subduces the spin-representation $d(\boldsymbol{L})$, meaning that $D(\boldsymbol{L}')$ is extended from $d(\boldsymbol{L})$ by defining the matrix $Z = D(\ell')$, satisfying the homomorphism condition $d(\bar{\ell}'\ell\ell') = \bar{Z}d(\ell)Z$. Consequently, only the representations of $\boldsymbol{L}$ satisfying this condition, i.e. the self ℓ'-conjugated [62] ones are extendable to $\boldsymbol{L}'$, and all their inequivalent extensions are all spin representations of $\boldsymbol{L}'$. Further, the irreducible components of SC representations may be either SC themselves, or mutually ℓ'-conjugated. Detailed but simple analysis of possible cases gives that each extendable representation generates 2 (if $D(\boldsymbol{L})$ consists of 2 MC and 1 SC irreducible component), 4 (3 equal SC or one two-dimensional and one one-dimensional SC), 6 (3 SC, two identical among them) or 8 (3 inequivalent SC) inequivalent spin representations of $\boldsymbol{L}'$.

As far as the arrangements are considered there are two possible cases of atomic orbits. If there is an element ℓ_0 in $\boldsymbol{L}$ such that $\ell'\ell_0$ leaves $\boldsymbol{r}_0$ unchanged, the $\boldsymbol{L}'$-orbit of $\boldsymbol{r}_0$ coincides with the orbit of $\boldsymbol{L}$. Then, $\boldsymbol{L}'$ must generate the same arrangement as $\boldsymbol{L}$, and this is possible if and only if $d(\boldsymbol{L})$ is extendable and $D(\ell'\ell_0)\boldsymbol{s}_0 = Zd(\ell_0)\boldsymbol{s}_0 = \boldsymbol{s}_0$. Hence, an $\boldsymbol{L}$-arrangement over such orbit is also an $\boldsymbol{L}'$-arrangement if and only if it can be generated by an extendable $d(\boldsymbol{L})$ with some of the extensions satisfying the stabilizer condition. Otherwise, the orbit of $\boldsymbol{L}'$ contains two $\boldsymbol{L}$-orbits with the representatives $\boldsymbol{r}_0$ and $\ell'\boldsymbol{r}_0$. Then any extendable representation $d(\boldsymbol{L})$ generates equivalent arrangements over the two orbits, which together give a spin orbit of $\boldsymbol{L}'$; such spin orbits are equivalent if and only if $\boldsymbol{s}_0$ is from the subspace of the common irreducible components of the extensions.

For the line group families 2-8 (having halving subgroups from the first family) one constructs spin representations and then arrangements directly applying the above described procedures. After this, the prescription has to be repeated for the rest of the line groups (families 9-13), as they have halving subgroups from the families 2-8.

Chapter 6

Quasi-classical ground state

As the ground state within the quasi-classical approach is the spin arrangement minimizing the energy functional, the corresponding optimization is a variational problem with the number of independent variables proportional to (by the factor two due to the fixed length of spins along any orbit) the number of the sites. Therefore, for infinite systems the exact optimization in general case is not possible, even numerically.

In Section 6.1 general conditions for local minima are given, and then, in Section 6.2, the application of the symmetry is analysed. Precisely, the trial set of the arrangements is restricted to the regular ones only, enabling us to obtain an expression for the total energy with the tremendously reduced number of variational parameters. For general interactions among the site spins, such an approach may give an incorrect solution. However, models which deal with non-symmetric arrangements can not be handled by group-theoretical methods at all. Therefore, the present discussion refers to the classical Hamiltonians with ground states generated by spin groups. Since this approach largely generalizes the scope of magnetic groups, it is expected that it is suitable at least for the most of the observed ordered, e.g. helical spin systems.

6.1 Constrained optimization

According to the definition of the ground state spin arrangement, the constrained minimum of (4.8) is achieved through the optimization of the new functional

$$F[\dots \varepsilon_p^P; \boldsymbol{s}_p^P, \dots] = F[\boldsymbol{\varepsilon} \oplus \boldsymbol{S}] = \varepsilon^{\mathrm{Cl}}[\dots \boldsymbol{s}_p^P \dots] - \sum_{Pp} \varepsilon_p^P (\bar{\boldsymbol{s}}_p^P \boldsymbol{s}_p^P - S^{P^2}), \qquad (6.1)$$

where $\boldsymbol{\varepsilon} = \sum_{Pp} E^{Pp} \otimes \varepsilon_p^P$ is the column of Lagrange multipliers ε_p^P.

The Taylor series at a point $\boldsymbol{\varepsilon} \oplus \boldsymbol{S}$ is

$$\begin{aligned} F[\boldsymbol{\varepsilon} + \mathrm{d}\boldsymbol{\varepsilon} \oplus \boldsymbol{S} + \mathrm{d}\boldsymbol{S}] &= F[\boldsymbol{\varepsilon} \oplus \boldsymbol{S}] + (\bar{F}_{\boldsymbol{\varepsilon}} \oplus \bar{F}_{\boldsymbol{S}})(\mathrm{d}\boldsymbol{\varepsilon} \oplus \mathrm{d}\boldsymbol{S}) \\ &+ \frac{1}{2}(\mathrm{d}\bar{\boldsymbol{\varepsilon}} \oplus \mathrm{d}\bar{\boldsymbol{S}}) \begin{pmatrix} 0 & \bar{F}_{\boldsymbol{S}\boldsymbol{\varepsilon}} \\ F_{\boldsymbol{S}\boldsymbol{\varepsilon}} & F_{\boldsymbol{S}\boldsymbol{S}} \end{pmatrix} (\mathrm{d}\boldsymbol{\varepsilon} \oplus \mathrm{d}\boldsymbol{S}) + \ldots, \end{aligned} \tag{6.2}$$

where the first partial derivatives (gradients) are N- and $3N$-dimensional columns $F_{\boldsymbol{\varepsilon}} = F_{\boldsymbol{\varepsilon}}[\boldsymbol{\varepsilon} \oplus \boldsymbol{S}]$ and $F_{\boldsymbol{S}} = F_{\boldsymbol{S}}[\boldsymbol{\varepsilon} \oplus \boldsymbol{S}]$, respectively:

$$F_{\boldsymbol{\varepsilon}} = \sum_{Pp} E^{Pp} \otimes \frac{\partial F[\boldsymbol{\varepsilon} \oplus \boldsymbol{S}]}{\partial \varepsilon_p^P} = -\sum_{Pp} E^{Pp} \otimes \left(\bar{\boldsymbol{s}}_p^P \boldsymbol{s}_p^P - S^{P2} \right), \tag{6.3}$$

$$F_{\boldsymbol{S}} = \sum_{Pp\alpha} E^{Pp\alpha} \otimes \frac{\partial F[\boldsymbol{\varepsilon} \oplus \boldsymbol{S}]}{\partial s_p^{P\alpha}} = \sum_{Pp} E^{Pp} \otimes \left(\sum_{Qq} h_{Qq}^{Pp} \boldsymbol{s}_q^Q - 2\varepsilon_p^P \boldsymbol{s}_p^P \right). \tag{6.4}$$

The bordered Hessian matrix $\begin{pmatrix} 0 & \bar{F}_{\boldsymbol{S}\boldsymbol{\varepsilon}} \\ F_{\boldsymbol{S}\boldsymbol{\varepsilon}} & F_{\boldsymbol{S}\boldsymbol{S}} \end{pmatrix}$ is composed of the submatrices $F_{\boldsymbol{S}\boldsymbol{S}} = F_{\boldsymbol{S}\boldsymbol{S}}[\boldsymbol{\varepsilon} \oplus \boldsymbol{S}]$ and $F_{\boldsymbol{S}\boldsymbol{\varepsilon}} = F_{\boldsymbol{S}\boldsymbol{\varepsilon}}[\boldsymbol{\varepsilon} \oplus \boldsymbol{S}]$:

$$F_{\boldsymbol{S}\boldsymbol{S}} = \sum_{PQpq\alpha\beta} E_{Qq\beta}^{Pp\alpha} \otimes \frac{\partial^2 F[\boldsymbol{\varepsilon} \oplus \boldsymbol{S}]}{\partial s_p^{P\alpha} \partial s_q^{Q\beta}} = \sum_{PQpq} E_{Qq}^{Pp} \otimes \left(h_{Qq}^{Pp} - 2\varepsilon_p^P \delta_Q^P \delta_q^p \mathbb{1}_3 \right), \tag{6.5}$$

$$F_{\boldsymbol{S}\boldsymbol{\varepsilon}} = \sum_{PQpq\alpha} E_{Qq}^{Pp\alpha} \otimes \frac{\partial^2 F[\boldsymbol{\varepsilon} \oplus \boldsymbol{S}]}{\partial s_p^{P\alpha} \partial \varepsilon_q^Q} = -\sum_{Pp} E_{Pp}^{Pp} \otimes \boldsymbol{s}_p^P. \tag{6.6}$$

The latter is a rectangular matrix of the dimension $3N \times N$.

Note that if $\boldsymbol{S}$ is a stationary point ($F_{\boldsymbol{\varepsilon}} = 0$ and $F_{\boldsymbol{S}} = 0$), the Lagrange multipliers are actually the site energy contributions (4.12) to the total energy, which follows from (6.4). A stationary point $\boldsymbol{S}$ is a local minimum of $\varepsilon^{\mathrm{Cl}}[\boldsymbol{S}]$ on the manifold $\mathcal{S}^{\mathrm{Cl}}$ if $\mathrm{d}\bar{\boldsymbol{S}}\, F_{\boldsymbol{S}\boldsymbol{S}}\, \mathrm{d}\boldsymbol{S} \geq 0$ for each vector $\mathrm{d}\boldsymbol{S}$ from the null-space of $\bar{F}_{\boldsymbol{S}\boldsymbol{\varepsilon}}$ ($\bar{F}_{\boldsymbol{S}\boldsymbol{\varepsilon}} \mathrm{d}\boldsymbol{S} = 0$). Its dimension is $2N$, and a corresponding basis is denoted by the set $\{\boldsymbol{T}_p^{P\alpha} \mid \forall P; p = 1, \ldots, |\boldsymbol{Z}^P|; \alpha = 1, 2\}$. These vectors are used to form the matrix $T = [\ldots, \boldsymbol{T}_p^{P1}, \boldsymbol{T}_p^{P2}, \ldots]$ (columns are $\boldsymbol{T}_p^{P\alpha}$) of the dimension $3N \times 2N$ giving the positive semi-definite $2N$-dimensional matrix $M = \bar{T} F_{\boldsymbol{S}\boldsymbol{S}} T$.

6.2 Symmetry in optimization

As mentioned in the introduction of this Chapter, only the regular ground state arrangements are considered. In general, a transversal, counting sites, is a subset of

the group, and to facilitate the application of the standard group theoretical tools the energy is extended to the sum over the whole group. To this end the stabilizer is incorporated, and due to the condition (2.2) for the regular arrangement (5.5), the energy (4.2) becomes (Theorem B.3.4):

$$\varepsilon^{\mathrm{Cl}}[\boldsymbol{S}_0, D] = \frac{1}{2}\sum_Q |\boldsymbol{Z}^Q| \sum_{Pp} \bar{\boldsymbol{s}}_0^P d^P(\bar{z}_p^P) h_{Q0}^{Pp}(D) \boldsymbol{s}_0^Q. \tag{6.7}$$

where $\boldsymbol{S}_0 = \sum_P E^P \otimes \boldsymbol{s}_0^P$ is the column comprised of the symcell spins. Here, *effective* Hamiltonian $H(D)$ with blocs

$$h_{Qq}^{Pp}(D) \stackrel{\mathrm{def}}{=} \frac{1}{|\boldsymbol{G}|}\sum_g [d^P(\bar{g})a(g)] h_{Qq}^{Pp} [d^Q(\bar{g})a(g)]^T \tag{6.8}$$

is the spin representation depended. Once these blocks are determined the summation in (6.7) is reduced to the neighbours of the symcell sites only. Though the finding of $H(D)$, including the summation over the group seems difficult for crystals, it may be simplified due to symmetry. Namely, the summands in (6.8) are the g-independent tensors h_{Q0}^{Pp} of interactions (of the symcell spins with their neighbours) conjugated by the g-dependent product $d^P(\bar{g})a(g)$ of the representations. When a 3-dimensional matrix A is written as the 9-dimensional column $\mathbf{A} = [A_1^1, A_2^1, A_3^1, \ldots, A_3^3]^T$ (the inverse procedure is obvious), (6.8) gets the form

$$\boldsymbol{h}_{Q0}^{Pp}(D) = P_Q^P(D)\boldsymbol{h}_{Q0}^{Pp}, \quad P_Q^P(D) \stackrel{\mathrm{def}}{=} \frac{1}{|\boldsymbol{G}|}\sum_g [d^P(\bar{g})a(g)] \otimes [d^Q(\bar{g})a(g)]. \tag{6.9}$$

Alternatively, since the substitution of the group elements by their inverses does not affects the sum, the rule $(A \otimes B)(C \otimes D) = (AC) \otimes (BD)$ leads to

$$P_Q^P(D) = \frac{1}{|\boldsymbol{G}|}\sum_g [d^P(g) \otimes d^Q(g)][a(g) \otimes a(g)]^T. \tag{6.10}$$

This allows us to introduce group theoretical apparatus, applying Theorem B.2.1. Indeed, in the notation of (B.2), Equation (6.10) reads

$$\boldsymbol{P}_Q^P(D) = \boldsymbol{G}(d_Q^P)\mathbb{1}, \quad d_Q^P \stackrel{\mathrm{def}}{=} [d^P \otimes d^Q] \otimes [a \otimes a]. \tag{6.11}$$

Here, the 81-dimensional columns $\boldsymbol{P}_Q^P(D)$ and $\mathbb{1}$ originate respectively from $P_Q^P(D)$ and the 9-dimensional identity matrix $\mathbb{1}$ as described above, while

$$\boldsymbol{G}([d^P \otimes d^Q] \otimes [a \otimes a]) = \frac{1}{|\boldsymbol{G}|}\sum_g [d^P \otimes d^Q] \otimes [a \otimes a](g) \tag{6.12}$$

is a group projector. The obtained form enables us to use the advantages developed for the operators (B.2) manifesting in the reducing of the summation over the whole group to the operations involving only group generators g_i: using (B.14) the projector (6.12) is

$$\boldsymbol{G}(d^P_Q) = F\left(\prod_i F\left(d^P_Q(g_i)\right)\right). \tag{6.13}$$

6.2.1 Some special cases

A (classical) Hamiltonian often has more symmetry than it is required by the axiomatic commutation (2.17a) with the (induced) axial representation. A typical example is the time reversal leading to magnetic groups, which are generalized, in a sense, by the spin groups. This inspires a further analysis of the obtained expressions, and some cases when the operator $P^P_Q(D)$ gets simplified forms are singled out here.

Compatibility of axial and spin representations

Let $[\bar{d}^P(g)a(g), d^P(g')] = 0$ for every g, g' and P. Then $\bar{d}^P(\boldsymbol{G})a(\boldsymbol{G})$ is a representation, as well as $[d^P(\bar{g})a(g)] \otimes [d^Q(\bar{g})a(g)]$. Consequently, $P^P_Q(D)$ defined in (6.10) is the group projector efficiently calculated by (B.14):

$$P^P_Q(D) = F\left(\prod_i F\left([d^P(\bar{g}_i)a(g_i)] \otimes [d^Q(\bar{g}_i)a(g_i)]\right)\right). \tag{6.14}$$

This insight may be useful when some suitable forms of interaction tensor are looked for. One may find a set $\{D_{\boldsymbol{\mu}}\}$ of the spin representations having the same projectors $\{P^P_Q(D_{\boldsymbol{\mu}})\}$. If the interaction tensors satisfy $h^{Pp}_{Q0}(D_{\boldsymbol{\mu}}) = h^{Pp}_{Q0}$ (fixed points for P^P_Q), the energy functional becomes

$$\varepsilon^{\mathrm{Cl}}[\boldsymbol{S}_0, \boldsymbol{\mu}] = \frac{1}{2}\sum_Q |\boldsymbol{Z}^Q| \sum_{Pp} \bar{\boldsymbol{s}}^P_0 d^P_{\boldsymbol{\mu}}(\bar{z}^P_p) h^{Pp}_{Q0} \boldsymbol{s}^Q_0. \tag{6.15}$$

It is to be optimized over the spin representations ($\boldsymbol{\mu}$ denotes the spin representations parameters) and the symcell spins $\boldsymbol{S}_0 = \sum_P E^{P0} \otimes \boldsymbol{s}^P_0$.

Compatibility of classical Hamiltonian with spin representations

Besides the first principle conditions on the form of the classical Hamiltonian (4.11), its possible enlarged symmetry may be manifested as the commutation

$$[D(\boldsymbol{G}), H] = 0 \quad \Leftrightarrow \quad h^{Pp}_{Qq} = d^P(\bar{g}) h^{P,gp}_{Q,gq} d^Q(g), \quad g \in \boldsymbol{G}, \tag{6.16}$$

with a spin representation $D(\boldsymbol{G})$. Then combining this with (2.17a), one finds

$$h^{P,\bar{g}p}_{Q,\bar{g}q} = [a(\bar{g}) d^P(g)] h^{P,\bar{g}p}_{Q,\bar{g}q} [a(\bar{g}) d^Q(g)]^\dagger, \quad g \in \boldsymbol{G}. \tag{6.17}$$

The commutation $[D_{\boldsymbol{\mu}}(\boldsymbol{G}), H] = 0$ of the classical Hamiltonian with the spin representations from a class $\{D_{\boldsymbol{\mu}}\}$ leads to the corresponding effective interaction tensors $h^{Pp}_{Qq}(D_{\boldsymbol{\mu}})$, which are all equal to h^{Pp}_{Qq} (Theorem B.3.5); the optimized spin configuration is looked for by the energy (6.15). Still, recall that the requirement that the classical Hamiltonian commutes with the symmetry of the ground state solution is an additional dynamical symmetry of the spin system, and we will assume in the following that this is the case.

6.2.2 Analysis of ground state solutions

Once the ground state regular spin arrangement $\boldsymbol{S} = \sum_{Pp} E^{Pp} \otimes d^P(z^P_p) \boldsymbol{s}^P_0$ is determined, then the state $\boldsymbol{S}^g \stackrel{\text{def}}{=} A(g)\boldsymbol{S}$ for every $g \in \boldsymbol{G}$ is also a ground state arrangement, since $\bar{\boldsymbol{S}} H \boldsymbol{S} = \bar{\boldsymbol{S}} A(\bar{g}) H A(g) \boldsymbol{S}$ due to the commutation (4.11). It is generated (Theorem B.3.8) from the site vector $\boldsymbol{s}^{gP}_0 \stackrel{\text{def}}{=} a(g) d^P(\bar{g}) \boldsymbol{s}^P_0$ by the spin representation $d^{gP}(z^P_p) = a(g) d^P(\bar{g} z^P_p g) a(\bar{g})$, i.e. $\boldsymbol{S}^g = \sum_{Pp} E^{Pp} \otimes d^{gP}(z^P_p) \boldsymbol{s}^{gP}_0$. Precisely, if $\boldsymbol{S}^g = \boldsymbol{S}$, the induced axial representation of the group element g stabilizes the arrangement $\boldsymbol{S}$, and the set of such elements $\boldsymbol{F}_{\boldsymbol{S}} = \{g \mid \boldsymbol{S}^g = \boldsymbol{S} \Leftrightarrow \boldsymbol{s}^{gP}_0 = \boldsymbol{s}^P_0\}$ leaves the arrangement invariant; otherwise the equivalent arrangements (Section 4.2) are obtained, since each new site spin vector $\boldsymbol{s}^{gP}_p = a(g) d^P(\bar{g}) \boldsymbol{s}^P_p$ is the corresponding initial one mapped by the nonsingular matrix $a(g) d^P(\bar{g})$. The set of the arrangements equivalent to $\boldsymbol{S}$ is generated by the transversal $\boldsymbol{Z}_{\boldsymbol{S}} = \boldsymbol{G}/\boldsymbol{F}_{\boldsymbol{S}}$, and the dimension of $\mathrm{span}\{\boldsymbol{Z}_{\boldsymbol{S}} \boldsymbol{S}\}$ is the degeneracy of the ground state.

Chapter 7

Linear theory of spin waves

The objective of this Chapter is the symmetry based analysis of the low-energy spin excitations. The first part of Section 7.1 follows up the general constrained optimization procedure exposed in Section 6.1 in order to give an insight to the mathematical structure of the state space of the spin wave Hamiltonian, quadratic with respect to the bosonic creation and annihilation operators. Its diagonalization is to be performed by the Bogoliubov-Valatin transformation, and a brief reminder of it is presented. Finally, the implementation of symmetry in the diagonalization is developed only for regular arrangements. Still, some difficulties arise and an algorithm to overcome a part of them is proposed.

7.1 Spin wave Hamiltonian

After the quasi-classical ground state $\boldsymbol{S}$ is found, small deviations from it can be analysed. According to the results of Chapter 6.1, such collective deviation $\mathrm{d}\boldsymbol{S} = \sum_{Pp\alpha} c_p^{P\alpha} \boldsymbol{T}_p^{P\alpha}$ is a vector from the null-space $\mathcal{N}(\bar{F}_{\boldsymbol{S}\boldsymbol{\varepsilon}})$. Its energy is

$$\varepsilon^{\mathrm{Cl}}[\mathrm{d}\boldsymbol{S}] = \frac{1}{2}\mathrm{d}\bar{\boldsymbol{S}}\boldsymbol{F}_{\boldsymbol{S}\boldsymbol{S}}\mathrm{d}\boldsymbol{S}. \tag{7.1}$$

The structure of the state space manifold enables us to find the basis vector $\boldsymbol{T}_p^{P\alpha}$ by a reduction to the site spheres $S^2(\boldsymbol{r}_p^P, S^P)$, i.e. by the choice $\boldsymbol{T}_p^{P\alpha} = E^{Pp} \otimes \boldsymbol{t}_p^{P\alpha}$ where $\boldsymbol{t}_p^{P\alpha}$ ($\alpha = 1, 2$) are the unit vectors ($\|\boldsymbol{t}_p^{P\alpha}\| = 1$) from $\mathbb{R}^3$, such that:

$$\bar{\boldsymbol{s}}_p^P \boldsymbol{t}_p^{P\alpha} = 0, \quad \bar{\boldsymbol{t}}_p^{P\alpha} \boldsymbol{t}_p^{P\beta} = \delta_\beta^\alpha. \tag{7.2}$$

The first condition provides that each $\boldsymbol{T}_p^{P\alpha}$ is from $\mathcal{N}(\bar{F}_{\boldsymbol{S}\boldsymbol{\varepsilon}})$, while the second one ensures that the set $\{\boldsymbol{T}_p^{P\alpha} \mid \forall P; p = 1, \ldots, |\boldsymbol{Z}^P|; \alpha = 1, 2\}$ is a basis in that space.

Clearly, the Lie algebra structure of the site space immediately gives such vectors: in the complexified site space one may find CWB $\{\boldsymbol{t}_p^{P\alpha} \mid \alpha = +, -, 3\}$; once the ground state is determined ($\boldsymbol{s}_p^P = S^P \boldsymbol{t}_p^{P3}$ for all P and p), the adjoint representation $\xi \stackrel{\text{def}}{=} \mathrm{i}\,\mathrm{ad}$ of $\boldsymbol{t}_p^{P3}$ (obtained by (2.10)) is to be used since its eigenvectors are $\boldsymbol{t}_p^{P\pm}$ for the eigenvalues ± 1:

$$\xi(\boldsymbol{t}_p^{P3})\boldsymbol{t}_p^{P\pi} = \pi \boldsymbol{t}_p^{P\pi}, \quad \pi = \pm 1, \tag{7.3}$$

while $\boldsymbol{s}_p^P$ is from the null-space of $\xi(\boldsymbol{t}_p^{P3})$.

In this way the Jacobian

$$T = \sum_{Pp} E_{Pp}^{Pp} \otimes t_p^P, \quad t_p^P = [\boldsymbol{t}_p^{P+}, \boldsymbol{t}_p^{P-}], \tag{7.4}$$

composed of the 3×2 matrices t_p^P as sub-matrices on its blocks, is obtained. The range of t_p^P is the tangent space of the site sphere $S^2(\boldsymbol{r}_p^P, S^P)$ at the point $\boldsymbol{s}_p^P$, and consequently, the range of T makes the tangent space $\mathcal{S}^{\mathrm{SW}}$ (isomorphic to $\mathbb{R}^{2N}$) of the manifold $\mathcal{S}^{\mathrm{Cl}}$ at $\boldsymbol{S}$; the Hessian $\boldsymbol{F_{SS}}$ is mapped to

$$M = \bar{T} F_{\boldsymbol{SS}} T = \sum_{PQpq} E_{Qq}^{Pp} \otimes m_{Qq}^{Pp}, \quad m_{Qq}^{Pp} = \bar{t}_p^P \left(h_{Qq}^{Pp} - 2\varepsilon_p^P \delta_Q^P \delta_q^p \mathbb{1}_3 \right) t_q^Q. \tag{7.5}$$

Since the site unit vector $\boldsymbol{t}_p^{P\alpha}$ ($\alpha = \pm$) defines the projection $\hat{S}^{t_p^{P\alpha}}$ of the site spin vector operator, the Hamiltonian of the spin waves is:

$$\hat{H}^{\mathrm{SW}} = \frac{1}{2} \sum_{PQpq\alpha\beta} \tilde{\hat{S}}_p^{P\alpha} m_{Qq\beta}^{Pp\alpha} \tilde{\hat{S}}_q^{Q\beta}, \quad \alpha, \beta = \pm, \tag{7.6}$$

where $\tilde{\hat{S}}_p^{P\pm} = \tilde{\hat{S}}_p^{P\mp}$. Further, using the Holstein-Primakoff transformation [63] the lowering and raising spin operators:

$$\tilde{\hat{S}}_p^{P+} = \sqrt{S^P} \sqrt{1 - \frac{\hat{c}_p^{P+} \hat{c}_p^{P-}}{2S^P}}\, \hat{c}_p^{P-}, \quad \tilde{\hat{S}}_p^{P-} = \sqrt{S^P}\, \hat{c}_p^{P+} \sqrt{1 - \frac{\hat{c}_p^{P+} \hat{c}_p^{P-}}{2S^P}}, \tag{7.7}$$

are expressed in terms of the bosonic annihilation $\hat{c}_p^{P-}$ and creation $\hat{c}_p^{P+}$ operators, with the commutation relations:

$$[\hat{c}_p^{P-}, \hat{c}_q^{Q+}] = \delta_Q^P \delta_q^p, \quad [\hat{c}_p^{P\pm}, \hat{c}_q^{Q\pm}] = 0. \tag{7.8}$$

In the low-temperature approximation $\sqrt{1 - \frac{\hat{c}_p^{P+} \hat{c}_p^{P-}}{2S^P}} \approx 1$, where the total number of the flipped spin is small compared to the total number of spins, the relations (7.7) are

$$\tilde{\hat{S}}_p^{P+} \approx \sqrt{S^P} \hat{c}_p^{P-}, \quad \tilde{\hat{S}}_p^{P-} \approx \sqrt{S^P} \hat{c}_p^{P+}, \tag{7.9}$$

and the spin wave Hamiltonian is:

$$\hat{H}^{\mathrm{SW}} = \frac{1}{2}\hat{\bar{\boldsymbol{C}}} M \hat{\boldsymbol{C}} = \frac{1}{2}\sum_{PQpq}\sum_{\alpha\beta=\pm} \sqrt{S^P S^Q}\,\hat{c}_p^{P\alpha} m_{Qq\beta}^{Pp\alpha} \hat{c}_q^{Q\beta}, \quad \hat{\boldsymbol{C}} = \sum_{Pp} E^{Pp} \otimes \begin{pmatrix} \hat{c}_p^{P-} \\ \hat{c}_p^{P+} \end{pmatrix}. \tag{7.10}$$

Note that the matrix elements of M satisfy: $m_{Qq+}^{Pp+^*} = m_{Qq-}^{Pp-}$ and $m_{Qq-}^{Pp+^*} = m_{Qq+}^{Pp-}$, while its blocks are related as $\bar{m}_{Qq}^{Pp} = m_{Pp}^{Qq}$.

7.1.1 Diagonalization of the spin wave Hamiltonian

To determine the spin wave dispersions and the corresponding states, the new set of bosonic operators $\{\hat{b}_i^\pi \mid \pi = \pm,\ i = 1, \ldots, N\}$ which diagonalize the matrix M needs to be found. This means that in the same space the basis $\hat{b}_i^\pi$ of collective (in contrast to the site associated $\hat{c}_p^{P\pi}$) spin deviations are introduced, with the transformation matrix B:

$$\hat{\boldsymbol{C}} = B\hat{\boldsymbol{B}}, \quad \hat{\boldsymbol{B}} = \sum_i E^i \otimes \begin{pmatrix} \hat{b}_i^- \\ \hat{b}_i^+ \end{pmatrix} \tag{7.11}$$

such that

$$\hat{H}^{\mathrm{SW}} = \frac{1}{2}\hat{\bar{\boldsymbol{B}}}(\bar{B}MB)\hat{\boldsymbol{B}} = \sum_i \omega_i \hat{b}_i^+ \hat{b}_i^- + \frac{1}{2}\sum_i \omega_i. \tag{7.12}$$

The transformation B preserves the bosonic commutation relations of the operators $\hat{b}_i^\pi$ if and only if

$$\Lambda = \bar{B}\Lambda B, \tag{7.13}$$

where the *metric matrix* Λ reflects (7.8):

$$\Lambda = \sum_{Pp} E_{Qq\beta}^{Pp\alpha} \otimes [\hat{c}_p^{P\alpha}, \hat{c}_q^{Q\beta}] = \sum_{Pp} E_{Pp}^{Pp} \otimes \lambda, \quad \lambda = \left(\begin{smallmatrix} 1 & 0 \\ 0 & -1 \end{smallmatrix}\right). \tag{7.14}$$

According to the Bogoliubov-Valatin diagonalization [64,65], the transformation matrix B is composed of the eigenvectors of the dynamical matrix

$$W = \Lambda M = \sum_{PpQq} E_{Qq}^{Pp} \otimes w_{Qq}^{Pp}, \quad w_{Qq}^{Pp} = \lambda m_{Qq}^{Pp}. \tag{7.15}$$

The eigenvalues of W are reals and come in pairs: if there is an eigenvalue $w_i^+ = w_i$, then there is also the opposite sign one, $w_i^- = -w_i$. It is enough to find only a half of the solutions, say vectors $\boldsymbol{W}_i^+$, which correspond to the non-negative eigenvalues. When normalized to 1 with respect to the metric Λ, they yield the vectors $\boldsymbol{B}_i^+$:

$\boldsymbol{B}_i^+ = \frac{\boldsymbol{W}_i^+}{\bar{\boldsymbol{W}}_i^+\Lambda\boldsymbol{W}_i^+}$. The other half is $\boldsymbol{B}_i^- = \Sigma\bar{\boldsymbol{B}}_i^+$, where $\Sigma = \sum_i E_i^i \otimes \sigma$. Finally, arranging them in columns, the matrix $B = [\ldots, \boldsymbol{B}_i^+, \boldsymbol{B}_i^-, \ldots]$ from (7.12) is obtained. Obviously, the relation (7.13) is fulfilled since $\bar{\boldsymbol{B}}_i^\pm \Lambda \boldsymbol{B}_i^\pm = \pm 1$.

This is clarified utilizing the equation of motion (4.3) for the angular momentum $\boldsymbol{s}_p^P + \mathbf{c}_p^P$ with $\mathbf{c}_p^P = \sum_\alpha c_p^{P\alpha}\boldsymbol{t}_p^{P\alpha}$:

$$\frac{\mathrm{d}(\boldsymbol{s}_p^P + \mathbf{c}_p^P)}{\mathrm{d}t} = -(\boldsymbol{s}_p^P + \mathbf{c}_p^P) \times \sum_{Qq} h_{Qq}^{Pp}(\boldsymbol{s}_q^Q + \mathbf{c}_q^Q).$$

By virtue of the stationarity condition (6.4), the linear equation of motion of the site deviation vector $\mathbf{c}_p^P$ is $\frac{\mathrm{d}\mathbf{c}_p^P}{\mathrm{d}t} = -\boldsymbol{s}_p^P \times \sum_{Qq}(h_{Qq}^{Pp} - 2\varepsilon_p^P\delta_Q^P\delta_q^p)\mathbf{c}_q^Q$, or in a more suitable form

$$\frac{\mathrm{d}\mathbf{c}_p^P}{\mathrm{d}t} = -\mathrm{ad}(\boldsymbol{s}_p^P)\sum_{Qq}(h_{Qq}^{Pp} - 2\varepsilon_p^P\delta_Q^P\delta_q^p)\mathbf{c}_q^Q.$$

Its projection onto the vector $\boldsymbol{t}_p^{P\beta}$ is

$$\frac{\mathrm{d}c_p^{P\beta}}{\mathrm{d}t} = -\bar{\boldsymbol{t}}_p^{P\beta}\mathrm{ad}(\boldsymbol{s}_p^P)\sum_{Qq}(h_{Qq}^{Pp} - 2\varepsilon_p^P\delta_Q^P\delta_q^p)\mathbf{c}_q^Q,$$

and the substitution $\mathrm{ad}(\boldsymbol{s}_p^P)\boldsymbol{t}_p^{P\beta} = \beta\mathrm{i}S^P\boldsymbol{t}_p^{P\beta}$ leads to

$$\frac{\mathrm{d}c_p^{P\beta}}{\mathrm{d}t} = -\beta\mathrm{i}S^P\sum_{Qq\alpha}\bar{\boldsymbol{t}}_p^{P\beta}(h_{Qq}^{Pp} - 2\varepsilon_p^P\delta_Q^P\delta_q^p)\mathbf{t}_q^{Q\alpha}c_q^{Q\alpha} = -\beta\mathrm{i}S^P\sum_{Qq\alpha}m_{Qq\alpha}^{Pp\beta}c_q^{Q\alpha}.$$

For a stationary solution $\boldsymbol{B}_i$, the site deviations satisfy $[\boldsymbol{B}_i]_p^{P\beta}(t) = [\boldsymbol{B}_i]_p^{P\beta}\mathrm{e}^{-\mathrm{i}\omega_i t}$, which results in the system of the equations $\omega_i\frac{[\boldsymbol{B}_i]_p^{P\beta}}{\sqrt{S^P}} = \beta\sum_{Qq\alpha}(\sqrt{S^P}m_{Qq\alpha}^{Pp\beta}\sqrt{S^Q})\frac{[\boldsymbol{B}_i]_q^{Q\alpha}}{\sqrt{S^Q}}$. Explicating block forms, this becomes

$$\omega_i[\boldsymbol{B}_i]_p^P = \sum_{Qq}\sqrt{S^P}\lambda m_{Qq}^{Pp}\sqrt{S^Q}[\boldsymbol{B}_i]_p^P, \qquad [\boldsymbol{B}_i]_p^P = \frac{1}{\sqrt{S^P}}\begin{pmatrix}[\boldsymbol{B}_i]_p^{P+}\\ [\boldsymbol{B}_i]_p^{P-}\end{pmatrix}.$$

Visibly, the column $\boldsymbol{B}_i = \sum_{Pp\alpha}E^{Pp\alpha}\otimes[\boldsymbol{B}_i]_p^{P\alpha}$ of the site deviations is an eigenvector of the dynamical matrix (7.15).

7.2 Symmetry of magnons

Once the regular ground state $\boldsymbol{S} = \sum_{Pp}E^{Pp}\otimes d^P(z_p^P)\boldsymbol{s}_0^P$ of some quasi-classical Hamiltonian H with the property (6.16) is determined, the low-energy dynamics is

described by the spin wave Hamiltonian (7.10) which is to be constructed basically from the matrix M defined by (7.5). For the cases we study here, site contributions to the energy are mutually equal $\varepsilon_p^P = \varepsilon_0^P$ (due to Theorem B.3.7 in the view of Theorem B.3.5), giving an obvious extension of (6.16) on the hessian matrix

$$[\boldsymbol{F_{SS}}, D(\boldsymbol{G})] = 0 \quad \Leftrightarrow \quad h_{Qq}^{Pp} - 2\varepsilon_0^P \delta_Q^P \delta_q^p = d^P(\bar{g})(h_{Q,gq}^{P,gp} - 2\varepsilon_0^P \delta_Q^P \delta_q^p) d^Q(g). \quad (7.16)$$

On the other hand, the form of M depends on the site vectors $\boldsymbol{t}_p^{P\pi}$ ($\pi = \pm 1$), which are to be derived from the ground state. Since regular arrangements obey $S^P \boldsymbol{t}_p^{P3} = \boldsymbol{s}_p^P = d^P(z_p^P)\boldsymbol{s}_0^P = S^P d^P(z_p^P)\boldsymbol{t}_0^{P3}$, it follows that $\boldsymbol{t}_p^{P\pi}$ are generated by the same spin representation d^P from the pair of the symcell vectors $\boldsymbol{t}_0^{P\pm}$ according to:

$$\boldsymbol{t}_p^{P\pi} = d^P(z_p^P)\boldsymbol{t}_0^{P\pi\pi^P(z_p^P)}, \quad (7.17)$$

where $\pi^P(g)$ is defined in (5.6). To justify this rule it is sufficient to use in (7.3) the equality $\xi(A\boldsymbol{x}) = A\xi(\boldsymbol{x})\bar{A}\det A$ for an arbitrary orthogonal matrix A to get:

$$\xi(d^P(\bar{z}_p^P)\boldsymbol{t}_p^{P3})\boldsymbol{t}_0^{P\pi\pi^P(z_p^P)} = \pi\pi^P(z_p^P)\boldsymbol{t}_0^{P\pi\pi^P(z_p^P)}.$$

It follows that $\boldsymbol{t}_0^{P\pi\pi^P(z_p^P)}$ is the eigenvector of $\xi(\boldsymbol{t}_0^{P3} = d^P(\bar{z}_p^P)\boldsymbol{t}_p^{P3})$ for the eigenvalue $\pi\pi^P(z_p^P) = \pm 1$. Then, the rest of the vectors (7.17) are the eigenvectors of $\xi(\boldsymbol{t}_p^{P\pi})$ by the presumption.

The similar arguments together with the stabilizer condition (5.4) for a ground state regular arrangement give

$$\boldsymbol{t}_0^{P\pi} = d^P(f^P)\boldsymbol{t}_0^{P\pi\pi^P(f^P)}, \quad f^P \in \boldsymbol{F}^P. \quad (7.18)$$

Finally, inserting (7.17), as well as (7.16), in (7.5), the derivation of the matrix element is straightforward: $m_{Qq\beta}^{Pp\alpha} = \bar{t}_0^{P\alpha\pi^P(z_p^P)} \bar{d}^P(g z_p^P)[h_{Q,gq}^{P,gp} - 2\varepsilon_0^P \delta_Q^P \delta_q^p] d^Q(g z_q^Q) \boldsymbol{t}_0^{Q\beta\pi^P(z_q^Q)}$. Using the group relation (2.3), the right hand side of the central bracket becomes $d^Q(z_{gq}^Q) d^Q(f^Q(g,q))\boldsymbol{t}_0^{Q\beta\pi^Q(z_q^Q)}$. Further, applying successively (7.18) in the convenient form $d^Q(f^Q(g,q))\boldsymbol{t}_0^{Q\beta\pi^Q(z_q^Q)} = \boldsymbol{t}_0^{Q\beta\pi^Q(z_q^Q f^Q(g,q))}$, as well as (7.17) transformed to $d^Q(z_{gq}^Q)\boldsymbol{t}_0^{Q\beta\pi^Q(z_q^Q f^Q(g,q))} = \boldsymbol{t}_{gq}^{Q\beta\pi^Q(z_q^Q f^Q(g,q) z_{gq}^Q)} = \boldsymbol{t}_{gq}^{Q\beta\pi^Q(g)}$, one gets:

$$m_{Qq\beta}^{Pp\alpha} = \bar{\boldsymbol{t}}_{gp}^{P\alpha\pi^P(g)}[h_{Q,gq}^{P,gp} - 2\varepsilon_0^P \delta_Q^P \delta_q^p]\boldsymbol{t}_{gq}^{Q\beta\pi^Q(g)} = m_{Q,gq,\beta\pi^Q(g)}^{P,gp,\alpha\pi^P(g)}.$$

This important relation reveals that ($\Pi^P(g)$ is defined in (5.6)):

$$[M, \Delta(g)] = 0, \quad m_{Qq}^{Pp} = \sigma^{\Pi^P(\bar{g})} m_{Q,gq}^{P,gp} \sigma^{\Pi^Q(g)}, \quad (7.19)$$

where

$$\Delta(g) \stackrel{\text{def}}{=} \bar{T}D(g)T = \sum_{Pp} E_p^{P,gp} \otimes \sigma^{\Pi^P(g)}, \quad \sigma^{\Pi^P(g)} = \bar{t}_p^P d^P(g) t_p^P, \tag{7.20}$$

is a group representation (since $\pi^P(gg') = \pi^P(g)\pi^P(g')$, it is easy to see that $\sigma^{\Pi^P(gg')} = \sigma^{\Pi^P(g)}\sigma^{\Pi^P(g')}$). Due to

$$\sigma^{\Pi^P(g)}\lambda\sigma^{\Pi^P(g)} = \pi^P(g)\lambda, \tag{7.21}$$

the action of the group on Λ is

$$\Delta(g)\Lambda\Delta(\bar{g}) = \sum_{Pp} E_{P,gp}^{P,gp} \otimes \sigma^{\Pi^P(g)}\lambda\sigma^{\Pi^P(g)} = \sum_{Pp} E_{P,gp}^{P,gp} \otimes \pi^P(g)\lambda. \tag{7.22}$$

Further, as $w_{Qq}^{Pp} = \lambda m_{Qq}^{Pp}$, utilizing (7.19) and (7.21) one gets

$$w_{Qq}^{Pp} = \pi^P(g)\sigma^{\Pi^P(\bar{g})} w_{Q,gq}^{P,gp} \sigma^{\Pi^Q(g)}. \tag{7.23}$$

Consequently, $\Delta(\boldsymbol{G})$ does not commute with the dynamical matrix (7.15),

$$\Delta(g)W\Delta(\bar{g}) = \sum_{PpQq} E_{Q,gq}^{P,gp} \otimes \sigma^{\Pi^P(g)} w_{Qq}^{Pp} \sigma^{\Pi^Q(g)} = \sum_{PpQq} E_{Q,gq}^{P,gp} \otimes \pi^P(g) w_{Q,gq}^{P,gp}, \tag{7.24}$$

except in the case when $\pi^P(\boldsymbol{G}) = 1$ for all P. In general, only the positive subgroup $\boldsymbol{G}_+$ (see Section 5.2.1) of $\boldsymbol{G}$ commutes with W.

Thus, the spin wave problem can be solved by the determination of the subgroup $\boldsymbol{G}_+$, and its standard application (Appendix B.1) as the symmetry of a system. This reduction of symmetry is a manifestation of the incompatibility of orbits with regards to their spin-parities. Such an approach *a priori* leads to an unwanted loss of the constraints imposed by the full symmetry, and additionally to the technically more robust problem based on the larger symcell of magnons, which gathers the representatives of the orbits of the positive subgroup. Finally, though such a task is realizable for any concrete system, it is non-trivial enough to be *a priori* solved in general. Nevertheless, when all orbits have the same (though nontrivial) spin-parity, there is an alternative method, based on the full group and its symcell.

7.2.1 Arrangements with the same spin-parity of orbits

In the special case when the spin-parities of all orbits are the same $\pi^P(\boldsymbol{G}) = \pi(\boldsymbol{G})$, the action (7.24) becomes:

$$\Delta(\bar{g}_+)W\Delta(g_+) = \sum_{PpQq} E^{P,\bar{g}_+p}_{Q,\bar{g}_+q} \otimes w^{Pp}_{Qq}, \qquad w^{P,\bar{g}_+p}_{Q,\bar{g}_+q} = w^{Pp}_{Qq}, \quad g_+ \in \boldsymbol{G}_+$$
$$\Delta(\bar{g}_-)W\Delta(g_-) = -\sum_{PpQq} E^{P,\bar{g}_-p}_{Q,\bar{g}_-q} \otimes \sigma w^{Pp}_{Qq}\sigma, \qquad w^{P,\bar{g}_-p}_{Q,\bar{g}_-q} = \sigma w^{Pp}_{Qq}\sigma,$$

or, unified

$$\Delta(\bar{g})W\Delta(g) = \pi(g)W, \quad w^{P,\bar{g}p}_{Q,\bar{g}q} = \sigma^{\Pi(g)} w^{Pp}_{Qq} \sigma^{\Pi(g)}. \tag{7.25}$$

Denoting the eigenvector of W for an eigenvalue ω by $|\omega\rangle$, the relation (7.25) gives $\Delta(g)W\Delta(g)\,|\omega\rangle = \pi(g)W\,|\omega\rangle = \pi(g)\omega\,|\omega\rangle$, which implies

$$W(\Delta(g)\,|\omega\rangle) = \pi(g)\omega(\Delta(g)\,|\omega\rangle). \tag{7.26}$$

Hence, $\Delta(g_-)\,|\omega\rangle$ is also an eigenvector, but for the opposite eigenvalue $-\omega$, which is a manifestation of the chiral symmetry (7.25) of g_-.

Since, $[W, \Delta(\boldsymbol{G}_+)] = 0$, the eigenvectors of W may be chosen to be the SSAB of $\Delta(\boldsymbol{G}_+) = \Delta(\boldsymbol{G}) \downarrow \boldsymbol{G}_+ = \sum_{Pp} E^{P,g+p}_{Pp} \otimes \mathbb{1}_2$. Supposing the decomposition

$$\Delta(\boldsymbol{G}_+) = \oplus_\mu f^\mu d^{(\mu)}(\boldsymbol{G}_+), \tag{7.27}$$

the vectors $\{|\,\mu t_\mu m\rangle \mid \forall \mu; t_\mu = 1, \ldots, f^\mu; m = 1, \ldots, |\mu|\}$ are the eigenvectors of W,

$$W\,|\mu t_\mu m\rangle = \omega_{\mu t_\mu}\,|\mu t_\mu m\rangle, \tag{7.28}$$

with the transformation properties

$$\Delta(g_+)\,|\mu t_\mu m\rangle = \sum_{m'} d^{(\mu)}_{m'm}(g_+)\,|\mu t_\mu m'\rangle. \tag{7.29}$$

Since the dynamical matrix W has paired real eigenvalues, the eigensubspace of a positive eigenvalue $\omega_{\mu t_\mu}$ is $\mathcal{S}^{(\mu t_\mu)}_+ = \text{span}\{|\,\mu t_\mu m\rangle \mid m = 1, \ldots, |\mu|\}$; here m counts the group degeneracy (not the accidental one). According to (7.26) the opposite value eigensubspace is spanned by the vectors $\Delta(g_-)\,|\mu t_\mu m\rangle$ $(m = 1, \ldots, |\mu|)$, which are transformed under the group $\boldsymbol{G}_+$ according to the g_--conjugated irreducible representation $d^{(g-\mu)}(g_+) \stackrel{\text{def}}{=} d^{(\mu)}(\bar{g}_- g_+ g_-)$ of $d^{(\mu)}(\boldsymbol{G}_+)$:

$$\Delta(g_+)(\Delta(g_-)\,|\mu t_\mu m\rangle) = \sum_{m'} d^{(g-\mu)}_{m'm}(g_+)(\Delta(g_-)\,|\mu t_\mu m'\rangle). \tag{7.30}$$

Obviously, the two types of pairing of the opposite value eigenspaces are possible: the set of the vectors fulfilling (7.30) is either a basis (not necessarily adapted with respect to an arbitrary chosen form of IRs of $\boldsymbol{G}_+$) in the space $\mathcal{S}_-^{(\mu',t_\mu)}$ of the different IR of the same dimension ($\mu' \nsim \mu$, $t_\mu = t_{\mu'}$, and $f^\mu = f^{\mu'}$), or $\mathcal{S}_-^{(\mu,t'_\mu)}$, which is the space of the same IR, but for another appearance ($t'_\mu \neq t_\mu$; consequently f^μ is even). The operator $\Delta(g_-)$ connects the irreducible stationary subspaces in the following ways: $\Delta(g_-)\mathcal{S}_+^{(\mu t_\mu)} = \mathcal{S}_-^{(\mu',t_\mu)}$, or $\Delta(g_-)\mathcal{S}_+^{(\mu t_\mu)} = \mathcal{S}_-^{(\mu,t'_\mu)}$.

$\boldsymbol{G}$-SAB and $\boldsymbol{G}_+$-SSAB relations

In the first case there is a nonsingular operator Z in $\mathcal{S}_-^{(\mu',t_\mu)}$ which maps the basis $\{\Delta(g_-)\,|\mu t_\mu m\rangle \mid m = 1,\ldots,|\mu|\}$ into the standard one $|\mu' t_\mu m\rangle = Z(\Delta(g_-)\,|\mu t_\mu m\rangle)$; therefore, (7.30) gives $d^{(\mu')} = \bar{Z} d^{(g_-\mu)} Z$. According to the induction of representations from an invariant index-two subgroup, the set

$$\{|\mu t_\mu m\rangle, \Delta(g_-)\,|\mu t_\mu m\rangle \mid m = 1,\ldots,|\mu|\}$$

forms the multiplet of the whole group $\boldsymbol{G}$ irreducible representation $D^{(\mu^0)}(\boldsymbol{G})$ given by the matrices:

$$D^{(\mu^0)}(g_+) = \begin{pmatrix} d^{(\mu)}(g_+) & 0 \\ 0 & d^{(g_-\mu)}(g_+) \end{pmatrix}, \quad D^{(\mu^0)}(g_-) = \begin{pmatrix} 0 & d^{(\mu)}(g_-^2) \\ \mathbb{1} & 0 \end{pmatrix}, \tag{7.31}$$

of the dimension $|\mu^0| = 2|\mu|$. Using the Theorem B.3.10 we may rewrite:

$$|\mu^0 t_\mu m\rangle = \begin{cases} |\mu t_\mu m\rangle, & 1 \leq m \leq |\mu| \\ \Delta(g_-)\,|\mu t_\mu, m - |\mu|\rangle, & |\mu| < m \leq 2|\mu| \end{cases}. \tag{7.32}$$

In the second mentioned case, for $g_-\mu \sim \mu$, the induced representation (7.31) is not irreducible, but decomposes into the irreducible ones $D^{(\mu^\pm)}(\boldsymbol{G})$:

$$D^{(\mu^\pm)}(g_+) = D^{(\mu)}(g_+), \quad D^{(\mu^\pm)}(g_-) = \pm Z, \tag{7.33}$$

by the matrix $U = \frac{1}{\sqrt{2}}\begin{pmatrix} \mathbb{1} & Z \\ \mathbb{1} & -Z \end{pmatrix}$, i.e. $U D^{(\mu^0)} \bar{U} = D^{(\mu^+)} \oplus D^{(\mu^-)}$. Consequently, the corresponding multiplets $|\,\mu^\pm t_\mu m\rangle$ ($t_\mu = 1,\ldots,\frac{f^\mu}{2}$, since $f^{\mu^+} = f^{\mu^-} = \frac{f^\mu}{2}$) are obtained by the transition matrix U from $\{|\mu^0 t_\mu m\rangle \mid m = 1,\ldots,2|\mu|\}$:

$$|\mu^\pm t_\mu m\rangle = \frac{1}{\sqrt{2}}(|\mu t_\mu m\rangle \pm Z\Delta(g_-)\,|\mu t_\mu m\rangle), \quad 1 \leq m \leq |\mu|. \tag{7.34}$$

From (7.26) it follows that

$$W\,|\mu^0 t_\mu m\rangle = \begin{cases} \omega_{\mu t_\mu}\,|\mu t_\mu m\rangle, & 1 \le m \le |\mu| \\ -\omega_{\mu t_\mu}\Delta(g_-)\,|\mu t_\mu, m-|\mu|\rangle, & |\mu| < m \le 2|\mu| \end{cases} \tag{7.35}$$

$$W\,|\mu^\pm t_\mu m\rangle = \omega_{\mu t_\mu}\,|\mu^\mp t_\mu m\rangle. \tag{7.36}$$

Extension of the eigenproblem

On the other hand, the relation (7.21) may be analysed in the similar manner as (7.25), since λ also has the paired eigenvalues 1 and -1. The corresponding eigenvectors are respectively $|+\rangle$ and $|-\rangle = \sigma^{\Pi(g_-)}\,|+\rangle = \sigma\,|+\rangle$. Both $|\pm\rangle$ are obviously invariant under $\sigma^{\Pi(\boldsymbol{G})} \downarrow \boldsymbol{G}_+ = 2A(\boldsymbol{G}_+)$, where $A(\boldsymbol{G}_+) = \mathbb{1}(\boldsymbol{G}_+)$. The corresponding g_--conjugated IR is equivalent, $A(\bar{g}_- g_+ g_-) = A(g_+)$, and the second type of IR, $A^\pm(\boldsymbol{G})$, is obtained, i.e the decomposition of the representation is $\sigma^{\Pi(\boldsymbol{G})} = \mathbb{1}(\boldsymbol{G}) \oplus \pi(\boldsymbol{G})$ ($A^+(\boldsymbol{G}) = \mathbb{1}(\boldsymbol{G})$, $A^-(\boldsymbol{G}) = \pi(\boldsymbol{G})$).

From the above it follows that one may construct the extended matrix $W \otimes \lambda$ and the representation $\Delta(\boldsymbol{G}) \otimes \sigma^{\Pi(\boldsymbol{G})}$, which mutually commute:

$$[W \otimes \lambda, \Delta(\boldsymbol{G}) \otimes \sigma^{\Pi(\boldsymbol{G})}] = 0. \tag{7.37}$$

The decomposition $\Delta(\boldsymbol{G}) = \oplus_{\mu^\rho} f^{\mu^\rho} D^{(\mu^\rho)}(\boldsymbol{G})$ (here $\rho = 0, \pm$ indicates the type of IR) implies $\Delta(\boldsymbol{G}) \otimes \sigma^{\Pi(\boldsymbol{G})} = \oplus_{\mu^\rho}(f^{\mu^\rho} D^{(\mu^\rho)}(\boldsymbol{G}) \oplus f^{\mu^\rho} D^{(\mu^\rho)}(\boldsymbol{G}) \otimes \pi(\boldsymbol{G}))$. For $\rho = 0$ IR's type, the representation $D^{(\mu^0)}(\boldsymbol{G}) \otimes \pi(\boldsymbol{G})$ is equivalent to $D^{(\mu^0)}(\boldsymbol{G})$, while for $\rho = \pm$ this is not the case, but $D^{(\mu^\pm)}(\boldsymbol{G}) \otimes \pi(\boldsymbol{G}) = D^{(\mu^\mp)}(\boldsymbol{G})$. Therefore, the decomposition of the extended representation is

$$\begin{aligned} \Delta(\boldsymbol{G}) \otimes \sigma^{\Pi(\boldsymbol{G})} &= \oplus_{\mu^\rho} \varphi^{\mu^\rho} D^{(\mu^\rho)}(\boldsymbol{G}), \\ \varphi^{\mu^0} &= 2f^{\mu^0} = 2f^{\mu} = 2f^{\mu'}, \\ \varphi^{\mu^\pm} &= f^{\mu^+} + f^{\mu^-} = f^{\mu} \quad (f^{\mu^+} = f^{\mu^-} = \frac{f^\mu}{2}), \end{aligned} \tag{7.38}$$

and the frequencies in the extended representation are twice as much as the frequencies in $\Delta(\boldsymbol{G})$. This means that it is enough to extend the notation of the SAB of $\Delta(\boldsymbol{G})$ by a new binary counter. It is easy to show, using the Theorem B.3.10, that

the vectors

$$|\,\mu^0 t_\mu m;\omega_{\mu t_\mu}\rangle = \begin{cases} |\,\mu t_\mu m\rangle\,|+\rangle, & 1\le m\le|\mu| \\ \Delta(g_-)\,|\,\mu t_\mu m-|\mu|\rangle\,|-\rangle, & |\mu|<m\le 2|\mu|, \end{cases} \tag{7.39}$$

$$|\,\mu^0 t_\mu m;-\omega_{\mu,t_\mu}\rangle = \begin{cases} |\,\mu t_\mu m\rangle\,|-\rangle, & 1\le m\le|\mu| \\ \Delta(g_-)\,|\,\mu t_\mu, m-|\mu|\rangle\,|+\rangle, & |\mu|<m\le 2|\mu|, \end{cases} \tag{7.40}$$

as well as the vectors

$$|\,\mu^\pm t_\mu m;\omega_{\mu t_\mu}\rangle = \frac{1}{\sqrt{2}}(|\,\mu t_\mu m\rangle\,|+\rangle \pm Z\Delta(g_-)\,|\,\mu t_\mu m\rangle\,|-\rangle),\ 1\le m\le|\mu|, \tag{7.41}$$

$$|\,\mu^\pm t_\mu m;-\omega_{\mu t_\mu}\rangle = \frac{1}{\sqrt{2}}(|\,\mu t_\mu m\rangle\,|-\rangle \pm Z\Delta(g_-)\,|\,\mu t_\mu m\rangle\,|+\rangle),\ 1\le m\le|\mu|, \tag{7.42}$$

are the eigenvectors for $W\otimes\lambda$. Under the action of $\Delta(\boldsymbol{G})\otimes\sigma^{\Pi(\boldsymbol{G})}$ they are transformed according to $D^{(\mu^\rho)}(\boldsymbol{G})$ being thus the standard basis. Note, the additional counter, the eigenvalue of $W\otimes\lambda$, corresponds to the doubled appearance of the corresponding IR in the extended representation with respect to the unextended one.

Obviously, the looked for eigenvectors of W are obtained by the partial scalar product in the second factor space by $|\,\pm\rangle$. Still, in this way found vectors are dependent, and the selection of a basis is to be performed. First, one should take the partial scalar product only of those vectors with the non-negative eigenvalues: for the IRs $\rho=0$ the half of them with $m=1,\dots,|\mu|$ will be non-zero $\langle+\mid\mu^0,t_\mu,m;\omega_{\mu t_\mu}\rangle=|\,\mu t_\mu m\rangle$, while $\langle+\mid\mu^0,t_\mu,m;\omega_{\mu t_\mu}\rangle=0$ for $m=|\mu|,\dots,2|\mu|$; for the IRs $\rho=\pm$ it is enough to take only the vectors corresponding to one IR, e.g. $\sqrt{2}\langle+\mid\mu^+,t_\mu,m;\omega_{\mu t_\mu}\rangle=|\,\mu t_\mu m\rangle$. Finally, note that in (7.31) the special forms of the matrices (suited to the subgroup $\boldsymbol{G}_+$) are assumed. In general, this IR may be given in an equivalent form $UD^{(\mu^0)}\bar{U}$ and then the corresponding multiplet $|\,U\mu^0,t_\mu,m;\omega_{\mu t_\mu}\rangle$ $(1\le m\le|\mu|)$ for the eigenvalue $\omega_{\mu t_\mu}$ will be some linear combination of $|\,\mu t_\mu m\rangle\,|+\rangle$ $(1\le m\le|\mu|)$ and $\Delta(g_-)\,|\,\mu t_\mu m-|\mu|\rangle\,|-\rangle$ $(|\mu|<m\le 2|\mu|)$. Thus, $\langle+\mid U\mu^0,t_\mu,m;\omega_{\mu t_\mu}\rangle\sim|\,\mu t_\mu m\rangle$ for all m will give twice as much vectors than it is needed and one must select only $|\mu|$ linear independent among them.

Types of the IRs

To determine the type of the IR μ^ρ in the decomposition (7.38) it is enough to determine whether $\mathrm{Tr}\,\boldsymbol{G}(D^{(\mu)}\otimes D^{(\nu)^*})$ is equal to 1 (for equivalent IRs), or it

is 0 (inequivalent ones). The projector $\boldsymbol{G}(D^{(\mu)} \otimes D^{(\nu)^*})$ of the type (B.2) is easily calculated even for infinite groups using the elaborated technique to obtain it in the form (B.14). Thus, the first of the relations

$$\mathrm{Tr}\,\boldsymbol{G}(D^{(\mu^\rho)} \otimes \pi \otimes D^{(\mu^\rho)^*}) = \begin{cases} 1, & \rho = 0 \\ 0, & \rho = \pm \end{cases}, \tag{7.43}$$

$$\mathrm{Tr}\,\boldsymbol{G}(D^{(\mu^+)} \otimes \pi \otimes D^{(\mu^-)^*}) = \mathrm{Tr}\,\boldsymbol{G}(D^{(\mu^-)} \otimes \pi \otimes D^{(\mu^+)^*}) = 1, \tag{7.44}$$

differs between the types of IRs μ^ρ, and the second one gives the paired IRs among them as far as the type $\rho = \pm$ is considered.

Calculation on the symcell

Since the eigenvectors of the extended matrix $W \otimes \lambda = (M \otimes \mathbb{1}_2)(\Lambda \otimes \lambda)$ are to be found, the modified group projector technique (Appendix B.1) turns out to be an efficient one. The frequency numbers in the decomposition (7.38) are

$$\varphi^{\mu^\rho} = \sum_P \varphi_P^{\mu^\rho}, \quad \varphi_P^{\mu^\rho} = \mathrm{Tr}\boldsymbol{F}^P(\gamma^{P\mu^\rho}), \tag{7.45}$$

where

$$\gamma^{P\mu^\rho}(\boldsymbol{F}^P) = \sigma^{\Pi(\boldsymbol{F}^P)} \otimes \sigma^{\Pi(\boldsymbol{F}^P)} \otimes D^{(\mu^{\rho *})}(\boldsymbol{F}^P), \quad \boldsymbol{F}^P(\gamma^{P\mu^\rho}) = \frac{1}{|\boldsymbol{F}^P|} \sum_{f^P} \gamma^{P\mu^\rho}(f^P).$$

For each[1] IR μ^ρ one needs to pull-down to the symcell space the extended operators $M \otimes \mathbb{1}_2 \otimes \mathbb{1}_{\mu^\rho}$ and $\Lambda \otimes \lambda \otimes \mathbb{1}_{\mu^\rho}$, i.e.

$$\begin{aligned} (M \otimes \mathbb{1}_2)^{\downarrow}_{0\mu^\rho} &= \sum_{PQ} E^{P0}_{Q0} \otimes \sqrt{\frac{|\boldsymbol{F}^P|}{|\boldsymbol{F}^Q|}} \boldsymbol{F}^P(\gamma^{P\mu^\rho})(M \otimes \mathbb{1}_2)^{\mu^\rho}_{PQ}, \\ (M \otimes \mathbb{1}_2)^{\mu^\rho}_{PQ} &= \sum_p (\sigma^{\Pi(\bar{z}^P_p)} \otimes \sigma^{\Pi(\bar{z}^P_p)})(m^{Pp}_{Q0} \otimes \mathbb{1}_2) \otimes D^{(\mu^{\rho *})}(\bar{z}^P_p), \\ (\Lambda \otimes \lambda)^{\downarrow}_{0\mu^\rho} &= \sum_P E^{P0}_{P0} \otimes \boldsymbol{F}^P(\gamma^{P\mu^\rho})(\lambda \otimes \lambda \otimes \mathbb{1}_{\mu^\rho}). \end{aligned} \tag{7.46}$$

Then the task is reduced to the eigenproblem of $(W \otimes \lambda)^{\downarrow}_{0\mu^\rho} = (M \otimes \mathbb{1}_2)^{\downarrow}_{0\mu^\rho}(\Lambda \otimes \lambda)^{\downarrow}_{0\mu^\rho}$, i.e. $(W \otimes \lambda)^{\downarrow}_{0\mu^\rho}\ |\mu^\rho t_\mu; \pm\omega_{\mu t_\mu}\rangle^0 = \pm\omega_{\mu t_\mu}\ |\mu^\rho t_\mu; \pm\omega_{\mu t_\mu}\rangle^0$ ($t_\mu = 1, \ldots, \varphi^{\mu^\rho}/2 = f^\mu$) giving

[1] Actually, it is not necessary to do what follows for the paired IRs of the type $\rho = \pm$; it is enough to perform the procedure only for one of them.

φ^{μ^ρ} vectors which corresponds to the eigenvalues $\pm\omega_{\mu t_\mu}$ of W (Equation (7.28)), where μ are the representations appearing in the decomposition (7.27). The obtained vectors $\mid \mu^\rho t_\mu; \pm\omega_{\mu t_\mu}\rangle^0 = \sum_P E^{P0}\otimes \mid \mu^\rho t_\mu; \pm\omega_{\mu t_\mu}\rangle^{P0}$, being from the range of the projector $\boldsymbol{G}^{\downarrow}(\Delta\otimes\sigma\otimes d^{(\mu^{\rho *})})$, are to be normalized with respect to the metric from (7.47), i.e. ${}^0\langle\mu^\rho t_\mu; \pm\omega_{\mu t_\mu}\mid (\Lambda\otimes\lambda)^{\downarrow}_{0\mu^\rho}\mid \mu^\rho t_\mu; \pm\omega_{\mu t_\mu}\rangle^0 = \pm 1$. Finally, arranging them into a matrix, the diagonal form of $(M\otimes \mathbb{1}_2)^{\downarrow}_{0\mu^\rho}$ is achieved, since:

$$ {}^0\langle\mu^\rho t_\mu; \pi\omega_{\mu t_\mu}\mid (M\otimes\mathbb{1}_2)^{\downarrow}_{0\mu^\rho}\mid \mu^\rho t'_\mu; \pi'\omega_{\mu t'_\mu}\rangle^0 = \omega_{\mu t_\mu}\delta_{t_\mu t'_\mu}\delta_{\pi\pi'},\quad \pi,\pi' = \pm. \tag{7.47} $$

If, in addition, one needs to find the explicit form of vectors that diagonalize M, it is enough to take only those which corresponds to the non-negative eigenvalues $\mid \mu^\rho t_\mu; \omega_{\mu t_\mu}\rangle^0$ and the partial scalar product is to be carried out with $\mid \mu^{\rho *} m\rangle$ (see Equation (B.12)). Then the pulling-up (B.13)

$$ \begin{aligned} \mid \mu^\rho t_\mu m; \omega_{\mu t_\mu}\rangle &= \sum_{Pp} E^{Pp}\otimes \mid \mu^\rho t_\mu m; \omega_{\mu t_\mu}\rangle^{Pp}, && (7.48)\\ \mid \mu^\rho t_\mu m; \omega_{\mu t_\mu}\rangle^{Pp} &= \sigma^{\Pi(z_p^P)}\otimes\sigma^{\Pi(z_p^P)}\sum_{m'} D^{(\mu^{\rho *})}_{mm'}(z_p^P)\mid \mu^\rho t_\mu m'; \omega_{\mu t_\mu}\rangle^{P0}, && (7.49)\\ \mid \mu^\rho t_\mu m; \omega_{\mu t_\mu}\rangle^{P0} &= \langle \mu^{\rho *} m\mid \mu^\rho t_\mu; \omega_{\mu t_\mu}\rangle^{P0}, \end{aligned} $$

gives the vectors (7.39) or (7.41) depending on the IRs type. The another partial scalar product leads to:

$$ \begin{aligned} \langle +\mid \mu^\rho t_\mu m; \omega_{\mu t_\mu}\rangle &= \sum_{Pp} E^{Pp}\otimes\langle +\mid \mu^\rho t_\mu m; \omega_{\mu t_\mu}\rangle^{Pp},\\ \langle +\mid \mu^\rho t_\mu m; \omega_{\mu t_\mu}\rangle^{Pp} &= \sigma^{\Pi(z_p^P)}\sum_{m'} D^{(\mu^{\rho *})}_{mm'}(z_p^P)\langle \pi(z_p^P)\mid \mu^\rho t_\mu m'; \omega_{\mu t_\mu}\rangle^{P0}. && (7.50) \end{aligned} $$

As elaborated, the linear independent ones are to be determined. Since they form just a half of the needed vectors, the other half is obtained by the action of $\Delta(g_-)$ on each of them.

Chapter 8

Applications to ^{13}C nanotubes

Symmetry based analysis is performed on ^{13}C single wall nanotubes [67–69]. Though this approach assumes nanotubes completely built of C^{13} isotope, the findings should be relevant for the realistic samples, which achieve even 99% purity. In metallic ones, the RKKY interaction stabilizes nuclear spins (of magnitude $S = 1/2$) in helimagnetic order [70]. However, for semiconducting nanotubes the itinerant electrons are induced when the chemical potential is tuned to the conduction band which is split by the spin-orbit interaction [71]. The resulting interesting scenarios with a variety of ground states, giving insight to the ordering in Q1D systems, could have a number of applications [72, 73].

After a brief reminder on the symmetries of nanotubes, their spin groups are singled out as the relevant entities for symmetries of regular magnetic arrangements. Then the expression for energy of such magnetic configurations with an arbitrary spin susceptibility tensor is found, as well as the form of the corresponding dynamical matrix. Recently determined [71] spin susceptibility tensor treating thoroughly RKKY interaction is singled out as the relevant dynamical model. This makes a necessary framework to look for the ground state and the consequently low-energy excitations in ^{13}C nanotubes. For infinite tubes, analysis of the short and long range contributions is sufficient to find the ground state exactly. An insight to the behaviour of the spin susceptibility is used as a hint to get an analytical estimation of the ground state in agreement with complementary performed numerical calculations. Finally, summarizing the obtained results we stress out their universality in the sense that there is essentially a single phase diagram referring to all semiconducting nanotubes (when the parameters are suitably scaled); symmetry based

interpretation of this feature gives rise to further generalization to other nanowires.

8.1 General symmetry analyses

A physically plausible interaction model for Q1D systems such as nanotubes assumes that itinerant electrons are confined to the cylinder of diameter D. Accordingly, the spin susceptibility χ is a tensor field over the cylinder: $\chi(\boldsymbol{r}_\ell, \boldsymbol{r}_{\ell'}) = \chi(\Delta_{\ell\ell'})$, where $\Delta_{\ell\ell'} = (\Delta\varphi_{\ell\ell'}, \Delta z_{\ell\ell'})$, i.e. χ depends on the oriented cylindrical arc length between sites with the coordinates $\boldsymbol{r}_\ell = (D/2, \varphi_\ell, z_\ell)$ and $\boldsymbol{r}_{\ell'} = (D/2, \varphi_\ell + \Delta\varphi_{\ell\ell'}, z_\ell + \Delta z_{\ell\ell'})$. As an inherent property of the system, this field shares its symmetry. As shown in Section 3.3, such lattices are described by the cylindrical susceptibility tensor (3.8) allowing the longitudinal component of the Dzyaloshinskii-Moriya vector in addition to the XXZ Heisenberg terms and frustration is unavoidable. This introduces further complexity into rich phase diagrams [74] of Q1D systems. Carbon nanotubes, with the 5th family line group symmetry considered below, illustrate the general situation.

8.1.1 Geometry

Single wall carbon nanotube [75–77] is a graphene ribbon rolled up into the cylinder of circumference $c = a_0\sqrt{N}$, with $N = {n_1}^2 + n_1 n_2 + {n_2}^2$ corresponding to chiral vector $\boldsymbol{c} = n_1\boldsymbol{a}_1 + n_2\boldsymbol{a}_1$ where $\boldsymbol{a}_1 = \frac{a_0}{2}(\sqrt{3}\boldsymbol{e}^1 - \boldsymbol{e}^2)$ and $\boldsymbol{a}_2 = \frac{a_0}{2}(\sqrt{3}\boldsymbol{e}^1 + \boldsymbol{e}^2)$ (graphene period $a_0 = |\boldsymbol{a}_1| = |\boldsymbol{a}_2| = 2.461$Å) are the unit cell vectors of the graphene honeycomb lattice and n_1, n_2 are integers. Thus, a SWCNT is characterized by chiral indexes (n_1, n_2), or alternatively by chiral angle θ between $\boldsymbol{a}_1$ and $\boldsymbol{c}$, i.e. $\cos\theta = \frac{\boldsymbol{a}_1\boldsymbol{c}}{|\boldsymbol{a}_1||\boldsymbol{c}|} = \frac{2n_1+n_2}{2\sqrt{N}}$, and diameter $D = \frac{|\boldsymbol{c}|}{\pi} = \frac{a_0\sqrt{N}}{\pi}$. Zig-zag and armchair nanotubes have the chiral indexes $n_1 = n_2 > 0$ and $n_1 > n_2 = 0$ respectively, while those with $n_1 > n_2 > 0$ are chiral. If $\delta = (2n_1 + n_2) \bmod 3 = -(n_1 - n_2) \bmod 3$ is ± 1 the nanotube is semiconducting, while for $\delta = 0$ it is metallic. Translations of SWCNT are generated by the vector $\boldsymbol{a} = \frac{n_1+2n_2}{n\mathcal{R}}\boldsymbol{a}_1 - \frac{2n_1+n_2}{n\mathcal{R}}\boldsymbol{a}_2$ perpendicular to $\boldsymbol{c}$, where $n = \mathrm{GCD}(n_1, n_2)$, while $\mathcal{R} = \mathrm{GCD}(\frac{2n_1+n_2}{n}, \frac{n_1+2n_2}{n})$ is equal to 3 if $\frac{(n_1-n_2)}{3n}$ is an integer or 1 otherwise. The graphene unit cell contains two atoms, positioned at $\frac{1}{3}(\boldsymbol{a}_1 + \boldsymbol{a}_2)$ and $\frac{2}{3}(\boldsymbol{a}_1 + \boldsymbol{a}_2)$; they define two graphene sublattices. In the translational period $a = |\boldsymbol{a}| = \frac{\sqrt{3N}}{n\mathcal{R}}a_0$ of a SWCNT there are $2q$ atoms, where $q = \frac{2N}{n\mathcal{R}}$.

Full symmetry of a SWCNT is described by the fifth family line group [46, 78], $\boldsymbol{L}^{(5)} = \boldsymbol{T}_Q(f)\boldsymbol{D}_n = \boldsymbol{L}^{(1)} + U\boldsymbol{L}^{(1)}$ if it is chiral, and by the thirteenth family one,

$\boldsymbol{L}^{(13)} = \boldsymbol{T}_{2n}(f)\boldsymbol{D}_{n\mathrm{h}} = \boldsymbol{L}^{(5)} + \sigma_{\mathrm{h}}\boldsymbol{L}^{(5)}$ if it is achiral. Line group parameters of non-relaxed nanotubes [79] are functions [46, 78] of n_1 and n_2; namely, $f = an/q$ and $Q = q/r$ with $r = \frac{n_1+2n_2-(\frac{n_2}{n})^{\mathrm{Eu}(\frac{n_2}{n})-1}q\mathcal{R}}{n_1\mathcal{R}} \mathrm{mod} \frac{q}{n}$. All nanotubes, including achiral ones, are generated by the fifth family line groups, making these groups sufficient to analyse the properties we are interested in. Since the elements of the fifth family line group are $\ell = \ell_{tsu} = (C_Q|f)^t C_n^s U^u$ ($t = 0, \pm 1, \ldots$, $s = 0, \ldots, n-1$ and $u = 0, 1$), sites of a nanotube are counted by an additiononal index u with respect to the first family orbit (2.5):

$$\boldsymbol{r}_{tsu} = \ell_{tsu}\boldsymbol{r}_0 = (\frac{D}{2}, (-1)^u\varphi_0 + 2\pi(\frac{rt}{q} + \frac{s}{n}), (-1)^u z_0 + t\frac{n}{q}a), \tag{8.1}$$

where the cylindrical coordinates of the orbit representative $\boldsymbol{r}_0 = \boldsymbol{r}_{000}$ in the frame xyz (conventionally, the tube axis is the z-direction) are

$$\boldsymbol{r}_0 = (\frac{D}{2}, \varphi_0, z_0), \quad \varphi_0 = 2\pi\frac{n_1+n_2}{nq\mathcal{R}}, \quad z_0 = \frac{n_1-n_2}{\sqrt{6nq\mathcal{R}}}a_0. \tag{8.2}$$

The atoms on a cross-section (the xy-plane) of the tube are counted by s, those differing only by t are on a helix along the tube, while u distinguishes two graphene sublattices. For a fixed t one gets a monomer with $2n$ atoms. Site $\boldsymbol{r}_{tsu}$ makes with $\boldsymbol{r}_0$ arch defined by:

$$\begin{aligned} \Delta\varphi_{tsu} &= \Delta\varphi_{0,tsu} = -2\delta_{u,1}\varphi_0 + 2\pi(\frac{tr}{q} + \frac{s}{n}), \\ \Delta z_{tsu} &= \Delta z_{0,tsu} = -2\delta_{u,1}z_0 + tf. \end{aligned} \tag{8.3}$$

8.1.2 Magnetic orders

Tightly related to the nanotube geometrical symmetry is the form of the corresponding spin susceptibility tensor

$$\chi(\Delta_{tsu}) = \begin{pmatrix} \chi^{xx}(\Delta_{tsu}) & \chi^{xy}(\Delta_{tsu}) & 0 \\ -\chi^{xy}(\Delta_{tsu}) & \chi^{xx}(\Delta_{tsu}) & 0 \\ 0 & 0 & \chi^{zz}(\Delta_{tsu}) \end{pmatrix}, \quad \Delta_{tsu} = (\Delta\varphi_{tsu}, \Delta z_{tsu}). \tag{8.4}$$

Also, possible symmetries of the arrangement of nuclear spins are described by the fifth family spin line groups [60]. Following Equation (5.5) the site spins $\boldsymbol{s}_{tsu}$ are generated from $\boldsymbol{s}_0$ by spin representations: for even n there are 8 non-equivalent classes $c = 0, u, s, s+u, t, t+u, t+s, t+s+u$ with matrices

$${}_{\tilde{k}}d^c_{\tilde{m}}(\ell_{tsu}) = \begin{pmatrix} \cos(\phi_{ts}^{\tilde{k}\tilde{m}}) & -(-1)^u\sin(\phi_{ts}^{\tilde{k}\tilde{m}}) & 0 \\ \sin(\phi_{ts}^{\tilde{k}\tilde{m}}) & (-1)^u\cos(\phi_{ts}^{\tilde{k}\tilde{m}}) & 0 \\ 0 & 0 & (-1)^c \end{pmatrix}, \quad \begin{matrix} \tilde{k}\in[0, \frac{\pi}{f}] \\ \tilde{m}\in(-\frac{n}{2}, \frac{n}{2}] \end{matrix} \tag{8.5a}$$

Table 8.1: Real irreducible representations of $\boldsymbol{L}^{(5)} = \boldsymbol{T}_Q(f)\boldsymbol{D}_n$ (matrices of the generators) given by the symbol ($D^{(\mu)}$) and corresponding quantum numbers (μ). Two-dimensional matrix $R(\varphi)$ is the rotation for the angle φ and parity Π_U takes the values ± 1.

$D^{(\mu)}$	μ	$(C_Q\|f)$	C_n	U
${}_{\tilde{k}}E_{\tilde{m}}$	$\tilde{k}\in(0,\frac{\pi}{f})$ $\tilde{m}\in(-\frac{n}{2},\frac{n}{2}]$	$R(\tilde{k}f)$	$R(\tilde{m}\frac{2\pi}{n})$	$\left(\begin{smallmatrix}1 & 0\\ 0 & -1\end{smallmatrix}\right)$
${}_{\tilde{k}}C^{\Pi_U}_{\tilde{m}}$	$\tilde{k}=0,\frac{\pi}{f}$ $\tilde{m}=0,\frac{n}{2}$	$\mathrm{e}^{\mathrm{i}\tilde{k}f}$	$\mathrm{e}^{\mathrm{i}\tilde{m}\frac{2\pi}{n}}$	Π_U

($\phi_{ts}^{\tilde{k}\tilde{m}}$ as in (5.8)), while non-equivalent diagonal spin representations are

$$\mathrm{diag}[(-1)^{c_1},(-1)^{c_2},(-1)^{c_3}]. \tag{8.5b}$$

Among the latter, 32 are included in the classes (for $\tilde{k}=0,\frac{\pi}{f}$ and $\tilde{m}=0,\frac{n}{2}$), and the remaining 88 are exceptional. For the odd n there are 4 classes ($c=0,u,t,t+u$) and 12 exceptional representations (altogether 20 diagonal ones). The SRs (8.5) are nothing but the combinations of RIRs into the forms (5.7), since the RIRs of the fifth family line groups are 1- and 2-dimensional as tabulated in 8.1. The most general form of SRs is additionally characterized by the Euler angles.

8.1.3 Ground states

For single orbit systems such as SWCNT, the compatibility (6.17) is reduced to $[a(\bar{\ell})d(\ell),\chi(\bar{\ell}\Delta_{tsu})]=0$ for any group element ℓ. This leads to the compatibility of the nanotube spin susceptibility (8.4) with the whole class (8.5a) of spin representations. Thus, the averaged energy of the regular spin arrangement

$$\varepsilon[\boldsymbol{s}_0,\tilde{k},\tilde{m},c]=\frac{J^2}{2}\sum_{tsu}\bar{\boldsymbol{s}}_{0\tilde{k}}d^c_{\tilde{m}}(\ell_{tsu})\chi(\Delta_{tsu})\boldsymbol{s}_0, \tag{8.6}$$

is to be optimized over the spin representation quantum numbers and the initial spin vector $\boldsymbol{s}_0$. Note that there are also equivalent forms of SRs, e.g. extensions by rotations around the z-axis, satisfying (6.17). Besides these, the diagonal SRs having $c_2=u+c_1$ ($c_3\neq c_1\neq c_1+u$) are also compatible with the susceptibility. However, it turns out that SRs (8.5a) are sufficient for the ground state determination.

In fact, the form of the susceptibility tensor allows us to separate the energy of planar (the xy-plane) and linear (the z-axis) arrangements. Thus, in the planar

case, when $\boldsymbol{s}_0 = \cos\phi_0 \boldsymbol{e}_x + \sin\phi_0 \boldsymbol{e}_y$, the energy per site is the function

$$\begin{aligned} \varepsilon^{(\tilde{k},\tilde{m},\phi_0)} &= \sum_{tsu} \varepsilon_{tsu}^{(\tilde{k},\tilde{m},\phi_0)}, \qquad (8.7a) \\ \varepsilon_{tsu}^{(\tilde{k},\tilde{m},\phi_0)} &= \frac{J^2}{2}\left(\chi^{xx}(\Delta_{tsu})\cos(\Delta\phi_{tsu}^{\tilde{k}\tilde{m}}) + \chi^{xy}(\Delta_{tsu})\sin(\Delta\phi_{tsu}^{\tilde{k}\tilde{m}})\right) \end{aligned}$$

of two continual parameters $\tilde{k}$, ϕ_0 and discrete one $\tilde{m}$ (here, $\Delta\phi_{tsu}^{\tilde{k}\tilde{m}} = -2\delta_{u,1}\phi_0 + \phi_{ts}^{\tilde{k}\tilde{m}}$ is the difference $\phi_{tsu}^{\tilde{k}\tilde{m}} - \phi_0$ of the azimuthal angles of $\boldsymbol{s}_{tsu}$ and $\boldsymbol{s}_0$). The geometrical meaning of the quantum numbers of the spin representations in this context is enlightened: $\frac{2\pi}{n}\tilde{m} = \phi_{t,s+1,u}^{\tilde{k}\tilde{m}} - \phi_{tsu}^{\tilde{k}\tilde{m}}$ and $\tilde{k}f = \phi_{t+1,s,u}^{\tilde{k}\tilde{m}} - \phi_{tsu}^{\tilde{k}\tilde{m}}$ are the angles between the spins of the closest sites along cross sections and along tube helices, respectively. In the view of Subsection 6.2.2, in the general case (when ground the SR and axial one differ) the induced axial representation (B.6) is not symmetry of the ground state, and in the planar case it introduces mutually rotated arrangements (vectors $a(\ell_{tsu})_{\tilde{k}} d^c_{tm}(\bar{\ell}_{tsu})\boldsymbol{s}_0$ span the xy-plane). The same holds for all other SRs of the classes (as they commute with the Hamiltonian, but do not fix the ground state), which results in the additional $\mathrm{SO}(2,\mathbb{R})$ continual degeneracy of the ground state. Thus, ϕ_0 essentially characterizes not a spin direction, but only the angle $-2\phi_0$ between $\boldsymbol{s}_{ts0}$ and $\boldsymbol{s}_{ts1}$ of the different sublattices. This clarify that SRs (8.5a) are sufficient to find ground state arrangements and why their equivalent forms are not taken into account in (8.6). In addition, (8.5a) also corresponds to the cases when a planar arrangement is invariant under a diagonal SR of the form $\mathrm{diag}[(-1)^{c_1}, (-1)^{c_1+u}, (-1)^{c_3}]$, e.g. the planar arrangement generated by the diagonal SR with $c_1 = s$ are recovered by the SRs of the type ${}_0d^c_{n/2}$. Specially, for $\phi_0 = 0$ or $\pi/2$ the spins on the two sublattices are mutually aligned parallel or anti-parallel; if in addition $\tilde{m} = 0, \pi/2$ and $\tilde{k} = 0, \pi/f$ various linear arrangements along the x- or the y-axis are obtained.

For linear arrangements with $\boldsymbol{s}_0 = \boldsymbol{e}_z$, the energies are

$$\varepsilon^c = \sum_{tsu} \varepsilon^c_{tsu}, \quad \varepsilon^c_{tsu} = \frac{J^2}{2}(-1)^c \chi^{zz}(\Delta_{tsu}). \qquad (8.7b)$$

There is the finite number of such arrangements, each corresponding to one c which determines the orientation of $\boldsymbol{s}_{tsu}$ along the z-axis. In contrast to the planar case, they are axially invariant and thus non-degenerated. Both the arrangements with site spins $\boldsymbol{s}_{tsu}$ and $a(U)_{\tilde{k}} d^c_{\tilde{m}}(U)\boldsymbol{s}_{tsu} = -\boldsymbol{s}_{tsu}$ ($c = 0, s, t$) have the same energy, but this can not be account as degeneracy since they are linearly dependent vectors (of the form (4.6)) in $\mathcal{S}^{\mathrm{Cl}}$ (see Subsection 6.2.2).

Finally, the energies (8.7) are to be mutually compared to obtain the ground state. The range of the interaction is included as the number N of neighbors along the z-axis restricting sums to $t = -N, \ldots, N$; for further purposes N will be used as the interaction cut-off.

8.1.4 Magnons

Whether the ground state arrangement is planar or linear, it is surely generated by a SR which fulfills (7.16) and the theory exposed in Section 7.2 is applicable.

Let us discuss the planar ground arrangement, described by the triple $(\tilde{k}_0, \tilde{m}_0, \phi_0)$, corresponding to the minimal energy $\varepsilon^{(\tilde{k}_0,\tilde{m}_0,\phi_0)}$ of (8.7a). The arbitrariness of the class c of the spin representation ${}_{\tilde{k}_0}d^c_{\tilde{m}_0}$ which generates the arrangement allows us to take $c = u$ giving the positive spin-parity, since $\det\left({}_{\tilde{k}_0}d^c_{\tilde{m}_0}\right) = (-1)^{c+u}$ for all ℓ_{tsu}. Hence, the representation (7.20) is $\Delta(\ell) = \sum_{\ell'} E^{\ell\ell'}_{\ell'} \otimes \mathbb{1}_2$, and commutes both with M and Λ. This immediately establishes the framework necessary to apply the MGPT (Appendix B) in the diagonalization of the dynamical matrix (7.15).

Indeed, since $[\Delta(\ell), W] = 0$, the pulled-down dynamical matrix W, spin wave Hamiltonian and metric are:

$$\begin{aligned} W^{\downarrow}_{0\mu} &= \Lambda^{\downarrow}_{0\mu} M^{\downarrow}_{0\mu} = \sum_{tsu} w^{tsu}_0 \otimes D^{(\mu^*)}(\bar{\ell}_{tsu}), \quad w^{tsu}_0 = \lambda m^{tsu}_0, \\ M^{\downarrow}_{0\mu} &= \sum_{tsu} m^{tsu}_0 \otimes D^{(\mu^*)}(\bar{\ell}_{tsu}), \\ \Lambda^{\downarrow}_{0\mu} &= \lambda \otimes \mathbb{1}_\mu. \end{aligned} \tag{8.8}$$

here, $D^{(\mu)}$ goes over the irreducible representations of the fifth family line group. The Jacobian matrix (7.4) is composed of the site vectors

$$\boldsymbol{t}^{\pi}_{tsu} =_{\tilde{k}_0} d^u_{\tilde{m}_0}(\ell_{tsu})\boldsymbol{t}^{\pi}_0 = \frac{1}{\sqrt{2}} \begin{pmatrix} \mathrm{i}\pi(-1)^u \sin\left(\phi^{\tilde{k}_0\tilde{m}_0}_{ts} + (-1)^u\phi_0\right) \\ -\mathrm{i}\pi(-1)^u \cos\left(\phi^{\tilde{k}_0\tilde{m}_0}_{ts} + (-1)^u\phi_0\right) \\ (-1)^u \end{pmatrix}, \tag{8.9}$$

where $\boldsymbol{t}^{\pi}_0$ are the eigenvectors of $\xi(\boldsymbol{s}_0) = \begin{pmatrix} 0 & 0 & \sin\phi_0 \\ 0 & 0 & -\cos\phi_0 \\ -\sin\phi_0 & \cos\phi_0 & 0 \end{pmatrix}$ corresponding to the eigenvalues $\pi = \pm 1$. According to (7.5), the vectors (8.9) are used to evaluate the matrix elements

$$m^{tsu,\pi'}_{0,\pi} = (-1)^u \left(\varepsilon^0_{tsu} + \pi\pi' \varepsilon^{(\tilde{k}_0\tilde{m}_0\phi_0)}_{tsu}\right) - \delta_{\pi\pi'}\delta_{0,tsu} 2\varepsilon^{(\tilde{k}_0,\tilde{m}_0,\phi_0)},$$

of the two-dimensional blocks m_0^{tsu}, where the site energies $\varepsilon_{tsu}^{(\tilde{k}_0\tilde{m}_0\phi_0)}$ and ε_{tsu}^0 are defined in (8.7). Inserting this in (8.8) and using the two-dimensional RIRs from Table 8.1 leads to the 4-dimensional matrix

$$\begin{aligned} W^{\downarrow}_{0(\tilde{k},\tilde{m})} &= \sum_{tsu}(-1)^u \begin{pmatrix} \varepsilon^0_{tsu}+\varepsilon^{(\tilde{k}_0\tilde{m}_0\phi_0)}_{tsu} & \varepsilon^0_{tsu}-\varepsilon^{(\tilde{k}_0\tilde{m}_0\phi_0)}_{tsu} \\ -\varepsilon^0_{tsu}-\varepsilon^{(\tilde{k}_0\tilde{m}_0\phi_0)}_{tsu} & -\varepsilon^0_{tsu}+\varepsilon^{(\tilde{k}_0\tilde{m}_0\phi_0)}_{tsu} \end{pmatrix} \otimes_{\tilde{k}} E_{\tilde{m}}(\bar{\ell}_{tsu}) \\ &- 2\begin{pmatrix} \varepsilon^{(\tilde{k}_0,\tilde{m}_0,\phi_0)} & 0 \\ 0 & -\varepsilon^{(\tilde{k}_0,\tilde{m}_0,\phi_0)} \end{pmatrix} \otimes \mathbb{1}_2. \end{aligned} \tag{8.10a}$$

For each $\tilde{k}$ and $\tilde{m}$ it has the eigenvalues $\pm\omega_{\tilde{m}}(\tilde{k})$ with eigenvectors $\mid(\tilde{k},\tilde{m}),\pm,m\rangle^0$ $(m=1,2)$ normalized as ${}^0\langle(\tilde{k},\tilde{m}),\pm,m \mid \lambda\otimes\mathbb{1}_2 \mid (\tilde{k},\tilde{m}),\pm,m\rangle^0 = \pm 1$. These vectors make the transformation matrix diagonalizing $M^{\downarrow}_{0(\tilde{k},\tilde{m})}$ by the congruence. The partial scalar product with vectors $\binom{1}{0}$ and $\binom{0}{1}$ gives the zero site vectors which are distributed on the rest of the sites by (B.13). The action of the matrix (7.4), composed of (8.9), gives the directions of site deviations. Thus, $\omega_{\tilde{m}}(\tilde{k})$ is the spin wave dispersion in the interval $\tilde{k}\in(0,\pi/f)$ where $\tilde{m}$ counts the branches. The values on the boundaries $\tilde{k}=0,\pi/f$ of the reduced Brillouin zone $[0,\pi/f]$ are determined by the one-dimensional RIRs (see Table 8.1) for which (8.8) is:

$$\sum_{tsu}(-1)^{u-c}\begin{pmatrix} \varepsilon^0_{tsu}+\varepsilon^{(\tilde{k}_0\tilde{m}_0\phi_0)}_{tsu} & \varepsilon^0_{tsu}-\varepsilon^{(\tilde{k}_0\tilde{m}_0\phi_0)}_{tsu} \\ -\varepsilon^0_{tsu}-\varepsilon^{(\tilde{k}_0\tilde{m}_0\phi_0)}_{tsu} & -\varepsilon^0_{tsu}+\varepsilon^{(\tilde{k}_0\tilde{m}_0\phi_0)}_{tsu} \end{pmatrix} - 2\begin{pmatrix} \varepsilon^{(\tilde{k}_0\tilde{m}_0\phi_0)} & 0 \\ 0 & -\varepsilon^{(\tilde{k}_0\tilde{m}_0\phi_0)} \end{pmatrix}. \tag{8.10b}$$

For each of the four RIRs a two-dimensional eigenproblem is to be solved. In particular, for $c=u$ (RIR ${}_0C_0^-$) one obtains $W^{\downarrow}_{0u} = \begin{pmatrix} \varepsilon^0-\varepsilon^{(\tilde{k}_0\tilde{m}_0\phi_0)} & \varepsilon^0-\varepsilon^{(\tilde{k}_0\tilde{m}_0\phi_0)} \\ -\varepsilon^0+\varepsilon^{(\tilde{k}_0\tilde{m}_0\phi_0)} & -\varepsilon^0+\varepsilon^{(\tilde{k}_0\tilde{m}_0\phi_0)} \end{pmatrix}$ giving the single Goldstone boson which corresponds to the global rotations around the z-axis. This has been already seen as continual degeneracy of the ground state. Nevertheless, the form of the dynamical matrix for this mode is not Bogoliubov-Valatin diagonalizabile [64,65] indicating the possibility of an unstable state [80,81] in the sense that quantum fluctuations may destroy the static spin order. Obviously, if $\varepsilon^0=\varepsilon^{(\tilde{k}_0\tilde{m}_0\phi_0)}$ site spins are ferromagnetically aligned, i.e. the ground state is $\mathrm{O}(3,\mathbb{R})$ degenerated.

Concerning linear arrangements along the z-axis, i.e. $\boldsymbol{s}_{tsu}=(-1)^c\boldsymbol{s}_0$, with $\boldsymbol{s}_0=\boldsymbol{e}_z$, the spin waves analysis is omitted here: it will be shown (Section 8.2) that for ^{13}C nanotubes the ground state belongs to the planar case. Let us only mention that for the cases with $c=0,t,s$ the spin representations have negative spin-parities and excitations are to be obtained using the algorithm described in Section 7.2.1.

8.2 ^{13}C nanotubes

The quite general approach elaborated above indicates the universality of the ground states and low-energy excitations. However, to get more refined results for ^{13}C nanotubes a concrete model of the spin susceptibility is utilized in the following text.

8.2.1 Spin susceptibility tensor

The reciprocal lattice of a SWCNT is determined by $\bar{\boldsymbol{k}}_\perp \boldsymbol{c} = 2\pi$, $\bar{\boldsymbol{k}}_\perp \boldsymbol{a} = 0$, $\bar{\boldsymbol{k}}\boldsymbol{c} = 0$ and $\bar{\boldsymbol{k}}\boldsymbol{a} = 2\pi$, from which follows that $k = \frac{2\pi}{a}$ ($k \in (-\frac{\pi}{a}, \frac{\pi}{a}]$) and $k_\perp^m = \frac{2m}{D}$ (takes discreet values $m = -q/2+1, \ldots, q/2$). The energy dispersions of SWCNT, in the zone folding approximation (thus non-relaxed [79]), are obtained by cutting the two dimensional dispersions of graphene along the lines determined by the tops of the allowed vectors $\boldsymbol{k}_\perp^m + \boldsymbol{k}$, where m is a band index. The low-energy physics takes place in the vicinities of the Dirac points of graphene, where the dispersions have well known conical shape $\epsilon(\boldsymbol{k}) = \pm\hbar v_F|\boldsymbol{k}|$ ($v_F = 10^{-6}\,\mathrm{m/s}$). The projection of the Dirac point $\boldsymbol{K} = \frac{1}{3}(2\boldsymbol{k}_1 + \boldsymbol{k}_2)$ on the chiral vector is $\frac{2}{D}(M + \frac{\delta}{3})$, with an integer

$$M = \frac{2n_1 + n_2 - \delta}{3}, \tag{8.11a}$$

while on the tube axis, it is

$$K = \frac{2\pi n_2}{an\mathcal{R}}. \tag{8.11b}$$

Here, $\boldsymbol{k}_1 = \frac{4\pi}{2a_0\sqrt{3}}(\boldsymbol{e}_1 + \sqrt{3}\boldsymbol{e}_2)$ and $\boldsymbol{k}_2 = \frac{4\pi}{2a_0\sqrt{3}}(\boldsymbol{e}_1 - \sqrt{3}\boldsymbol{e}_2)$ are graphene reciprocal lattice orts. Then, cutting the Dirac cone at $\boldsymbol{K}$ by the allowed planes determined by m, a set of hyperbolas is obtained:

$$\epsilon_m(k) = \pm\hbar v_F \sqrt{\left(\frac{2}{D}(m - M - \frac{\delta}{3})\right)^2 + k^2}. \tag{8.12}$$

The closest to $\boldsymbol{K}$ energy band is with $m = M$; for semiconducting nanotubes the gap is $\frac{4\hbar v_F}{D}$, while for metallic ones the dispersion is linear and gapless.

The inclusion of the spin-orbit interaction gives

$$\epsilon_m(k) = \beta s + \hbar v_F \sqrt{\left(\frac{\alpha s}{\hbar v_F} - \frac{2}{D}(m - M - \frac{\delta}{3})\right)^2 + k^2}, \quad s = \pm 1, \tag{8.13}$$

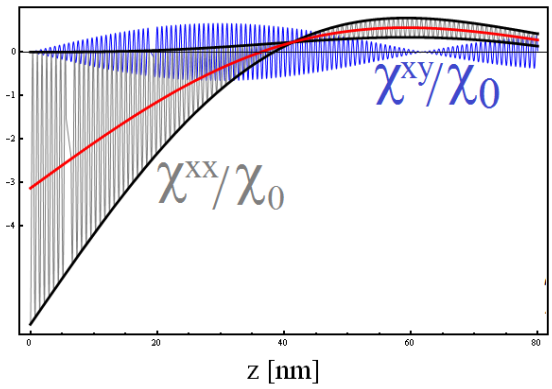

Figure 8.1: Dimensionless susceptibility functions χ^{xx}/χ_0 (gray) and χ^{xy}/χ_0 (blue) of the nanotube (17,6) for $\mu = 0.5$ meV and $\varphi = 0$ as the functions of length. The averaged function of envelopes (black) of χ^{xx}/χ_0 is the red one.

causing the splitting of the energy bands (8.12) by $\Delta = 2|\alpha+\beta|$, where $\alpha = -\frac{0.16\,\mathrm{meV}}{D\,[\mathrm{nm}]}$ and $\beta = -\frac{0.62\,\mathrm{meV}\cos 3\theta}{D\,[\mathrm{nm}]}$ are spin-orbit parameters [82].

If the chemical potential $\mu > 0$ crosses the conduction bands, there appear conduction electrons and consequently the RKKY interaction among nuclear spins. The states corresponding to (8.13) were used [71] in the perturbation technique to obtain the components of the spin susceptibility tensor (Figure 8.1):

$$\begin{aligned}
\chi^{zz}(\Delta_{tsu}) &= \chi_0\left[S(k_{++},|\Delta z_{tsu}|)+S(k_{--},|\Delta z_{tsu}|)+2\cos(2X_{tsu})S(k_{-+},|\Delta z_{tsu}|)\right],\\
\chi^{xx}(\Delta_{tsu}) &= \chi_0\left[2S(k_{-+},|\Delta z_{tsu}|)+\cos(2X_{tsu})[S(k_{++},|\Delta z_{tsu}|)+S(k_{--},|\Delta z_{tsu}|)]\right],\\
\chi^{xy}(\Delta_{tsu}) &= \chi_0\sin(2X_{tsu})\left[S(k_{++},|\Delta z_{tsu}|)-S(k_{--},|\Delta z_{tsu}|)\right]; \qquad (8.14)
\end{aligned}$$

here $S(k,z) = \mathrm{sgn}(k)\mathrm{si}(k|z|)$, $\mathrm{si}(x) = \int_0^x \frac{\sin t}{t}dt - \frac{\pi}{2}$, $X_{tsu} = K\Delta z_{tsu} + M\Delta\varphi_{tsu}$ and $\chi_0 = \frac{a_0^2 k_G}{2\pi\hbar v_F}$. The wave numbers $k_{\eta\eta'}$ (referring to k_{-+}, k_{--} and k_{++}) depend on the chemical potential $\mu \geq 0$. Precisely, $k_{++} = \frac{4}{U}\sqrt{\frac{\mu}{D}}$, with $U = \sqrt{3\hbar v_F} = 44.44\,\mathrm{meV}^{\frac{1}{2}}\mathrm{nm}^{\frac{1}{2}}$; if the chemical potential is inside the SO interaction gap, i.e. for $0 < \mu \leq \Delta$, then $k_{-+} = k_{++}/2$ and $k_{--} = 0$, while for $\mu > \Delta$ (above the gap) $k_{-+} = \frac{2}{U}(\sqrt{\frac{\mu}{D}} + \sqrt{\frac{\mu-\Delta}{D}})$ and $k_{--} = \frac{4}{U}\sqrt{\frac{\mu-\Delta}{D}}$.

8.2.2 Analytical approach to ground states

Despite the complexity of the susceptibility functions, in some limiting cases it is possible to analyse the ground state analytically.

Namely, inserting (8.14) in (8.7) and applying the identities $\sum_{s=0}^{n-1}\cos\frac{2\pi p}{n}s = n\delta_n^p$ and $\sum_{s=0}^{n-1}\sin\frac{2\pi p}{n}s = 0$ for integers n, s, and p, the energy of the planar arrangement (8.7a) is

$$\begin{aligned}\varepsilon^{(\tilde{k}\tilde{m}\phi_0)}(N) &\propto \sum_{t=-N}^{N}\sum_{u=0}^{1}[\delta_0^{\tilde{m}}2S(k_{-+},\Delta z_{t0u})\cos(\Delta\phi_{t0u}^{\tilde{k}0}) \\ &+ \sum_{\eta=\pm1}\delta_{2\eta M}^{\tilde{m}}S(k_{\eta\eta},\Delta z_{t0u})\cos(2X_{t0u}-\eta\Delta\phi_{t0u}^{\tilde{k}0})],\end{aligned} \tag{8.15a}$$

where $\delta_x^{\tilde{m}} = 1$ if $\tilde{m}-x$ is a multiple of n, otherwise 0. Analogously, for the linear magnetic order the energy (8.7b) becomes

$$\begin{aligned}\varepsilon^{c}(N) &\propto \sum_{t=-N}^{N}\sum_{s=0}^{n-1}\sum_{u=0}^{1}(-1)^c[2S(k_{-+},\Delta z_{tsu})\cos(2X_{tsu}) \\ &+ S(k_{++},\Delta z_{tsu})+S(k_{--},\Delta z_{tsu})].\end{aligned} \tag{8.15b}$$

To this end we extend the energy (8.7b) to the function

$$f^z_{\tilde{k},\tilde{m},\Pi} = \sum_{tsu}\cos(\tilde{k}ft+\tilde{m}\frac{2\pi}{n}s+\Pi\pi u)\chi^{zz}(\Delta_{tsu})$$

of continual parameters $\tilde{k}$ and Π, coinciding with the physically relevant ε^c only for $\tilde{k} = 0,\pi/f$, $\tilde{m} = 0,n/2$ and $\Pi = 0,1$. Consequently, (8.15b) is extended also, and summation in s gives

$$\begin{aligned}f^z_{\tilde{k},\tilde{m},\Pi}(N) \propto n\sum_{t=-N}^{N}\sum_{u=0,1}\sum_{\eta=\pm1}[&\delta_0^{\tilde{m}}S(k_{\eta\eta},\Delta z_{t0u})\cos(\Delta\phi_{t00}^{\tilde{k}0}+\Pi\pi u)) \\ +&\delta_{2\eta M}^{\tilde{m}}S(k_{-+},\Delta z_{t0u})\cos(2X_{t0u}-\eta(\Delta\phi_{t00}^{\tilde{k}0}+\Pi\pi u))].\end{aligned} \tag{8.16}$$

Both (8.15a) and (8.16) consist of the terms of the form

$$g(-N,N) = \sum_{t=-N}^{N}\sum_{u=0,1}\mathrm{S}(k_{\eta\eta'},\Delta z_{t0u})\cos\Psi_{tu}$$

multiplied by $\delta_x^{\tilde{m}}$, which are replaced by

$$g(-N,N) = g(-N^f+1,N^f-1)+\sum_{t=N^f}^{N}\sum_{\substack{u=0,1\\ \rho=\pm1}}\mathrm{sgn}(k_{\eta\eta'})\mathrm{si}(k_{\eta\eta'}(tf-2\rho\delta_{u,1}z_0))\cos\Psi_{\rho t,u},$$

where N^f is a finite integer grater than $2\delta_{u,1}z_0/f$.

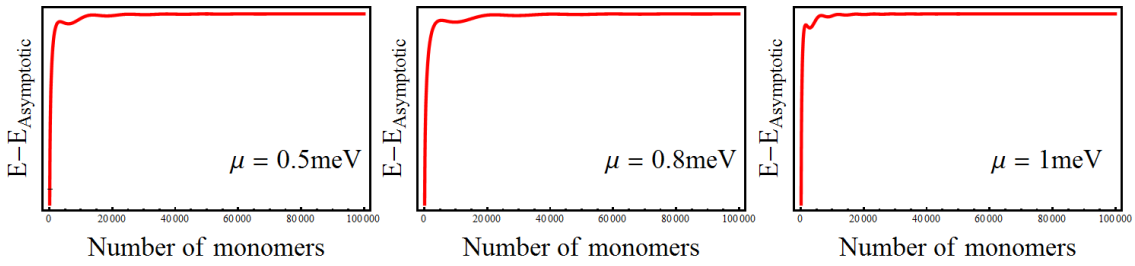

Figure 8.2: Differences between the energy and it's asymptotic form for the nanotube (17,6) as functions of the range of interactions for various regimes. The differences are finite and converge by increasing the range of interaction.

Infinite length nanotubes

The long range of the RKKY interaction suggests that total energy is dominated by its asymptotic behavior. Precisely, for arbitrary finite N^f, the sum in t, grouped for $|t| < N^f$ and for $N^f \leq |t| \leq N$, leads to the energy $\varepsilon(N) = \varepsilon(N^f) + \varepsilon(N^f, N)$ divided in the short and the long range parts; then, it is physically plausible to expect that for infinite tubes (large N limit), the contribution of the arbitrary finite part $\varepsilon(N^f)$ of the tube around the central ion, is overwhelmed by that of the rest of the tube, $\varepsilon(N^f, N)$. In the forthcoming analysis this is first justified and then used to obtain an analytical solution for the optimal arrangement.

Along this line, we start by substituting the large x asymptotic approximation $\mathrm{si}(x) \sim -\frac{\cos x}{x}$ in (8.15a). Clearly, for infinite N and sufficiently large N^f, the long range contribution $\varepsilon^{\mathrm{as}}(N^f, N)$ is approximately equals to $\varepsilon(N^f, N)$. Then, $\varepsilon(N) \approx \varepsilon(N^f) + \varepsilon^{\mathrm{as}}(N^f, N)$, and if in the same limit $\varepsilon^{\mathrm{as}}(N^f, N)$ diverges at the point (regular arrangement) of its minima (as we are going to show), then exactly the same point minimizes also $\varepsilon(N)$ due to the obvious finiteness of $\varepsilon(N^f)$ (Figure 8.2).

To find the minima of $\varepsilon^{\mathrm{as}}(N^f, N)$ and perceive the mentioned divergencies, we firstly use trigonometry to decompose $\varepsilon^{\mathrm{as}}(N^f, N)$ into several summands, each being a product of either $\delta_0^{\tilde{m}}$ or $\delta_{2\eta M}^{\tilde{m}}$ with a trigonometric function of the general form $f(x, y) = -\sum_{t=N^f}^{N} \alpha_t \cos(xt + y)$. Here, the factor $\alpha_t = n\,\mathrm{sgn} k_{\eta\eta'}/[f k_{\eta\eta'}(t - F)]$ is positive, since N^f can be always taken to be greater than the small geometrical constant $F = \pm 2\delta_{u1} z_0/f$ (less than 15 for the nanotubes with diameter less than 3 nm); x and y are term dependent combinations of regular arrangement parameters

$\tilde{k}$ and ϕ_0. For instance, one of the terms for $u = 1$ is

$$-n\delta_0^{\tilde{m}} \frac{\mathrm{sgn} k_{-+}}{f k_{-+}} \sum_{t=N^f}^{N} \frac{\cos\left[(k_{-+} - \tilde{k}) f t + k_{-+} z_0 - \phi_0\right]}{t + 2z_0/f}.$$

As $k_{\eta\eta'} \geq 0$, the function $f(x, y)$ is minorized by

$$-\sum_{t=N^f}^{N} \alpha_t = n \mathrm{sgn} k_{-+} [\psi(N^f - F) - \psi(1 - F + N)]/f k_{\eta\eta'}$$

(ψ is the digamma function); it reaches this minimum for the regular arrangement parameters such that $\cos(xt + y) = 1$ is satisfied for each t, i.e. in the points $(x_i, y_j) = (2\pi i, 2\pi j)$ (i, j arbitrary integers) which solve this equation. For large N, the constant $\psi(N^f - F)$ is negligible in comparison to logarithmically divergent $\psi(1 - F + N)$. Then, the absolutely minimal value of $\varepsilon^{\mathrm{as}}$ comes from the term with minimal positive $k_{\eta\eta'}$. The corresponding (x_i, y_j) determine $\tilde{k}_0$ and ϕ_0 of the ground states. This gives a clear algorithm to find the ground state.

Before we find the ground state, two comments may further enlighten the obtained result. First, the ratio $2z_0/f$ is a purely geometric characteristic of a nanotube, and for the semiconducting ones it is a number of the form $p \pm \frac{1}{3}$, with integer p; consequently, independently of N^f, none of the summands α_t diverges, and the total difference $\varepsilon(N) - \varepsilon^{\mathrm{as}}(N)$ must be finite (as a function of N, it converges to some finite value, through oscillations with a rapid dumping, as can be easily seen numerically). Thus, the obtained logarithmic divergence of a single site energy is strictly cumulative effect, stemming from the long range nature of the RKKY interaction. This hints that the described method of the determination of the ground state may be suitable for other such systems. Second, it is clear that for sufficiently large finite N optimal configuration of the corresponding finite length nanotube is arbitrarily close to the ground state of the infinite one found in this way; this offers a valuable criterion in validation of the numerical results on the finite nanotubes (Section 8.2.2).

Directly applying the described prescription to the planar case (8.15a), one instantly finds that for regular arrangements with $\tilde{m} = 0$, the minimal energy

$$\varepsilon^{(\tilde{k}^\nu, 0, \phi_0^\nu)}(N) \propto \frac{-2n \,\mathrm{sgn} k_{-+}}{f k_{-+}/2} \psi(N) \tag{8.17a}$$

is for $\tilde{k}^\nu = \nu k_{-+}$, $\phi_0^\nu = \nu k_{-+} z_0$ (here $\eta, \nu = \pm 1$). For $\tilde{m}^\eta = 2\eta M$ the minima at

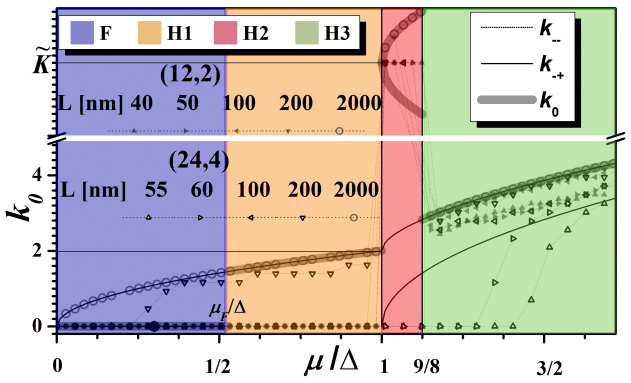

Figure 8.3: Ground state as a function of the chemical potential. Presented dependence $k_0 = \tilde{k}_0 U\sqrt{D/\Delta}$ of μ/Δ is universal for infinite tubes. Wide solid line is analytical prediction: ferromagnetic order, $\tilde{k}_0 = 0$, is retained until estimated μ_F (depicted for $L = 100\,\mathrm{nm}$); then follow long limit values showing H1, H2 and H3 regimes. Degenerate solutions $-\tilde{k}_0$ are omitted. For two tubes numerical results for different lengths L (indicated within the Figure) are depicted by symbols and dotted eye guides.

$\tilde{k}^{\eta\nu} = \eta[\frac{4\pi}{fq}(Mr + n_2) - \nu k_{\eta\eta}]$ and $\phi_0^{\eta\nu} = \eta[2(M\varphi_0 + Kz_0) - \nu k_{\eta\eta} z_0]$ give

$$\varepsilon^{(\tilde{k}^{\eta\nu}, \tilde{m}^{\eta}, \phi_0^{\eta\nu})}(N) \propto \frac{-2n\,\mathrm{sgn}\,k_{\eta\eta}}{f k_{\eta\eta}}\psi(N). \tag{8.17b}$$

Note that equalities in $\tilde{k}$ and $\tilde{m}$ are modulo their ranges given in (5.8). Thus, the ground state arrangement corresponds to the term with the minimal non-vanishing among the positive wave numbers $k_{-+}/2$, k_{++} and k_{--}. Analysing the linear case one obtains that the minima $\frac{-n\,\mathrm{sgn}k_{-+}}{f k_{-+}}\psi(N)$ and $\frac{-n\,\mathrm{sgn}k_{\eta\eta}}{f k_{\eta\eta}}\psi(N)$ of the asymptotic form of $f^z_{\tilde{k},\tilde{m},\Pi}$ are greater than those of the planar arrangements; moreover, the minimal points differ from the physically relevant ones, meaning that $\varepsilon^c(N)$ is even greater. Thus, the ground state is always a planar helical arrangement.

Finally, depending on the chemical potential, three regimes occur (Figure 8.3), with planar helimagnetic ground states of nuclear spins characterized by the triples $\tilde{m}_0$, $\tilde{k}_0$ and ϕ_0:

H1. $0 < \mu \leq \Delta$; minimal wave number $k_{-+}/2$ leads to double degenerate solution of (8.17a): $\tilde{m}_0 = 0$ with $\tilde{k}_0 = k_{-+}$, $\phi_0 = k_{-+}z_0$ and $\tilde{k}_0 = -k_{-+}$, $\phi_0 = -k_{-+}z_0$.

H2. $\Delta < \mu \leq 9\Delta/8$; preferred wave number k_{--} selects two degenerate minima from (8.17b): $\tilde{m}_0 = -2M$ with $\tilde{k}_0 = \tilde{K} \pm k_{--}$, $\phi_0 = -2(M\varphi_0 + Kz_0) \pm k_{--}z_0$; here, $\tilde{K} = -\frac{4\pi}{qf}(Mr + n_2)$ is defined by the nanotube (as is explained after (8.15a)).

H3. $\mu > 9\Delta/8$: solutions are the same as for H1.

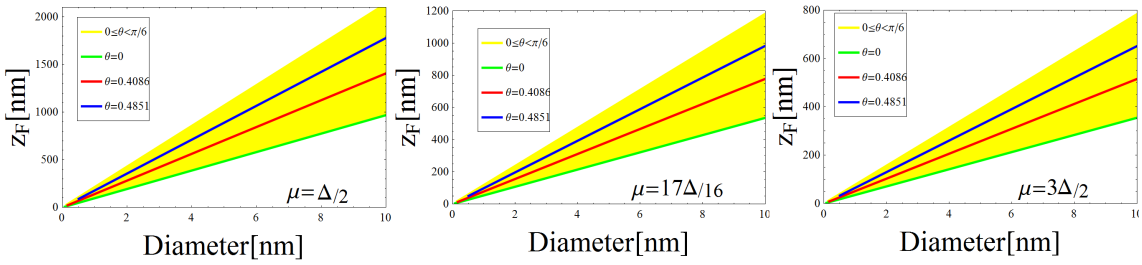

Figure 8.4: Dependence of the ferromagnetic interaction range on the tube diameter for various chiral angles in the first (left), the second (middle) and the third (right) regime.

Besides the considered symmetries of nanotubes, the interaction model is invariant under time reversal Θ. Reversing all momenta, Θ equalizes energies of the arrangements with opposite $\tilde{k}$ and $\tilde{m}$, providing that $-\tilde{k}_0$, $-\tilde{m}_0$ and $-\phi_0$ is the degenerate ground state of the opposite chirality. This doubles degeneracy only in the second regime: the energy does not depend on the sign of k_{--} and k_{-+}; in H1 and H3 this coincides with Θ degeneracy, but in H2 $\tilde{K} \pm k_{--}$ degeneracy is extended to $-\tilde{K} \pm k_{--}$ by Θ.

Finite length nanotubes

The above considerations, concerning sufficiently long tubes (large N), are to be completed by an insight to the tubes of realistic lengths L. As a function of z, the Heisenberg component [71] has rapid oscillations (with period na/n_2) between upper and lower envelopes, both negative for small z. The averaged envelope $2S(k_{-+}, z)$ slowly oscillates with damping, being negative until the first root at $k_{-+}z_F = 1.926$. Thus, χ^{xx} tends to parallelize spins spaced less than z_F. Further, damped fast oscillations of χ^{xy} introduce frustration, but in the region $k_{-+}z_F \le 1.926$ it is less than χ^{xx}, and the ferromagnetic pairwise interaction dominates; i.e., the tubes of length $L < 1.926/k_{-+}$ are ferromagnetically ordered. The expressions for k_{-+} show that z_F increases with D for fixed μ and ϑ, but for fixed tube z_F decreases with μ (Figure 8.4). Thus, there is a nanotube dependent critical value $\mu_F(D, \vartheta)$, after which frustration is significant. In this way a more complex phase diagram arises (Figure 8.5): $\mu_F = \frac{3.71DU^2}{4L^2}$ is linear in D until the H2 regime is reached, and then $\mu_F = \frac{(3.71D^2U^2+4\Delta DL^2)^2}{59.35D^3L^2U^2}$; i.e., it decreases but slower than the curves delimiting helical phases. Therefore, for $D > D_1 = 0.02L\sqrt{0.32 + 1.24\cos 3\vartheta}$ the ferromagnetic phase

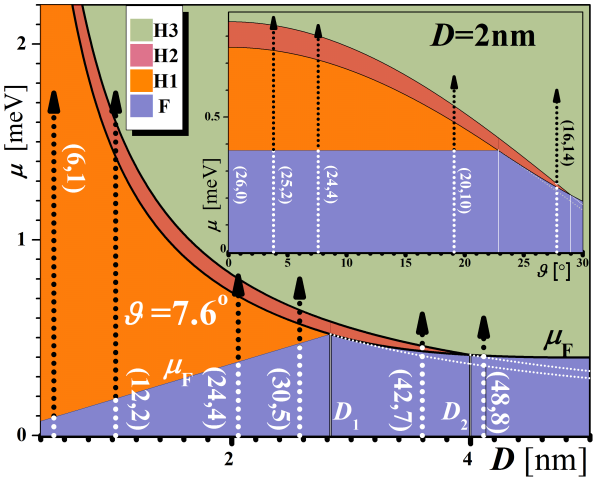

Figure 8.5: D-μ and ϑ-μ (inset) phase diagrams. Different colors stand for helical phases H1, H2 and H3, as well as for the approximate region of length dependent (here $L = 100\,\mathrm{nm}$) ferromagnetic phase F. Dotted arrows indicate tubes with $\vartheta = 7.6°$ on D-μ, and with $D \approx 2\,\mathrm{nm}$ on ϑ-μ diagram (as a pair, selected D and ϑ correspond only to the tube (24,4)). For μ_F, D_1 and D_2 see Section 8.2.2.

completely overrides phase H1, and for $D > D_2 = \sqrt{2}D_1$, increase of μ changes ferromagnetic phase directly to H3. For smaller ϑ the shorter tubes are sufficient to get the full range of μ controlled phases (Figure 8.5, inset). Let us emphasize that the ferromagnetic region is only roughly estimated; more insight is obtained numerically.

8.2.3 Numerical verification

These results, obtained analytically and physically justified in the limits of long (μ dependent helimagnets, Section 8.2.2) and short (ferromagnetic, Section 8.2.2) tubes, are further numerically tested. To get at least a qualitative interpolation of the two limits, various interaction cutoffs N, in the range of 500 to several hundreds thousands (lengths from 10 nm to 200 μm), are applied for 50 nanotubes with diameters between 1 nm and 3 nm and various chiral angles. The efficient optimization, as well as spin waves spectra are achieved by systematic use of the the full symmetry, through the modified group projector technique [66] within the POLSymm code [83]. All the analytically obtained predictions for ground states are completely verified (some of the numerical results are in Figure 8.3). For the fixed chemical potential the numerically obtained optimal configuration is used in calculation of the dynamical

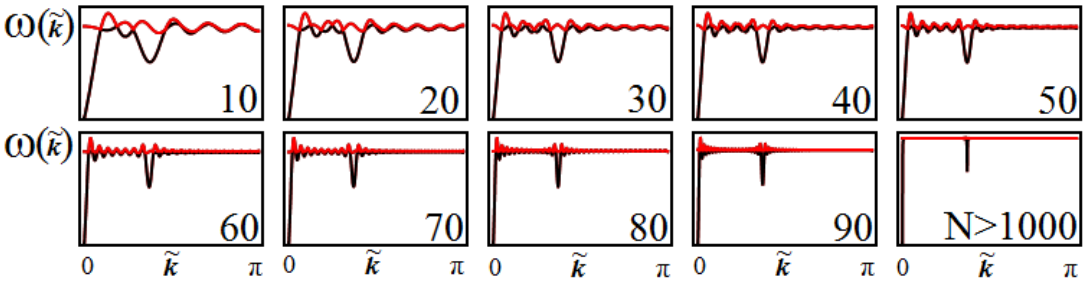

Figure 8.6: Spin waves dispersions of ^{13}C nanotube (12,2) of various lengths. Series of panels illustrates dependence of spectrum on the interaction range, simulated by the number of monomers N (except on the last panel, N is artificially small). The site reference frames correspond to the ground state (H1 regime depicted); the other local minimum refers to H2.

matrices (8.10). The corresponding eigenequations are solved on discretized irreducible Brillouin domain with the accuracy of the mesh of $10^{-3} - 10^{-5}$. Of course, when N is sufficiently increased, the ground state rapidly approaches that of the infinite nanotube, as has been anticipated. On the other hand, spin waves dispersion becomes narrower (as N increase), reflecting the long-ranged nature of RKKY interaction (sketched in Figure 8.6). Independently of the chosen regime, elementary excitations have the universal characteristics. In the region of high-wavelengths (for $\tilde{k}/f \to 0$), the gapless dispersion shows the linear tendency, analogously to the anti-ferromagnetic case. On the contrary to the Néel state, where two Goldstone bosons exists, here a single one is found and may be addressed as helimagnon [84]. It corresponds to the global rotations of the magnetic lattice around the system axis as indicated in the optimization. The ground states of other regimes are also visible through the additional local minima. In Figure 8.6, the chemical potential is tuned to the first regime; the sharp line is in the vicinity of $\tilde{K}/f$ and corresponds to H2, while another local minimum, very close to the global one, is in the point $2\tilde{k}_0/f$. This unambiguously reflects the chirality of helimagnetic arrangement. In contrast to the Goldstone boson, where the tunneling of magnetic system among the continual states is without energy cost, the change of the chirality of the magnetic lattice required an amount of energy. Except this pronounced lines, the rest of the spectra is flat probably indicating the stability of helimagnetic order.

Worth noticing is that numerically found μ_F is slightly greater than the estimate.

The ferro-helimagnet transition is continual, but more rapid when the tube geometry (L, D and ϑ) implies direct transition from ferro to H2 phase. Anyway, one should be aware that simulating finiteness of the nanotube by the interaction cut-off neglects edge effects and the results for short tubes may be only qualitatively close to realistic situations or (numerically too requiring) exact calculations.

8.2.4 Phase diagram

Before commenting the conclusions, which promote the C^{13} nanotubes as controllable helimagnets, we briefly consider the domain of the approach since some idealizations are introduced in the model. The used spin susceptibility is calculated [71] by the zero-temperature Fermi distribution, with tight-binding electronic states from the subband closest to the Fermi level. Therefore, the derivation is rigorous only for $T = 0\,\mathrm{K}$, when the occupation of the split subband is strictly determined by the chemical potential; nevertheless, as far as this model is considered, the physical description should be qualitatively preserved up to the temperatures of order of 10 K, corresponding to the spin-orbit gap of a few meVs. However, it has been exhaustively discussed [70, 85] that the order in 1D systems with RKKY interaction is possible in much lower temperatures, of order 10 mK. The appearance of the spin order can be observed by neutron diffraction technique [60, 86].

Concerning the results, the first important observation is richness of the phase diagram, with a number of the nanotube geometry and gate-voltage orchestrated phases. This can be expected [71] in the view of the complexity of the model. A more detailed understanding of the phenomena described in Section 8.2.2, is obtained analysing the qualitative difference between the second and other regimes. In H1 and H3 spin $\boldsymbol{s}_{tsu}$ is rotated for $\Delta\phi^{\pm}_{tsu} = \pm k_{-+}(ft - 2\delta_{u,1}z_0)$ with respect to $\boldsymbol{s}_0$; as $\tilde{m} = 0$, it is independent of s, indicating ferromagnetic order in cross sections. The angles $\pm k_{-+}f$, between the sections t and $t+1$ with the same u (along the helix) and $\pm 2k_{-+}z_0$, between $\boldsymbol{s}_{ts0}$ and $\boldsymbol{s}_{ts1}$ (the two sublattices), are small, typically of the order $10^{-2} - 10^{-3}$ degrees. Thus, these helimagnets are incommensurate deviations from the ferromagnet. However, ground state spins in H2 are for $n > 2$ helically ordered also within the cross sections, rotating from site to site for $2\pi\tilde{m}_0/n$ ($\tilde{m}_0 = 0$ for $n = 1, 2$); for different tubes with diameters up to 3 nm, $\tilde{m}_0$ is diverse, taking all the values from -10 to 10. Also, the rotation along the helix in H2 is much quicker than in other regimes: $\tilde{K}f$ is the main contribution to the angle $\tilde{k}_0 f$

between the consecutive spins (much greater than $k_{--}f \sim 10^{-2} - 10^{-3}$ degrees). Significantly, the arrangement corresponding to $\tilde{K}$ (at the very beginning of H2, $k_{--} = 0$) is commensurate, with the period a of the nanotube. Mild increase of the chemical potential triggers slow modulation by k_{--}, which results in the beating frequencies $\tilde{K} \pm k_{--}$, found as ground states. This can be explained by the inspection of the susceptibility functions [71] in the vicinity of the critical chemical potential $\mu = \Delta$. At this point, the wave numbers k_{++} and k_{-+} are finite, while k_{--} is zero for $\mu \leq \Delta$ and starts to increase being infinitesimally positive immediately after Δ. Therefore, for sufficiently large $|z|$, the functions $S(k_{++}, z)$ and $S(k_{-+}, z)$ are dumped, while $S(k_{--}, z)$ is almost constant. As these functions determine envelopes, both χ^{xx} and χ^{xy} are well approximated in this region (corresponding to the dominant part $\varepsilon(N^f, N)$ of energy) by the trigonometric factors ($\cos(2M\phi + 2Kz)$ and $\sin(2M\phi + 2Kz)$, respectively) multiplied by a constant. The decisive are these rapidly oscillating factors: sublimating within K and M the geometry of the system, they establish a resonant mechanism of the quantum transition [87] (with discontinuous energy and susceptibility in Δ) to the state with spin order which fully reflects the geometric symmetry of the nanotubes. It is important to remark that this opens the possibility to observe the effect by the recently proposed setup [85] allowing access of spin susceptibility, as its spatial distribution in the second regime neatly reflects the system symmetry and spin ordering.

Another important observation is universal behaviour of all semiconducting nanotubes (Figure 8.3). For $\mu = 0$ spin susceptibility infers no frustration, establishing ferromagnetic order, which is also the case when μ increases until some critical value μ_F (estimated above). After that, frustration is significant enough to induce spin rearrangement, which rapidly (but continually) reaches the long limit regime. Further increase of μ follows the long limit predictions: within the same regime continual change of helimagnetic order accompanies change of μ, but transition between the regimes is an abrupt switch to a quite different helimagnet. Critical values (enclosing the second regime) of the chemical potential decrease with chiral angle and with D (Figure 8.5). Thus, H1 and H2 get narrower for thicker tubes with chirality closer to the armchair ones; for thick tubes the third regime dominates, and in the infinite D limit (with vanishing electronic gap) only H3 exists.

The universality of the derived behaviour fully emerges when the ground state and chemical potential are described by the dimensionless quantities $\tilde{k}_0 U \sqrt{D/\Delta}$

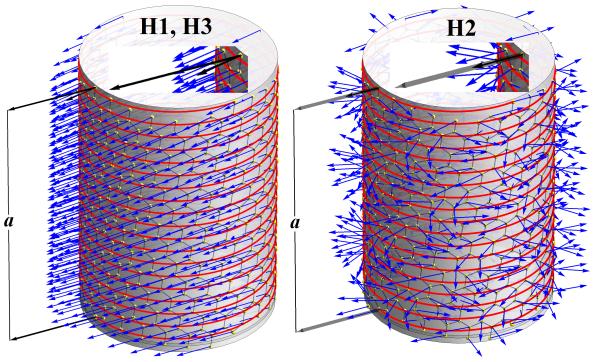

Figure 8.7: Spin arrangements of the nanotube (24,4) in all three helimagnetic regimes. Only a single period a is presented; tube helix generated by $(C_q^r|f)$ is visible. Spin $\boldsymbol{s}_0$ is emphasized by long black arrows at atoms in $\boldsymbol{r}_0$ and $\boldsymbol{a}+\boldsymbol{r}_0$. Spin vectors at $\boldsymbol{a}+\boldsymbol{r}_0$ (blown up in insets) and $\boldsymbol{s}_0$ coincide in H2 for $\tilde{k}_0 f = \tilde{K} f = 1.5$ and $\tilde{m}_0 = 2$, while in H1 and H3 ($\tilde{k}_0 f > 0$ and $\tilde{m}_0 = 0$) they slightly differ, pointing out incommensurability of spin order and geometry.

and μ/Δ. The diagram of their dependence, Figure 8.3, is the same for all infinitely long tubes, except the value of $\tilde{K}U$. On the contrary, quantum numbers $\tilde{K}$ and $\tilde{m}_0$, determining the H2 ground state, are for all C13NTs (with diameter less then 3 nm) unique, making the H2 regime an accurate fingerprint of a particular nanotube. Finally, the second regime reflects spin-orbit coupling, and disappears (as well as H1) when the SO interaction gap is neglected ($\Delta = 0$); within (the only remaining) H3 regime, spins in the cross-sections are parallel (no preferred plane), while the angle along the helix is $2k_F f = k_{-+} f = \frac{4f}{U}\sqrt{\frac{\mu}{D}}$, coinciding with the result for metallic nanotubes obtained by a different approach [70]. Thus, the ground state of nuclear spins for all C13NTs has universal chemical potential dependence.

It is important to point out that the $S(k,z)$ functions, being decisive in H1 and H3, are the same as in strictly 1D systems [88]. Only the H2 regime, resonant with the trigonometric rapidly oscillating parts, manifests the real, not strictly 1D structure of the tube [89]. Thus, it can be expected that all Q1D systems governed by the RKKY interaction have analogous susceptibility causing gate voltage tunable phases.

Conclusion

A general review of the existing literature reveals that magnetic dynamics of isolated crystals is mostly modeled by quadratic forms in non-vanishing magnetic moments (spins) of their sites (whether the spin carriers are electrons or ions). The Heisenberg coupling, Dzyaloshinskii-Moria vector, and symmetric anisotropy are enshrined in tensor field over the geometrical configuration of the system. Despite the crystals' symmetries are well known, numerous results are usually derived utilizing their translational periodicity through the Bloch's theorem, while rotations and roto-reflections are *a posteriori* considered.

In this research the full geometrical symmetry of a system is systematically incorporated in the description of the corresponding spin lattice (formed of the site magnetic moments) on various levels. In short, this includes the symmetry allowed interaction tensors and quasi-classical magnetic phases, as well as their usage in the dynamics through mean-field approach to ground states and non-interacting quasi-particle picture of elementary excitations. Though these highlights are thoroughly elaborated for monoperiodical systems (described by line groups), the methodological aspects of the presented study refer to the other dimensions also: layers (diperiodic group) and three-dimensional crystals (space groups). The studied concepts are applied to the already fabricated [67–69] nanotubes composed of the ^{13}C isotope, whose nuclear spins ($S = 1/2$) interacts via the itinerant electrons resulting in long-ranged RKKY type of coupling.

As usual, to make use of the geometrical symmetry group, in the state space of quantum spin lattice (being the tensorial product of site spaces) its action is defined by the corresponding representation in the site space, which when applied on the triple of spin operators expresses their pseudo-vector nature. Then, the fundamental concept of invariance of the Hamiltonian leads to restrictions on the interaction tensors imposed by the axial-vector representation of the rotations and roto-reflections from the group. Together with the hermiticity of Hamiltonian, this establishes the basis for the modeling of magnetic interactions. Let us only mention a possible practical benefit of such approach: since the tensorial components are matrix elements of the kinetic energy operator, Coulomb, and/or SO interactions, it is sufficient to calculate only a part of them, and then the others are immediately determined by the symmetry.

In contrast to three-dimensional crystals, where a single invariant selects the isotropic Dirac-Heisenberg Hamiltonian, in Q1D (as far as the system has non-trivial rotations) there are at least two of them introducing the XXZ Heisenberg form, i.e. the anisotropy along the system axis. Some symmetries allow an additional scalar, corresponding to the longitudinal component of DM vector. The rest of the components (either symmetric or antisymmetric ones) have vectorial or tensorial transformation properties. The generalization of the Moriya's rules [19] is also performed. Further on, the notions of homogenity and isotropy of materials are revisited in the context of Q1D systems: for some of those which are geometrically confined to a cylinder (such as nanotubes), the analysis suggests that the non-vanishing projection of DM vector on the system axis is to be considered on an equal footing with the XXZ components. The RKKY interaction in ^{13}C nanotubes fits to this form.

Commonly, difficulties in handling quantum correlations are partly overcome by an appropriate restriction of the state space. The simplest, single-particle approximation, utilized here, considers the product quantum states. These states are mapped into the space which is the direct sum of the site spaces spanned by classical spin vectors. Simultaneously, the matrix composed of the three-dimensional interaction tensors blocks takes the role of the classical Hamiltonian, while the group action becomes the induced axial representation. Within such mathematical framework dynamics is efficiently solved using a modification [66] of the Wigner's group projectors [61]. In general case, the lengths of the obtained classical site vectors vary (may be even zero). This is in contrast to the widely used mean-field prescription where spin operators are to be substituted by classical vectors of the fixed length, which seems to be a natural symmetry requirement. In fact, for spin 1/2, the restriction of the trial set to the pure states only gives the equal site spins lengths. Anyway, the constrained optimization leads to $2N$ variables (manifold composed of the site spheres, where N is the number of sites), and standard numerical techniques are to be employed. In general, the mean-field approximation may result in highly non-symmetric magnetic structures. Still, the number of variational parameters is tremendously reduced if symmetrical states are accounted.

The above discussion demands foundation of the spin line groups [59] and principles of their exploitation. This is a base for full implementation of the symmetry in the studies of the frustrated magnetics. The equivalence with the originally in-

troduced concept [31–33] is achieved by the notion of spin representation. Precisely, classical spins are arranged over the lattice by the action of a spin representation on some initial site spin vector. Combining one, two, and three-dimensional physically irreducible representations of the underlying group into three-dimensional orthogonal ones, the spin representations, preserving the vectors length, are obtained. This approach provides an efficient classification of the symmetry allowed magnetic phases. The diversity of the complex helimagnets in Q1D systems is found, including the situations with the site spins tilted along a singled out direction, as well as within the cross sections perpendicular to it. Besides the part of the results is presented here, the proposed algorithm is used elsewhere [60] to obtain all the possible spin arrangements for Q1D geometries and corresponding neutron diffraction amplitudes, providing experimentally verifiable fingerprints of such symmetric spin structures.

However, the determination of an overall criterion to select symmetry allowed models which are optimized by the symmetric magnetic structures is a non-trivial task. A possible algorithm, expressed through the commutation of the classical hamiltonian with the spin representations (besides the axial one) is proposed. Precisely, one may restrict the trial set of the classical states to the symmetrical spin configurations (which usually results in few parameters related to the spin representations and initial site spins), and *a posteriori* check whether the commutation requirement is fulfilled for the minimal one. Even more, it may turn out (as in the example of ^{13}C nanotubes) that the space of the classical spins of a particular interaction model is exhausted by the symmetric arrangements.

Concerning elementary excitations, they are treated within the linear approximation of spin waves. Similarly to the common textbook approach to magnons for ferromagnetic state, in the case of helimagnets it is usual to transform the site frames in such a way that classical site spin vectors of the ground state coincide with the local z-axes [48, 53]. In addition, these transformations of the site frames must be rotations in order to preserve angular momentum nature of the site spins. Then the site deviations are vectors in the tangent spaces on the site spheres at the points of minima. Consequently, the total state space is their orthogonal sum; the mapping of the Hessian matrix into that space leads to the spin waves Hamiltonian quadratic in bosonic operators. Normal coordinates are to be obtained by diagonalization of the associated dynamical matrix. Nevertheless, once the symmetrical ground spin

arrangement is determined by a corresponding spin representation, to make use of symmetry it must be incorporated into the mapping giving all the relevant quantities: spin waves Hamiltonian, its dynamical matrix, and the group representation. It turns out that using the full symmetry is straightforward through the MGPT whenever the spin representations are rotations, but in the cases when they are roto-reflections only a part of the underlying group fits to this approach. However, an algorithm restoring the full symmetry is proposed to overcome this problem.

The detailed analytical and numerical study of nuclear spin orders and magnons in semiconducting ^{13}C nanotubes justifies that use of symmetry reveals some universal characteristics of Q1D systems. Subtle interplay of the chemical potential, length, diameter and chirality, results in the complex four dimensional phase diagram of the helical ground states. This behaviour of ^{13}C nanotubes manifests long range of RKKY interaction and quasi one-dimensional geometry. It is expectable that for all RKKY interaction governed nanowires various scenarios of the helical order response to the gate voltage can be achieved.

It should be remarked that this study is to large extent relevant for Q2D lattices. In fact, the line, as well as the diperiodic groups preserve a singled out direction. This refers to the axis along (Q1D), or perpendicular (Q2D) to a system. Therefore, all the derived general transformational properties of the interaction tensors for Q1D are the same as in Q2D, while isotropy and homogenity should be accommodated.

To summarize, this study enlightens the scope of the application of symmetry within a basic domain of the theory of magnetism establishing an adequate formal framework. Starting from the exact quantum-mechanical description, the transition to the quasi-classical (thus single-particle mean-field) model is rigorously analyzed. The symmetry is completely incorporated within its two principle parts: determination of the ground state and low-energy dynamics. In this way formed firm foundation of symmetry in magnetism, should be, as in other fields of physics, a powerful tool for analysis of well known interesting sophisticated phenomena. Only to mention noticed appearance of the Goldstone mode manifesting the broken intrinsic isotropy, and its possible consequences on stability and phase transitions, and along the same line the higher order correlations treated by tensor network states [90], an approach which allows a direct implementation of the presented concepts.

Appendix A

Abbreviations and notation

A.1 List of abbreviations

- AFM: antiferromagnet;
- CWB: Cartan-Weyl basis;
- C13NT: ^{13}C nanotube;
- DH: Dirac-Heisenberg;
- DM: Dzyaloshinskii-Moria;
- ECS: equally contributing sites;
- FM: ferromagnet;
- IR: irreducible representation;
- MC: mutually conjugated;
- MGPT: modified group projector technique;
- Q1D: quasi-one-dimensional;
- Q2D: quasi-two-dimensional;
- RIR: real irreducible representation;
- RKKY: Ruderman-Kittel-Kasuya-Yosida;

- SAB: symmetry adapted (or standard) basis;
- SC: self-conjugated;
- SO: spin-orbit;
- SR: spin representation;
- SSAB: stationary symmetry adapted basis;
- SWCNT: single wall carbon nanotube.

A.2 Notation and conventions

- Bold: Sets, groups ($\boldsymbol{G}$, $\boldsymbol{F}$, $\boldsymbol{Z}$, $\boldsymbol{R}$, $\boldsymbol{S}$), vectors of any dimension ($\boldsymbol{r}$, $\boldsymbol{s}$).
- Calligraphic: vector spaces ($\mathcal{S}$, $\mathcal{H}$).
- Absolute value has contextual meaning: the dimension of the vector space ($|\mathcal{S}|$), cardinality of sets ($|\boldsymbol{G}|$, the order of the group $\boldsymbol{G}$, $|\boldsymbol{R}|$ for number of sites, $|\boldsymbol{Z}|$ for the order of transversal), dimension of the matrices and representations ($|\mu|$, $|D(\boldsymbol{G})|$).
- Braced label emphasizes irreducibility (representations $D^{(\mu)}$, spaces $\mathcal{H}^{(\mu)}$); however, when the same label is without brace, the corresponding quantity is not irreducible, though it is related to an irreducible representation ($\mathcal{H}^{\mu}$, $\mathcal{S}^{\mu}$).
- $\mathbb{1}$: the identity operator with indices specifying the space ($\mathbb{1}_3$, $\mathbb{1}_\delta$), or the unit representation, $\mathbb{1}(\boldsymbol{G})$.
- e: identity element of a group.
- E^i are the columns with coordinates $(E^i)_p = \delta_{pi}$; they satisfy $E_i E^j = \delta_{ji}$.
- E^i_j are the matrices with the elements $(E^i_j)_{pq} = \delta_{pi}\delta_{jq}$; they satisfy $E_i E^j_k = \delta_{ji} E_k$, and $E^i_j E^k_l = \delta_{kj} E_{il}$.
- Overbar: inverse of a group element ($\bar{g} = g^{-1}$), adjoint operator ($\bar{A} = A^\dagger$), when the standard notation is inconvenient. Also used as $E^{P\bar{p}}_{Qq}$ to denote the ordinal of the inverse of a transversal element (only when it is also the element of the transversal), i.e. $\bar{z}^P_p = z^P_{\bar{p}}$.
- $\mathrm{diag}\,[d_1, \ldots, d_n]$ is diagonal matrix, with elements $d_{ij} = d_i \delta_{ij}$.
- $\mathrm{O}(3,\mathbb{R})$ and $\mathrm{SO}(3,\mathbb{R})$ are the three-dimensional orthogonal group and its rotational subgroup; E(3) is the extended Euclidean group, $T_3 \wedge \mathrm{O}(3,\mathbb{R})$ (semidirect product).
- Koster-Seitz notation $(O|\boldsymbol{t})$: the Euclidian transformation $g = (O|\boldsymbol{t})$ is composed of an orthogonal transformation O (rotation R or roto-reflection $\mathcal{I}R$,

where $\mathcal{I} = -\mathbb{1}$) and a translation $\boldsymbol{t}$, with the action $(O|\boldsymbol{t})\boldsymbol{r} = O\boldsymbol{r} + \boldsymbol{t}$. The set of all such transformations form the Euclidian group $E(3) = T_3 \wedge \mathrm{O}(3, \mathbb{R})$. In the case of Q1D systems, translations are along the z-axis, and $(O|t)$ shortens $(O|t\boldsymbol{e}^z)$.

- σ^α are Pauli matrices: $\sigma = \sigma^1 = \left(\begin{smallmatrix} 0 & 1 \\ 1 & 0 \end{smallmatrix}\right)$, $\sigma^2 = \left(\begin{smallmatrix} 0 & -\mathrm{i} \\ \mathrm{i} & 0 \end{smallmatrix}\right)$, $\lambda = \sigma^3 = \left(\begin{smallmatrix} 1 & 0 \\ 0 & -1 \end{smallmatrix}\right)$.

- $\hbar = 1$;

- Partial trace: if A is an operator in the product space $\otimes_i \mathcal{S}_i$ (with a separable basis $|\,\psi_1, \ldots, \psi_N\rangle$), then the partial trace over the spaces $\mathcal{S}_{i_1}, \ldots, \mathcal{S}_{i_L}$, is the operator $\mathrm{Tr}_{i_1 \ldots i_L} A = \sum_{\psi_{i_1} \ldots \psi_{i_L}} \langle \psi_{i_1}, \ldots \psi_{i_L} \mid A \mid \psi_{i_1}, \ldots \psi_{i_L} \rangle$ in the product of the all the spaces but $\mathcal{S}_{i_1}, \ldots, \mathcal{S}_{i_L}$. Hat specifies the omitted factor spaces: $\mathrm{Tr}_{\widehat{i_1, \ldots, i_L}} A$ is the partial trace over all the spaces but $\mathcal{S}_{i_1}, \ldots, \mathcal{S}_{i_L}$, which is an operator in $\mathcal{S}_{i_1} \otimes \cdots \otimes \mathcal{S}_{i_L}$.

- Scalar product: $\bar{\boldsymbol{x}}\boldsymbol{y} = \sum_i {x_i}^* y_i$ of the vectors $\boldsymbol{x}$ and $\boldsymbol{y}$, where x_i and y_i are the coordinates of $\boldsymbol{x}$ and $\boldsymbol{y}$, respectively, and x^* is the complex-conjugation. Similarly, if operators $\hat{X}_i$ are arranged in the column $\hat{\boldsymbol{X}}$, then $\hat{\bar{\boldsymbol{X}}}\hat{\boldsymbol{Y}} = \sum_i {\hat{X}_i}^\dagger \hat{Y}_i$, and $\hat{X}^\dagger$ is the adjoint of $\hat{X}$.

- $\sim$ – Equivalence of representations: $D_1(\boldsymbol{G}) \sim D_2(\boldsymbol{G})$ means $D_1(\boldsymbol{G}) = X D_2(\boldsymbol{G}) \bar{X}$ for a nonsingular operator X.

All the representation used in the text are unitary (and orthogonal, if real).

Appendix B

Reminders on groups and proofs

B.1 Modified group projector technique

Unitary representation $D(\boldsymbol{G})$ of the group $\boldsymbol{G}$ in the state space $\mathcal{S}$ is decomposed into the orthogonal sum

$$D(\boldsymbol{G}) = \oplus_\mu f^\mu d^{(\mu)}(\boldsymbol{G}) \tag{B.1}$$

of the $|\mu|$-dimensional unitary irreducible components $d^{(\mu)}(\boldsymbol{G})$, with *frequency numbers* f^μ. Each representation $D(\boldsymbol{G})$ of a group $\boldsymbol{G}$ defines the group projector

$$\boldsymbol{G}(D) = \frac{1}{|\boldsymbol{G}|} \sum_g D(g). \tag{B.2}$$

The trace $\mathrm{Tr}\, \boldsymbol{G}(d^{(\mu)} \otimes d^{(\nu)^*})$ of the projector (B.2) for the product $d^{(\mu)} \otimes d^{(\nu)^*}$ of two IRs $d^{(\mu)}(\boldsymbol{G})$ and $d^{(\nu)}(\boldsymbol{G})$ equals to 1 if and only if the two IRs are equivalent, and otherwise it vanishes.

Symmetry adapted, or *standard basis*

$$\{|\, \mu t_\mu m\rangle \mid \forall \mu, t_\mu = 1, \ldots, f^\mu, m = 1, \ldots, |\mu|\} \tag{B.3}$$

is a basis in $\mathcal{S}$, in which (B.1) is block-diagonal, and its vectors are transformed as

$$D(g)\, |\mu t_\mu m\rangle = \sum_{m'} d^{(\mu)}_{m'm}(g)\, |\mu t_\mu m'\rangle. \tag{B.4}$$

For an operator H (usually Hamiltonian) such that $[H, D(\boldsymbol{G})] = 0$ (commutes with all operators $D(g)$), it is possible to find *stationary symmetry adapted basis*, i.e. the SAB which is also the eigenbasis of H:

$$H\, |\mu t_\mu m\rangle = E_{\mu t_\mu}\, |\mu t_\mu m\rangle. \tag{B.5}$$

The procedure for finding the SSAB is based on the Wigner's group operators [61].

Inductive type of the state space $\mathcal{S} = \oplus_{Pp}\mathcal{S}_p^P$ is the orthogonal sum of the spaces $\mathcal{S}_p^P = \mathcal{S}_0^P$ (e.g. site spin space, site deviation space) assigned to the sites of $\boldsymbol{G}$-lattice. For inductive group representation, with $d^P(\boldsymbol{G})$ being site space representations (assigned by the group orbits),

$$D(g) = \sum_{Pp} E_{Pp}^{P,gp} \otimes d^P(g), \tag{B.6}$$

the commutation $[H, D(\boldsymbol{G})] = 0$ implies

$$h_{Qq}^{Pp} = d^P(\bar{g}) h_{Q,gq}^{P,gp} d^Q(g), \tag{B.7}$$

where h_{Qq}^{Pp} are $|\mathcal{S}_0^P| \times |\mathcal{S}_0^Q|$ dimensional blocks of H. The corresponding SSAB is found using *modified group projector technique* [66]. The essence of the method is a reduction of the eigenproblem to the finite dimensional space $\mathcal{S}_0 \otimes \mathcal{S}^{(\mu^*)}$, which is the *symcell* space $\mathcal{S}_0 \stackrel{\text{def}}{=} \oplus_P \mathcal{S}_0^P$ extended by the state space $\mathcal{S}^{(\mu^*)}$ of the dual IR $d^{(\mu^*)}$. Namely, the operator $H \otimes \mathbb{1}_\mu$ commutes with the representation $D(\boldsymbol{G}) \otimes d^{(\mu^*)}(\boldsymbol{G})$, and thus with the *modified group projector* $\boldsymbol{G}(D \otimes d^{(\mu^*)}) = \frac{1}{|\boldsymbol{G}|}\sum_g D(g) \otimes d^{(\mu^*)}(g)$. When pulled-down to the space $\mathcal{S}_0 \otimes \mathcal{S}^{(\mu^*)}$, these quantities are:

$$H_{0\mu}^{\downarrow} = \sum_{PQ} E_{Q0}^{P0} \otimes \sqrt{\frac{|\boldsymbol{F}^P|}{|\boldsymbol{F}^Q|}} \boldsymbol{F}^P(\gamma^{P\mu}) H_{PQ}^{\mu}, \tag{B.8}$$

$$H_{PQ}^{\mu} = \sum_p d^P(\bar{z}_p^P) h_{Q0}^{Pp} \otimes D^{(\mu^{\rho *})}(\bar{z}_p^P);$$

$$\boldsymbol{G}^{\downarrow}(D \otimes d^{(\mu^*)}) = \sum_P E_{P0}^{P0} \otimes \boldsymbol{F}^P(\gamma^{P\mu}), \tag{B.9}$$

$$\gamma^{P\mu} = d^P(\boldsymbol{F}^P) \otimes d^{(\mu^*)}(\boldsymbol{F}^P), \quad \boldsymbol{F}^P(\gamma^{P\mu}) = \frac{1}{|\boldsymbol{F}^P|}\sum_{f^P} \gamma^{P\mu}(f^P).$$

Practically, the eigenproblems

$$H_{0\mu}^{\downarrow} \,|\mu t_\mu\rangle^0 = E_{\mu t_\mu} \,|\mu t_\mu\rangle^0, \quad \boldsymbol{G}^{\downarrow}(D \otimes d^{(\mu^*)}) \,|\mu t_\mu\rangle^0 = |\mu t_\mu\rangle^0, \tag{B.10}$$

are to be solved for each μ to obtain f^μ vectors ($t_\mu = 1, \ldots, f^\mu$):

$$f^\mu = \sum_P f_P^\mu, \quad f_P^\mu = \mathrm{Tr}\boldsymbol{F}^P(\gamma^{P\mu}). \tag{B.11}$$

The partial scalar products $\mid \mu t_\mu m\rangle^0 = \langle \mu^* m \mid \mu t_\mu \rangle^0$ with the standard basis $\{|\mu^* m\rangle \mid m = 1, \ldots, |\mu|\}$ of $\mathcal{S}^{(\mu^*)}$, satisfying

$$D^{(\mu^*)}(g)\,|\mu^* m\rangle = \sum_{m'} d^{(\mu^*)}_{m'm}(g)\,|\mu^* m'\rangle, \tag{B.12}$$

give the symmcell parts of the SSAB (Eqquations (B.4) and (B.5)), i.e.

$$|\mu t_\mu m\rangle = \sum_{Pp} E^{Pp} \otimes |\mu t_\mu m\rangle^{Pp}, \quad |\mu t_\mu m\rangle^{Pp} = d^P(z_p^P) \sum_{m'} d^{(\mu^*)}_{mm'}(z_p^P)\,|\mu t_\mu m'\rangle^{P0}. \tag{B.13}$$

In addition, the projector (B.2) can be calculated with help of the group generators g_i only, i.e. avoiding the summation over the whole group. The main task of the algorithm is finding the projector $F(X)$ on the fixed point space of an operator X; precisely, projectors $F(D(g_i))$ of the representation $D(\boldsymbol{G})$ for the group generators (usually several only), and $F\left(\prod_i F\left(D(g_i)\right)\right)$, the fixed point space projector of the operator $\prod_i F(D(g_i))$. The latter is equal to the needed projector:

$$\boldsymbol{G}(D) = F\left(\prod_i F\left(D(g_i)\right)\right). \tag{B.14}$$

B.2 Intertwining operators

Let $A(\boldsymbol{G})$ and $B(\boldsymbol{G})$ be representations of $\boldsymbol{G}$ in the spaces $\mathcal{A}$ and $\mathcal{B}$. *Intertwining operator* is any operator X satisfying $XA(g) = B(g)X$ for each g. Obviously, such operators form the subspace of homomorphisms of $\boldsymbol{G}$, $\mathrm{Hom}_{\boldsymbol{G}}(\mathcal{A}, \mathcal{B})$ in the space of endomorphisms $\mathrm{End}(\mathcal{A}, \mathcal{B})$.

Teorem B.2.1 *The range of the group super-projector*

$$\boldsymbol{G}(B \otimes A^*) = \frac{1}{|\boldsymbol{G}|} \sum_g B(g) \otimes A^*(g), \quad \boldsymbol{G}(B \otimes A^*)X \stackrel{def}{=} \frac{1}{|\boldsymbol{G}|} \sum_g B(g) X \bar{A}(g),$$

is $\mathrm{Hom}_{\boldsymbol{G}}(\mathcal{A}, \mathcal{B})$.

▬*Proof:* Let X be an operator mapping $\mathcal{A}$ into $\mathcal{B}$. Then

$$(\boldsymbol{G}(B \otimes A^*)X)A(h) = \frac{1}{|\boldsymbol{G}|} \sum_g B(g) X \bar{A}(g) \bar{A}(\bar{h}) = \frac{1}{|\boldsymbol{G}|} \sum_g B(g) X \bar{A}(\bar{h}g).$$

The rearrangement lemma with $k = \bar{h}g$ yields

$$(\boldsymbol{G}(B \otimes A^*)X)A(h) = B(h) \frac{1}{|\boldsymbol{G}|} \sum_k B(k) X \bar{A}(k) = B(h)(\boldsymbol{G}(B \otimes A^*)X),$$

i.e. X is an intertwining operator if and only if $\boldsymbol{G}(A \otimes B^*)X = X$.▮

B.3 Statements used in the text with proofs

Teorem B.3.1 *The action* (2.16) *is a representative of* $\tilde{\boldsymbol{G}}$.

▬*Proof:* Product of two representative operators satisfies

$$\begin{aligned} U(\tilde{h})U(\tilde{g})\,|\ldots,m^P_p,\ldots\rangle &= U(\tilde{h})\,|\ldots,u^P(\tilde{g})m^P_{\bar{g}p},\ldots\rangle = |\ldots,u^P(\tilde{h})u^P(\tilde{g})m^P_{\bar{g}\bar{h}p},\ldots\rangle \\ &= |\ldots,u^P(hg)m^P_{\overline{hg}p},\ldots\rangle = U(\tilde{h}\tilde{g})\,|\ldots,m^P_p,\ldots\rangle, \end{aligned}$$

which is the homomorphism looked for.∎

Teorem B.3.2 *The commutation of the Hamiltonian* (2.6) *with the operators of the representation* (2.16) *satisfying* (2.15) *is equivalent to* (2.17a).

▬*Proof:* Equality of the matrix elements of the both sides of $\hat{H} = U(\bar{g})\hat{H}U(g)$ in a separable basis $|\ldots,\boldsymbol{s}^P_p,\ldots\rangle$ reads:

$$\tfrac{1}{2}\textstyle\sum_{PQp'q'}\langle \boldsymbol{s}^P_{p'},\boldsymbol{s}^Q_{q'}|\,\hat{\boldsymbol{S}}^P_{p'}h^{Pp'}_{Qq'}\hat{\boldsymbol{S}}^Q_{q'}\,|\boldsymbol{s}^P_{p'},\boldsymbol{s}^Q_{q'}\rangle = \langle\ldots,\boldsymbol{s}^P_p,\ldots|\,U(\bar{g})\hat{H}U(g)\,|\ldots,\boldsymbol{s}^P_p,\ldots\rangle =$$
$$\tfrac{1}{2}\textstyle\sum_{PQpq}\sum_{\alpha\beta}h^{Pp\alpha}_{Qq\beta}\langle \boldsymbol{s}^P_{\bar{g}p}|\,u^P(\bar{g})\hat{\boldsymbol{S}}^\alpha u^P(g)\,|\boldsymbol{s}^P_{\bar{g}p}\rangle\langle \boldsymbol{s}^Q_{\bar{g}q}|\,u^Q(\bar{g})\hat{\boldsymbol{S}}^\beta u^Q(g)\,|\boldsymbol{s}^Q_{\bar{g}q}\rangle \overset{(2.15)}{=}$$
$$\tfrac{1}{2}\sum_{PQpq}\langle \boldsymbol{s}^P_{\bar{g}p},\boldsymbol{s}^Q_{\bar{g}q}|\,\hat{\boldsymbol{S}}^P_{\bar{g}p}a(\bar{g})h^{Pp}_{Qq}a(g)\hat{\boldsymbol{S}}^Q_{\bar{g}q}\,|\boldsymbol{s}^P_{\bar{g}p},\boldsymbol{s}^Q_{\bar{g}q}\rangle \overset{\substack{p'=\bar{g}p\\ q'=\bar{g}q}}{=} \tfrac{1}{2}\sum_{PQp'q'}\langle \boldsymbol{s}^P_{p'},\boldsymbol{s}^Q_{q'}|\,\hat{\boldsymbol{S}}^P_{p'}a(\bar{g})h^{Pgp'}_{Qgq'}a(g)\hat{\boldsymbol{S}}^Q_{q'}\,|\boldsymbol{s}^P_{p'},\boldsymbol{s}^Q_{q'}\rangle.$$

Equality of the first and the last part is (2.17a).∎

Teorem B.3.3 *The group action on a classical spin vector from* $\mathbb{R}^3$ *is given by* (4.4). *Consequently, the group action in* $\mathbb{R}^{3N}$ *is the representation* $A(\boldsymbol{G})$ *defined in* (4.10), *commuting with the classical Hamiltonian* H *given by* (4.7).

▬*Proof:* Form the definition (2.16) the action of the group on the separable state $\hat{\rho}_0$ is

$$\bar{U}(\tilde{g})\hat{\rho}_0U(\tilde{g}) = \ldots\otimes\bar{u}^P(\tilde{g})\hat{\rho}^P_{\bar{g}p}u^P(\tilde{g})\otimes\ldots.$$

Inserting the relation (2.15) in the identity

$$\mathrm{Tr}\hat{\boldsymbol{S}}^P_p\bar{U}(\tilde{g})\hat{\rho}_0U(\tilde{g}) = \mathrm{Tr}_{Pp}\hat{\boldsymbol{S}}\bar{u}^P(\tilde{g})\hat{\rho}^P_{\bar{g}p}u^P(\tilde{g}) = \mathrm{Tr}_{Pp}(u^P(\tilde{g})\hat{\boldsymbol{S}}\bar{u}^P(\tilde{g}))\hat{\rho}^P_{\bar{g}p}$$

leads to $a(\bar{g})\mathrm{Tr}_{Pp}\hat{S}\hat{\rho}^P_{\bar{g}p} = a(\bar{g})\boldsymbol{s}^P_{\bar{g}p}$, explicating the group action $g\boldsymbol{s}^P_p \overset{\mathrm{def}}{=} a(\bar{g})\boldsymbol{s}^P_{\bar{g}p}$, or equivalently $g\boldsymbol{S} \overset{\mathrm{def}}{=} A(g)\boldsymbol{S}$. The commutation $[A(\boldsymbol{G}),H] = 0$ has been justified by Theorem B.3.2.∎

Teorem B.3.4 *Let* $h^{Pp}_{Q0}(D) = \frac{1}{|\boldsymbol{G}|}\sum_g [d^P(\bar{g})a(g)]h^{Pp}_{Q0}[d^Q(\bar{g})a(g)]^T$. *Then the energy* (6.7) *is*

$$\varepsilon^{\mathrm{Cl}}[\boldsymbol{S}_0, D] = \frac{1}{2}\sum_Q |\boldsymbol{Z}^Q| \sum_{Pp} \bar{\boldsymbol{s}}^P_0 d^P(\bar{z}^P_p) h^{Pp}_{Q0}(D) \boldsymbol{s}^Q_0.$$

▬*Proof:* Since $d^P(\boldsymbol{F}^P)\boldsymbol{s}^P_0 = \boldsymbol{s}^P_0$ for every orbit P, then

$$\varepsilon^{\mathrm{Cl}} = \varepsilon^{\mathrm{Cl}}[\boldsymbol{S}_0, D]) = \frac{1}{2}\sum_{QP} \frac{1}{|\boldsymbol{F}^P||\boldsymbol{F}^Q|} \sum_{pq}\sum_{f^P f^Q} \bar{\boldsymbol{s}}^P_0 d^P(\bar{f}^P \bar{z}^P_p) h^{Pp}_{Qq} d^Q(z^Q_q f^Q) \boldsymbol{s}^Q_0.$$

Taking $g = z^P_p f^P$ and $g' = z^Q_q f^Q$ one obtains

$$\varepsilon^{\mathrm{Cl}} = \frac{1}{2}\sum_{QP} \frac{1}{|\boldsymbol{F}^P||\boldsymbol{F}^Q|} \sum_{gg'} \bar{\boldsymbol{s}}^P_0 d^P(\bar{g}) h^{Pg}_{Qg'} d^Q(g') \boldsymbol{s}^Q_0.$$

Here it is used that $h^{Pg}_{Qg'} = h(z^P_p f^P \boldsymbol{r}^P_0, z^Q_q f^Q \boldsymbol{r}^Q_0) = h(z^P_p \boldsymbol{r}^P_0, z^Q_q \boldsymbol{r}^Q_0) = h^{Pp}_{Qq}$. Application of the commutation relation $[H, A(\bar{g}')] = 0$ gives

$$\varepsilon^{\mathrm{Cl}} = \frac{1}{2}\sum_{QP} \frac{1}{|\boldsymbol{F}^P||\boldsymbol{F}^Q|} \sum_{gg'} \bar{\boldsymbol{s}}^P_0 d^P(\bar{g}) a(g') h^{P,\bar{g}'g}_{Q0} a(\bar{g}') d^Q(g') \boldsymbol{s}^Q_0.$$

The rearrangement lemma and the substitution $g'' = \bar{g}'g$ lead to

$$\varepsilon^{\mathrm{Cl}} = \frac{1}{2}\sum_{QP} \frac{1}{|\boldsymbol{F}^P||\boldsymbol{F}^Q|} \sum_{g'g''} \bar{\boldsymbol{s}}^P_0 d^P(\bar{g}'') [d^P(\bar{g}')a(g')] h^{Pg''}_{Q0} [d^Q(\bar{g}')a(g')]^T \boldsymbol{s}^Q_0.$$

The factorization $g'' = z^P_p f^P$ finally gives the expression

$$\varepsilon^{\mathrm{Cl}} = \frac{1}{2}\sum_{QP} \frac{1}{|\boldsymbol{F}^Q|} \sum_{g'p} \bar{\boldsymbol{s}}^P_0 d^P(\bar{z}^P_p) [d^P(\bar{g}')a(g')] h^{Pp}_{Q0} [d^Q(\bar{g}')a(g')]^T \boldsymbol{s}^Q_0.$$

As $h^{Pp}_{Q0}(D) = \frac{1}{|\boldsymbol{G}|}\sum_{g'} [d^P(\bar{g}')a(g')] h^{Pp}_{Q0} [d^Q(\bar{g}')a(g')]^T$, this is $\varepsilon^{\mathrm{Cl}} = \frac{1}{2}\sum_Q |\boldsymbol{Z}^Q| \sum_{Pp} \bar{\boldsymbol{s}}^P_0 d^P(\bar{z}^P_p) h^{Pp}_{Q0}(D) \boldsymbol{s}^Q_0$.▮

Teorem B.3.5 *If* $[D(\boldsymbol{G}), H] = 0$, *then* $h^{Pp}_{Q0}(D) = h^{Pp}_{Q0}$, *i.e.* $\boldsymbol{h}^{Pp}_{Q0}$ *is a fixed point of* $P^P_Q(D)$.

▬*Proof:* From the definition (6.8) it follows $h^{Pp}_{Q0}(D) = \frac{1}{|\boldsymbol{G}|}\sum_g [d^P(\bar{g})a(g)] h^{Pp}_{Q0} [d^Q(\bar{g})a(g)]^T$. Applying $a(g) h^{Pp}_{Q0} a(\bar{g}) = h^{P,\bar{g}p}_{Q\bar{g}}$ one finds $h^{Pp}_{Q0}(D) = \frac{1}{|\boldsymbol{G}|}\sum_g d^P(\bar{g}) h^{P,\bar{g}p}_{Q\bar{g}} d^Q(g) = \frac{1}{|\boldsymbol{G}|}\sum_g h^{Pp}_{Q0} = h^{Pp}_{Q0}$; here $[D(\boldsymbol{G}), H] = 0$ is used in the equivalent form $d^P(\bar{g}) h^{P,\bar{g}p}_{Q,\bar{g}q} d^Q(g) = h^{Pp}_{Qq}$.▮

Teorem B.3.6 *Let* $\boldsymbol{S} = \sum_{Pp} E^{Pp} \otimes d^P(z^P_p)\boldsymbol{s}^P_0$ *and* $h^{Pp}_{Q0}(D) = h^{Pp}_{Q0}$. *Then the averaged energy* $\varepsilon_0[\boldsymbol{S}]$ *(Equation* (4.9)*) is the expectation value* $\frac{1}{2}\frac{\bar{\boldsymbol{s}}_0 H^{\downarrow}_{01}(D)\boldsymbol{s}_0}{\bar{\boldsymbol{s}}_0 \boldsymbol{s}_0}$ *for the vector* $\boldsymbol{s}_0 = \sum_P E^{P0} \otimes \frac{\boldsymbol{s}^P_0}{\sqrt{|F^P|}}$ *(*$\|\boldsymbol{s}^P_0\| = S^P$*) of the pulled-down operator* $H^{\downarrow}_{01}(D)$ *(Equation* (B.9)*) for the unit IR* $d^{(\mu)}(\boldsymbol{G}) = \mathbb{1}(\boldsymbol{G})$.

▬*Proof*: The classical energy (6.7) is

$$\begin{aligned} 2\varepsilon^{\mathrm{Cl}}[\boldsymbol{S}] &= \sum_Q |\boldsymbol{Z}^Q| \sum_{Pp} \bar{\boldsymbol{s}}_0^P d^P(\bar{z}_p^P) h_{Q0}^{Pp} \boldsymbol{s}_0^Q = \sum_Q |\boldsymbol{Z}^Q| \sum_P \bar{\boldsymbol{s}}_0^P [\sum_p d^P(\bar{z}_p^P) h_{Q0}^{Pp}] \boldsymbol{s}_0^Q \\ &\overset{(B.9)}{=} \sum_Q |\boldsymbol{Z}^Q| \sum_P \bar{\boldsymbol{s}}_0^P H_{PQ}^1(D) \boldsymbol{s}_0^Q = \sum_Q |\boldsymbol{Z}^Q| \sum_P \bar{\boldsymbol{s}}_0^P \boldsymbol{F}^P(d^P) H_{PQ}^1(D) \boldsymbol{s}_0^Q \\ &= |G| \sum_{PQ} \frac{\bar{\boldsymbol{s}}_0^P}{\sqrt{|F^P|}} [\frac{\sqrt{|F^P|}}{\sqrt{|F^Q|}} \boldsymbol{F}^P(d^P) H_{PQ}^1(D)] \frac{\boldsymbol{s}_0^Q}{\sqrt{|F^Q|}} = |G| \bar{\boldsymbol{s}}_0 H_{01}^{\downarrow}(D) \boldsymbol{s}_0, \end{aligned}$$

where $\boldsymbol{F}^P(d^P) = \frac{1}{|F^P|} \sum_f d^P(f)$ is the subgroup projector (thus $\bar{\boldsymbol{F}}^P(d^P) = \boldsymbol{F}^P(d^P)$ and obviously $\boldsymbol{F}^P(d^P) = \boldsymbol{F}^P(\bar{d}^P)$), since by (5.4) $d^P(f)\boldsymbol{s}_0^P = \boldsymbol{s}_0^P$ for all $f \in \boldsymbol{F}^P$. Because of the normalization $\bar{\boldsymbol{s}}_0 \boldsymbol{s}_0 = \sum_P \frac{S^{P\,2}}{|\boldsymbol{F}^P|} = \frac{1}{|\boldsymbol{G}|} \sum_P S^{P\,2} |\boldsymbol{Z}^P| = \frac{\bar{\boldsymbol{S}}\boldsymbol{S}}{|\boldsymbol{G}|}$, the group order $|\boldsymbol{G}|$ can be substituted in the expression $\varepsilon^{\mathrm{Cl}}[\boldsymbol{S}] = \frac{|\boldsymbol{G}|}{2} \bar{\boldsymbol{s}}_0 H_{01}^{\downarrow}(D) \boldsymbol{s}_0$ to end with $\varepsilon^0[\boldsymbol{S}] = \frac{\varepsilon^{\mathrm{Cl}}[\boldsymbol{S}]}{\bar{\boldsymbol{S}}\boldsymbol{S}} = \frac{1}{2} \frac{\bar{\boldsymbol{s}}_0 H_{01}^{\downarrow}(D) \boldsymbol{s}_0}{\bar{\boldsymbol{s}}_0 \boldsymbol{s}_0}$.∎

Teorem B.3.7 *Let $h_{Q0}^{Pp}(D) = h_{Q0}^{Pp}$ and let $D(\boldsymbol{G})\boldsymbol{S} = \boldsymbol{S} = \sum_{Pp} E^{Pp} \otimes d^P(z_p^P)\boldsymbol{s}_0^P$ be a variational minimum of (6.7). Then:*

1. *$\boldsymbol{S}$ is an eigenvector of H;*
2. *$\boldsymbol{S}$ is an ESC vector.*

▬*Proof*: 1. By fixing D, each symcell stationary point $\boldsymbol{x}_0 = \sum_P E^{P0} \otimes \boldsymbol{x}_0^P$ of $\frac{\bar{\boldsymbol{x}}_0 H_{01}^{\downarrow}(D) \boldsymbol{x}_0}{\bar{\boldsymbol{x}}_0 \boldsymbol{x}_0}$ is an eigenvector of $H_{01}^{\downarrow}(D)$. According to Theorem B.3.6, and the assumption that $\boldsymbol{S}$ is the variational minimum, the symcell part $\boldsymbol{S}_0$ is among the stationary points, thus it is an eigenvector of $H_{01}^{\downarrow}(D)$. The application of (B.13) gives a regular arrangement $\boldsymbol{x} = \sum_{Pp} E^{Pp} \otimes d^P(z_p^P)\boldsymbol{x}_0^P$, which is an eigenvector of H, being exactly $\boldsymbol{S}$.

2. Since $\boldsymbol{S}$ is the eigenvector, $H\boldsymbol{S} = E\boldsymbol{S}$, it follows: $\varepsilon_q^Q = \frac{1}{2} \sum_{Pp} \bar{\boldsymbol{s}}_q^Q h_{Pp}^{Qq} \boldsymbol{s}_p^P = \frac{E}{2} \bar{\boldsymbol{s}}_q^Q \boldsymbol{s}_q^Q = \frac{E}{2} S^{Q\,2}$.∎

Teorem B.3.8 *Let $\boldsymbol{S} = \sum_{Pp} E^{Pp} \otimes d^P(z_p^P)\boldsymbol{s}_0^P$ be a regular spin arrangement. Then $\boldsymbol{S}^g \overset{def}{=} A(g)\boldsymbol{S}$ is also the regular spin arrangement generated from the representative site vector $\boldsymbol{s}^g{}_0^P \overset{def}{=} a(g) d^P(\bar{g}) \boldsymbol{s}_0^P$ by the spin representation $d^{gP}(z_p^P) \overset{def}{=} a(g) d^P(\bar{g} z_p^P g) a(\bar{g})$.*

▬*Proof*: Using the relations $gp = p'$, $g z_p^P = z_{gp}^P f^P(g,p)$ and $d^P(\boldsymbol{F}^P)\boldsymbol{s}_0^P = \boldsymbol{s}_0^P$, one finds:

$$\begin{aligned} A(g)\boldsymbol{S} = & \sum_{Pp} E^{P,gp} \otimes a(g) d^P(z_p^P) \boldsymbol{s}_0^P = \sum_{Pp'} E^{Pp'} \otimes a(g) d^P(z_{\bar{g}p'}^P) \boldsymbol{s}_0^P = \\ & \sum_{Pp'} E^{Pp'} \otimes a(g) d^P(\bar{g} z_{p'}^P \bar{f}^P(\bar{g}, p')) \boldsymbol{s}_0^P = \sum_{Pp'} E^{Pp'} \otimes a(g) d^P(\bar{g} z_{p'}^P) \boldsymbol{s}_0^P = \\ & \sum_{Pp'} E^{Pp'} \otimes a(g) d^P(\bar{g}) \boldsymbol{s}_{p'}^P. \end{aligned}$$

This means that $\boldsymbol{s}_{p'}^P = d^P(g) a(\bar{g}) \boldsymbol{s}^g{}_{p'}^P$, and the representative spin vector is obtained for $p' = e$. When the obtained relation is inserted in $\boldsymbol{s}_{p'}^P = d^P(z_{p'}^P)\boldsymbol{s}_0^P$, the form of $d^{gP}(z_{p'}^P)$ appears.∎

Teorem B.3.9 *If* $\{|\ \mu t_\mu m\rangle \mid m = 1, \dots, |\mu|\}$ *is a multiplet of* $\Delta(\boldsymbol{G}_+)$ *for IR* $d^{(\mu)}(\boldsymbol{G}_+)$*, then* $\{\Delta(g_-) \mid \mu t_\mu m\rangle\}$ *is the multiplet for* $d^{(g-\mu)}(g_+) = d^{(\mu)}(\bar{g}_- g_+ g_-)$*, where* $\boldsymbol{G} = \boldsymbol{G}_+ + g_- \boldsymbol{G}_+$*.*

▬*Proof:* $\Delta(g_+)(\Delta(g_-) \mid \mu t_\mu m\rangle) = \Delta(g_- \bar{g}_- g_+)(\Delta(g_-) \mid \mu t_\mu m\rangle) = \Delta(g_-)\Delta(\bar{g}_- g_+ g_-) \mid \mu t_\mu m\rangle$. Since $\bar{g}_- g_+ g_-$ is an element from $\boldsymbol{G}_+$ then $\Delta(\bar{g}_- g_+ g_-) \mid \mu t_\mu m\rangle = \sum_{m'} d^{(g-\mu)}_{m'm}(g_+) \mid \mu t_\mu m'\rangle$ and $\Delta(g_+)(\Delta(g_-) \mid \mu t_\mu m\rangle) = \sum_{m'} d^{(g-\mu)}_{m'm}(g_+)(\Delta(g_-) \mid \mu t_\mu m'\rangle)$.∎

Teorem B.3.10 *Let* $\{|\ \mu^0 t_{\mu^0} m\rangle \mid m = 1, \dots, |\mu^0|\}$ *be a multiplet of* $\Delta(\boldsymbol{G})$ *for IR* (7.31) *and* $\{|\ \mu t_\mu m\rangle \mid m = 1, \dots, |\mu|\}$ *a multiplet of* $\Delta(\boldsymbol{G}_+)$ *for some IR* $d^{(\mu)}(\boldsymbol{G}_+)$*, where* $\boldsymbol{G} = \boldsymbol{G}_+ + g_- \boldsymbol{G}_+$*. Then the half of the vectors* $|\ \mu^0 t_{\mu^0} m\rangle$*, with* $m = 1, \dots, |\mu|$*, is transformed according to* $d^{(\mu)}(\boldsymbol{G}_+)$ *and the other half, with* $m = |\mu| + 1, \dots, 2|\mu|$*, according to the* g_-*-conjugated representation* $d^{(g-\mu)}(\boldsymbol{G}_+)$*; also, it holds*

$$\Delta(g_-) \mid \mu^0 t_{\mu^0} m\rangle = \mid \mu^0 t_{\mu^0}, m + |\mu|\rangle, \quad m = 1, \dots, |\mu|.$$

▬*Proof:* The multiplet $\{|\ \mu^0 t_{\mu^0} m\rangle | m = 1, \dots, 2|\mu|\}$ is transformed under $\Delta(\boldsymbol{G})$ as usual:

$$\Delta(g) \mid \mu^0 t_{\mu^0} m\rangle = \sum_{m'=1}^{|\mu^0|} D^{(\mu^0)}_{m'm}(g) \mid \mu^0 t_{\mu^0} m'\rangle. \tag{B.15}$$

From (7.31) it follows that

$$D^{(\mu^0)}_{m'm}(g_+) = \begin{cases} d^{(\mu)}_{m'm}(g_+), & 1 \le m, m' \le |\mu| \\ d^{(g-\mu)}_{m'm}(g_+), & |\mu| < m, m' \le 2|\mu| \\ 0, & 1 \le m \le |\mu|, |\mu| < m' \le 2|\mu| \\ 0, & |\mu| < m \le 2|\mu|, 1 \le m' \le |\mu|, \end{cases}$$

$$D^{(\mu^0)}_{m'm}(g_-) = \begin{cases} 0, & 1 \le m, m' \le |\mu| \\ 0, & |\mu| < m, m' \le 2|\mu| \\ \delta_{m',|\mu|+m}, & 1 \le m \le |\mu|, |\mu| < m' \le 2|\mu| \\ d^{(\mu)}_{m'm}(g_-^2), & |\mu| < m \le 2|\mu|, 1 \le m' \le |\mu|. \end{cases}$$

Therefore the first $|\mu|$ vectors are transformed as the SAB of $d^{(\mu)}(\boldsymbol{G}_+)$:

$$\Delta(g_+) \mid \mu^0 t_{\mu^0} m\rangle = \sum_{m'=1}^{|\mu|} d^{(\mu)}_{m'm}(g_+) \mid \mu^0 t_{\mu^0} m'\rangle, \quad 1 \le m \le |\mu|,$$

and the rest of them according to $d^{(g-\mu)}(\boldsymbol{G}_+)$:

$$\Delta(g_+) \mid \mu^0 t_{\mu^0} m\rangle = \sum_{m'=|\mu|}^{2|\mu|} d^{(g-\mu)}_{m'm}(g_+) \mid \mu^0 t_{\mu^0} m'\rangle, \quad |\mu| < m \le 2|\mu|.$$

The action of $\Delta(g_-)$ on the first half of vectors gives the second half of them, i.e:

$$\Delta(g_-)\,|\,\mu^0 t_{\mu^0}, 1 \le m \le |\mu|\rangle = \sum_{m'=|\mu|}^{2|\mu|} \delta_{|\mu|+m,m'}\,|\,\mu^0, t_{\mu^0}, m'\rangle = |\,\mu^0 t_{\mu^0}, m+|\mu|\rangle,$$

and in the last case:

$$\Delta(g_-)\,|\,\mu^0 t_{\mu^0}, |\mu| < m \le 2|\mu|\rangle = \sum_{m'=1}^{|\mu|} d^{(\mu)}_{m'm}(g_-^2)\,|\,\mu^0 t_{\mu^0} m'\rangle = \Delta(g_-^2)\,|\,\mu^0 t_{\mu^0}, m-|\mu|\rangle$$

according to the first relation, since $g_-^2 \in \boldsymbol{G}_+$.∎

Bibliography

[1] R. R. P. Singh, W. E. Pickett, D. W. Hone, and D. J. Scalapino, *Comments on Modern Physics* **2**, B1 (2000)

[2] H. Kageyama et al., *Phys. Rev. Lett.* **82**, 3168 (1999)

[3] N. A. Spaldin, *Magnetic Materials: Fundamentals and Applications*, 2nd Edition (Cambridge University Press, 2011)

[4] F. Bloch, *Zeitschrift fur Physik* **52**, 555-600 (1928)

[5] N. W. Ashcroft, and N. D. Mermin, *Solid State Physics* (Saunders College Publishing, 1976)

[6] H. Bethe, *Zeitschrift fur Physik* **71**, 205-226 (1931)

[7] M. Karbach and G. Muller, *Computers in Physics* **11**, 36-43 (1997) (cond-mat/9809162)

[8] M. Karbach, K. Hu, and G. Muller,*Computers in Physics* **12**, 565-573 (1998) (cond-mat/9809163)

[9] C. K. Majumdar, and D. Ghosh, *J. Math. Phys.* **10**, 1388 (1969)

[10] C. K. Majumdar, *J. Phys. C: Solid State Phys.* **3**, 911-915 (1969)

[11] F. D. M. Haldane, *Phys. Rev. Lett.* **60**, 635 (1988)

[12] B. S. Shastry,*Phys. Rev. Lett.* **60**, 639 (1988)

[13] I. Bose, *Quantum magnets: a brief overview* (2001) arXiv:cond-mat/0107399

[14] F. Mila, *Eur. J. Phys.* **21**, 499-510 (2000)

[15] L. Balents, *Nature* **464**, 199-208 (2010)

[16] J. L. Atwood, *Nature Materials* **1**, 91-92 (2002)

[17] B. Bernu, C. Lhuillier, and L. Pierre, *Phys. Rev. Lett.* **69**, 2590 (1992)

[18] I. Dzyaloshinsky, *Journal of Physics and Chemistry of Solids* **4**, 241-255 (1958)

[19] T. Moriya, *Phys. Rev.* **120**, 1 (1960)

[20] T. Yildirim, A. B. Harris, A. Aharony, and O. Entin-Wohlman, *Phys. Rev. B* **52**, 10239 (1995)

[21] I.A. Sergienko, and E. Dagotto, *Phys. Rev. B* **73**, 094434 (2006)

[22] S. W. Cheong, and M. Mostovoy, *Nature Materials* **6**, 13-20 (2007)

[23] Y. Tokunaga, Y. Kaneko, D. Okuyama, S. Ishiwata, T. Arima, S. Wakimoto, K. Kakurai, Y. Taguchi, and Y. Tokura, *Phys. Rev. Lett.* **105**, 257201 (2010)

[24] C. Kittel, *Quantum Theory of Solids* (Wiley, 1987)

[25] J. Nygård, D. H. Cobden and P. E. Lindelof, *Nature* **408**, 342-346 (2000)

[26] P. Jarillo-Herrero et al., *Nature* **434**, 484-488 (2005)

[27] M. R. Buitelaar et al., *Phys. Rev. Lett.* **88**, 156801 (2002)

[28] A. V. Shubnikov, *Simmetriya i antisimmetriya konechnykh figur* (Akad. Nauk., Moscow, 1951)

[29] C. Bradley, and A. Cracknell, *The Mathematical Theory of Symmetry in Solids: Representation Theory for Point Groups and Space Groups* (Clarendon Press, Oxford, 1972)

[30] M. S. Dresselhaus, G. Dresselhaus, and A. Jorio, *Group Theory: Application to the Physics of Condensed Matter* (Springer, Berlin 2008)

[31] W. F. Brinkman, and R. J. Elliott, *Proc. R. Soc. Lond. A* **294**, 343-358 (1966)

[32] D. B. Litvin, Acta Cryst. A **29**, 651-660 (1973)

[33] D. B. Litvin, and W. Opechowski, *Physica* **76**, 538-554 (1974)

[34] E. F. Bertaut, *Le Journal de Physique Colloques* **32**, 462-470 (1971)

[35] Yu. A. Izyumov, V. E. Naish, and R. P. Ozerov, *Neutron Diffraction Of Magnetic Materials* (Consultants Bureau, New York, 1991)

[36] R. Lifshitz, *Phys. Rev. Lett.* **80**, 2717 (1998)

[37] R. Lifshitz, and S. Even-Dar Mandel, *Acta Cryst. A* **60**, 167-178 (2004)

[38] L. Messio, C. Lhuillier, and G. Misguich, *Phys. Rev. B* **83**, 184401 (2011)

[39] N. Lazić, M. Damnjanović, *Phys. Rev. B* **90**, 195447 (2014)

[40] S. D. Bader, *Rev. Mod. Phys.* **78**, 1 (2006)

[41] P. Lemmensa, G. Gúntherodtb, and C. Grosc, *Physics Reports* **375**, 1-103 (2003)

[42] T. Masuda et al., *Phys. Rev. B* **72**, 014405 (2005)

[43] L. Mihaly, B. Dora, A. Vanyolos, H. Berger, and L. Forro, *Phys. Rev. Lett.* **97**, 067206 (2006)

[44] F. Cinti, A. Rettori, M. G. Pini, M. Mariani, E. Micotti, A. Lascialfari, N. Papinutto, A. Amato, A. Caneschi, D. Gatteschi, and M. Affronte *Phys. Rev. Lett.* **100**, 057203 (2008)

[45] J. M. Higgins, R. Ding, J. P. DeGrave, and S. Jin, *Nano Lett.* **10**, 1605-1610 (2010)

[46] M. Damnjanović, and I. Milošević, *Line Groups in Physics* (Springer-Verlag, Berlin, 2010)

[47] P. A. M. Dirac, *The Principles of Quantum Mechanics*, 4th Edition (Oxford University Press, 1958)

[48] S. V. Tjablikov, *Methods in the Quantum Theory of Magnetism* (Plenum Press, New York, 1967)

[49] N. Majlis, *The Quantum Theory of Magnetism* (World Scientific Publishing, 2000)

[50] H.-J. Mikeska, and A.K. Kolezhuk, *One-Dimensional Magnetism, Lect. Notes Phys.* **645**, 1-83 (2004) arXiv:cond-mat/0501603

[51] F. H. L. Essler, H. Frahm, F. Gohmann, A. Klumper and V.E. Korepin, *The One-dimensional Hubbard Model* (Cambridge University Press, 2005)

[52] D. C. Mattis, *The Theory of Magnetism Made Simple. An Introduction to Physical Concepts and to Some Useful Mathematical Methods* (World Scientific Publishing, 2006)

[53] I. A. Zaliznyak, *Spin Structures and Spin Wave Excitations. Handbook of Magnetism and Advanced Magnetic Materials* (Wiley, 2007)

[54] D. D. Stancil, and A. Prabhakar, *Spin Waves Theory and Applications* (Springer, Berlin, 2009)

[55] J. Keeling, *Quantum Magnetism*, University of Cambridge (2010) https://www.st-andrews.ac.uk/ jmjk/keeling/teaching/magnetism-notes.pdf

[56] J. R. Schrieffer, and P. A. Wolff, *Phys. Rev.* **149**, 2 (1966)

[57] P. W. Anderson, *Phys. Rev.* **124**, 41 (1961)

[58] N. Lazić, M. Milivojević, and M. Damnjanović, *Phys. Status Solidi B* **249**, 2558-2561 (2012)

[59] N. Lazić, M. Milivojević, and M. Damnjanović, *Acta Cryst. A* **69**, 611-619 (2013)

[60] M. Milivojević, N. Lazić, T. Vuković, and M. Damnjanović, *Phys. Rev. B* **92**, 165410 (2015)

[61] E. P. Wigner, *Group Theory and Its Application to the Quantum Mechanics of Atomic Spectra* (Academic Press, New York, 1959)

[62] Representation $d(\ell'^{-1}\ell\ell')$ is called ℓ'-conjugated to $d(\ell)$; if it is equivalent to $d(\ell)$ it is called self ℓ'-conjugated; otherwise the two are mutually ℓ'-conjugated. L. Jansen and M. Boon, *Theory of finite groups. Applications in Physics* (North-Holland, Amsterdam, 1967)

[63] T. Holstein, and H. Primakoff, *Phys. Rev.* **58**, 1098-1113 (1940)

[64] M-w. Xiao, arXiv:0908.0787 (2009)

[65] A. Zagoskin, *Quantum Theory of Many-Body Systems* (Springer, Berlin, 2014)

[66] M. Damnjanović, and I. Milošević, *Physics Reports* **581**, 1-43 (2015)

[67] F. Simon et al., *Phys. Rev. Lett.* **95**, 017401 (2005)

[68] M. H. Rummeli et al., *J. Phys. Chem. C* **111**, 4094 (2007)

[69] H. O. H. Churchill et al., *Nature Physics* **5**, 321 (2009)

[70] B. Braunecker, P. Simon, and D. Loss, *Phys. Rev. Lett.* **102**, 116403 (2009)

[71] J. Klinovaja, and D. Loss, *Phys. Rev. B* **87**, 045422 (2013)

[72] B. Trauzettel, and D. Loss, *Nature Physics* **5**, 317-318 (2009)

[73] F. Kuemmeth et al., *Materials Today* **13**, 18-26 (2010)

[74] H. Schenck, V. L. Pokrovsky, and T. Nattermann, *Phys. Rev. Lett.* **112**, 157201 (2014)

[75] S. Reich, C. Thomsen, and J. Maultzsch, *Carbon Nanotubes* (Wiley, 2003)

[76] R. Saito, G. Dresselhaus, and M. S. Dresselhaus, *Physical Properties of Carbon Nanotubes* (Imperial College Press, 1998)

[77] E. B. Barros et al., *Physics Reports* **431**, 261-302 (2006)

[78] M. Damnjanović, I. Milošević, T. Vuković, and R. Sredanović, *Phys. Rev. B* **60**, 2728 (1999)

[79] N. Lazić, T. Vuković, G. Volonakis, I. Milošević, S. Logothetidis, and M. Damnjanović, *Journal of Physics: Condensed Matter* **24**, 485302 (2012)

[80] V. S. Shchesnovich, *Physics Letters A* **349**, 398-403 (2006)

[81] J. Chalker, *Quantum Theory of Condensed Matter*, Oxford University (2013) http://www-thphys.physics.ox.ac.uk/people/JohnChalker/qtcm/lecture-notes.pdf

[82] J. Klinovaja, M. J. Schmidt, B. Braunecker, and D. Loss, *Phys. Rev. Lett.* **106**, 156809 (2011)

[83] M. Damnjanović, I. Milošević, E. Dobardžić, T. Vuković, and B. Nikolić, Ch. 2 in: *Applied Physics of Carbon Nanotubes: Fundamentals of Theory, Optics and Transport Devices*, eds. S. V. Rotkin and S. Subramoney, Springer Series in Nanoscience and Technology (Springer, Berlin, 2005)

[84] D. Belitz, T. R. Kirkpatrick, and A. Rosch, *Phys. Rev. B* **73**, 054431 (2006)

[85] B. Braunecker, P. Simon, and D. Loss, *Phys. Rev. B*, **80**, 165119 (2009)

[86] Yu. A. Izyumov, V. E. Naish, and R. P. Ozerov, *Neutron Diffraction of Magnetic Materials* (Springer, 1991)

[87] I. Herbut, *A Modern Approach to Critical Phenomena* (Cambridge University Press, 2007)

[88] V. I. Litvinov, and V. K. Dugaev, *Phys. Rev. B* **58**, 3584 (1998)

[89] V. B. Shenoy, *Phys. Rev. B* **71**, 125431 (2005)

[90] R. Orús, *Annals of Physics* **349**, 117-158 (2014) arXiv:1306.2164

BIOGRAFIJA

Nataša Lazić je rodjena 1980. godine u Beogradu, gde je završila osnovnu školu i gimnaziju, a zatim upisala Fizički fakultet Univerziteta u Beogradu, smer teorijska i eksperimentalna fizika. Nakon diplomiranja 2010, upisala je doktorske studije fizike na istom fakultetu. Do sada je položila sve ispite i 2012. godine odbranila temu pred Kolegijumom doktorskih studija. Od 2010. godine je zaposlena na Fizičkom fakultetu kao istraživač pripravnik, a 2013. godine je izabrana u zvanje istraživač saradnik. Do sada je objavila šest naučnih članaka u međunarodnim časopisima. Trenutno je angažovana na projektu "Niskodimenzionalne nanostrukture" Ministarstva prosvete, nauke i tehnološkog razvoja Republike Srbije.
Naučna aktivnost Nataše Lazić zasniva se na analizi simetrije u fizici kondenzovane materije, prvenstveno kod kvazi-jednodimenzionalnih sistema. To obuhvata rezultate o stabilnim položajima ugljeničnih nanotuba i metodologiju kvazi-klasične teorije magnetizma.

Прилог 1.

Изјава о ауторству

Потписани-а Наташа Лазић

број уписа Д-35/2010.

Изјављујем

да је докторска дисертација под насловом

Quasi-classical ground states and magnons in monoperiodic spin systems

- резултат сопственог истраживачког рада,
- да предложена дисертација у целини ни у деловима није била предложена за добијање било које дипломе према студијским програмима других високошколских установа,
- да су резултати коректно наведени и
- да нисам кршио/ла ауторска права и користио интелектуалну својину других лица.

Потпис докторанда

У Београду, 19.09.2016.

Прилог 2.

Изјава о истоветности штампане и електронске верзије докторског рада

Име и презиме аутора Наташа Лазић

Број уписа Д-35/2010.

Студијски програм Квантна, математичка и нано-физика

Наслов рада Quasi-classical ground states and magnons in monoperiodic spin systems

Ментор Милан Дамњановић

Потписани Наташа Лазић

изјављујем да је штампана верзија мог докторског рада истоветна електронској верзији коју сам предао/ла за објављивање на порталу **Дигиталног репозиторијума Универзитета у Београду.**

Дозвољавам да се објаве моји лични подаци везани за добијање академског звања доктора наука, као што су име и презиме, година и место рођења и датум одбране рада.

Ови лични подаци могу се објавити на мрежним страницама дигиталне библиотеке, у електронском каталогу и у публикацијама Универзитета у Београду.

Потпис докторанда

У Београду, 19.09.2016.

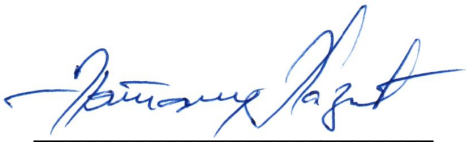

Прилог 3.

Изјава о коришћењу

Овлашћујем Универзитетску библиотеку „Светозар Марковић“ да у Дигитални репозиторијум Универзитета у Београду унесе моју докторску дисертацију под насловом:

Quasi-classical ground states and magnons in monoperiodic spin systems

која је моје ауторско дело.

Дисертацију са свим прилозима предао/ла сам у електронском формату погодном за трајно архивирање.

Моју докторску дисертацију похрањену у Дигитални репозиторијум Универзитета у Београду могу да користе сви који поштују одредбе садржане у одабраном типу лиценце Креативне заједнице (Creative Commons) за коју сам се одлучио/ла.

1. Ауторство

2. Ауторство - некомерцијално

3. Ауторство – некомерцијално – без прераде

4. Ауторство – некомерцијално – делити под истим условима

5. Ауторство – без прераде

6. Ауторство – делити под истим условима

(Молимо да заокружите само једну од шест понуђених лиценци, кратак опис лиценци дат је на полеђини листа).

Потпис докторанда

У Београду, 19.09.2016.

1. Ауторство - Дозвољавате умножавање, дистрибуцију и јавно саопштавање дела, и прераде, ако се наведе име аутора на начин одређен од стране аутора или даваоца лиценце, чак и у комерцијалне сврхе. Ово је најслободнија од свих лиценци.

2. Ауторство – некомерцијално. Дозвољавате умножавање, дистрибуцију и јавно саопштавање дела, и прераде, ако се наведе име аутора на начин одређен од стране аутора или даваоца лиценце. Ова лиценца не дозвољава комерцијалну употребу дела.

3. Ауторство - некомерцијално – без прераде. Дозвољавате умножавање, дистрибуцију и јавно саопштавање дела, без промена, преобликовања или употребе дела у свом делу, ако се наведе име аутора на начин одређен од стране аутора или даваоца лиценце. Ова лиценца не дозвољава комерцијалну употребу дела. У односу на све остале лиценце, овом лиценцом се ограничава највећи обим права коришћења дела.

4. Ауторство - некомерцијално – делити под истим условима. Дозвољавате умножавање, дистрибуцију и јавно саопштавање дела, и прераде, ако се наведе име аутора на начин одређен од стране аутора или даваоца лиценце и ако се прерада дистрибуира под истом или сличном лиценцом. Ова лиценца не дозвољава комерцијалну употребу дела и прерада.

5. Ауторство – без прераде. Дозвољавате умножавање, дистрибуцију и јавно саопштавање дела, без промена, преобликовања или употребе дела у свом делу, ако се наведе име аутора на начин одређен од стране аутора или даваоца лиценце. Ова лиценца дозвољава комерцијалну употребу дела.

6. Ауторство - делити под истим условима. Дозвољавате умножавање, дистрибуцију и јавно саопштавање дела, и прераде, ако се наведе име аутора на начин одређен од стране аутора или даваоца лиценце и ако се прерада дистрибуира под истом или сличном лиценцом. Ова лиценца дозвољава комерцијалну употребу дела и прерада. Слична је софтверским лиценцама, односно лиценцама отвореног кода.